FAST GC: APPLICATIONS AND THEORETICAL STUDIES

by

Gail L. Reed

Dissertation submitted to the Faculty of
Virginia Polytechnic Institute and State University
in partial fulfillment of the requirements for the degree of

Doctor of Philosophy
in
Chemistry

Committee:
Dr. Harold M. McNair, Chairman
Dr. Larry T. Taylor
Dr. James O. Glanville
Dr. Gary L. Long
Dr. Paul A. Deck

September 15, 1999
Blacksburg, Virginia

Keywords: Fast GC, Gas Chromatography, flash temperature programming, theoretical, food, BHT, Blumberg equation, microwave assisted extraction

FAST GC: APPLICATIONS AND THEORETICAL STUDIES

Gail L. Reed

Abstract

Experimental data are presented for the first time in support of a theoretical model of band broadening proposed by Blumberg (1997). This model addresses the effects of the compressibility of the mobile phase in gas chromatography and presents an equation derived from only two mutually independent variables. Solutions of decane and tridecane in hexane were analyzed at pressures ranging from 15 to 150 psi. Six different columns were used that varied in length, internal diameter and film thickness. Theoretical plate heights were obtained from this data and plotted versus the average linear carrier gas velocity (Golay type plots). These plots showed that at high pressures the Blumberg model fit the experimental data statistically significantly better than the earlier model proposed by Golay. The Blumberg model also accurately predicts the relationship between the optimum linear carrier gas velocity and the temperature.

The second part of this work explores the scope and limitations of fast temperature programming in the fast GC analyses of various sample types. These samples included polycyclic aromatic hydrocarbons (PAHs), hydrocarbons and food samples. Programming rates of up to 1200 °C/min were used. These fast programming rates were obtained by using "flash"™ temperature programming, controlled by resistive heating of a metal tube that enclosed a capillary column. The precision of peak data was found to be good, less than 5% for peak areas and 4% for retention times. However, a slight, but statistically significant decrease in peak areas was seen above programming rates of 240 °C/min.

Microwave assisted extraction (MAE) was used to extract 2,6-di-(tert-butyl)-4-methylphenol, BHT, from chewing gum and breakfast cereal. The extraction was followed by a fast GC analysis (less than 4 minutes) using "flash"™ temperature programming. MAE reduced the sample preparation time, from hours to minutes, and consequently reduced, the total analysis time. Extraction times longer than 5 minutes gave decreased recoveries of BHT.

Acknowledgements

I have been blessed in my life in many ways and have achieved many goals set before me. I have not obtained them alone. Many people have helped me realize my potential and have shown me the benefits of working hard. To them I am grateful. I thank my family for supporting me and believing in me. I thank my husband, Matt for his support through this time. I thank Dr. Harold McNair, my research advisor, for all the support, teaching, and opportunities he has given me during my time in his research group at Virginia Tech. Thanks to the research group for their help, especially, Dr. Stephanye Armstrong, Dr. Yuwen Wang and Dr. Marisa Bonilla. Thanks to all the people who have been in the research group in the last four years for the help and suggestions that they provided. Lastly, but most importantly, I thank God for guiding my life and giving me the strength needed to persevere.

Dedication

This work is dedicated my parents, Frank and Lois Reed.

Table of Contents

List of Figures

List of Tables

Chapter 1 - Introduction

The capillary gas chromatography (GC) column, introduced by Marcel Golay in the late 1950's[1], brought about a revolution in gas chromatography. The wall coated open tubular (WCOT) capillary column that he introduced offered distinct advantages compared to the then used packed columns. In particular, the lower flow impedance of capillary columns made it possible to use higher flow rates and longer columns, which led to higher efficiencies. These higher efficiencies enabled faster and more complex analyses compared to packed columns. These complex samples included perfumes, wines, natural products, gasoline, and crude oil. The properties of these WCOT capillary columns were described at the first GC Symposium held in the United States in 1956 at the spring national ACS meeting.[1] The WCOT capillary column itself was introduced in Europe at the International meeting on GC held in Amsterdam in 1958.[2]

Prior to the introduction of GC complex samples were impossible to separate and time consuming to study. Packed column GC made the work much easier than distillation techniques, however, the capillary columns yielded even better results due to their higher efficiencies. The longer capillary columns led to some analyses with very long analysis times. The most notable being a naptha analysis that was done on a 1300 m column and lasted 18 hours.[3] Despite some of the long analyses, there were several people who foresaw the possibilities of doing fast GC with capillary columns.

In 1960, D. H. Desty wrote, "it is apparent from the few results we have obtained to date that, if suitable high-speed sample introduction methods and automatic recording equipment could be developed, exciting possibilities for capillary column chromatography lie ahead".[4] With this comment he summarized the problems with fast GC as early as 1960. Introducing small amounts of samples in very narrow bands onto capillary columns with small internal diameters, thin films and short lengths is still a problem today. However, over the years improvements in technology have made great changes in all aspects of GC.

Since 1960 great strides have been made in the instrumentation available for GC, as well as in our understanding of GC as a science. Today GC is a mature, well

developed field. Currently, GC is being pushed to a new level, a level that will allow for the rapid, quantitative acquisition of data. Industry is demanding rapid analyses and rapid throughput of samples to reduce costs and increase profits. One objective of this thesis is to demonstrate that these rapid analyses are possible, and can be done without sacrificing the integrity of the results.

This study of fast GC is composed of four segments. Chapter One is the introduction to fast GC. Chapter Two is a review of the literature concerning fast GC. Chapter Three discusses the theoretical implications of the high pressure drops that occur when using small internal diameter columns for fast GC. Recently the Blumberg equation, a modification of the Golay equation, has been proposed. The Blumberg equation takes into account the effect of high pressure drops on carrier gas viscosity and the resultant effect on band broadening. At high pressure drops the compressibility of the mobile phase is more significant than at low pressure drops. This in turn affects the mass transfer in the mobile phase. The work presented here provides, for the first time, experimental validation of the Blumberg model.

Chapter Four is an investigation of the capabilities of fast oven temperature programming, (up to 1200 °C/min) and its effects on various analyses. Resistive heating of metal is applied to capillary GC columns in order to achieve very fast rates of temperature programming. Chapter Five of this work presents some research on practical applications of fast GC. The work in Chapter Five incorporates microwave assisted extraction as a fast sample preparation technique preceding a fast GC analysis. This research demonstrates that the quantitative integrity of an analysis can be maintained under fast GC conditions. Chapter Six draws together what has been discovered in this work and expresses where the future of fast GC lies.

Chapter 2 –Literature Review and Background

Historical

The patent[5] for capillary columns, submitted by Golay in 1957, demonstrated the separation of five analytes in 10 seconds (Figure 1). The peaks present in the analysis are air, acetone, carbon disulfide, methanol, and methylene chloride from left to right. The analysis was done on a 32 foot long capillary column with an internal diameter of ten thousandths of an inch and a carrier gas head pressure of 15 p.s.i. The detector was a thermal conductivity detector and instead of a chromatogram it was called a fractogram (Perkin Elmer terminology). This result was an incredible decrease in analysis time compared to the packed columns being used at that time.

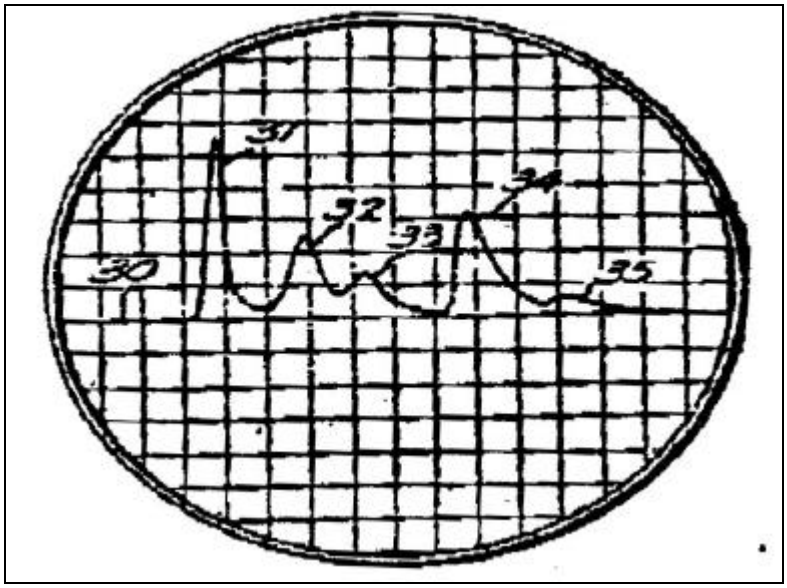

Figure 1. Fast Analysis From Golay Patent

Conditions: 32 ft x 0.001 in. i.d. column, head pressure of 15 p.s.i., thermal conductivity detector, peaks – air, acetone, carbon disulfide, methanol, and methylene chloride

Using the then recently introduced capillary columns, Desty separated the isomeric heptanes, (without baseline resolution), in less than 1 minute. This corresponds to over 17,000 theoretical plates for the column efficiency. Desty also minimized his injection

times by depressing the button of his syringe with a mallet. The conditions for his fast analysis are noted on the chromatogram in Figure 2. This work was presented at the Third International GC Symposium held in Edinburgh (1960).[6]

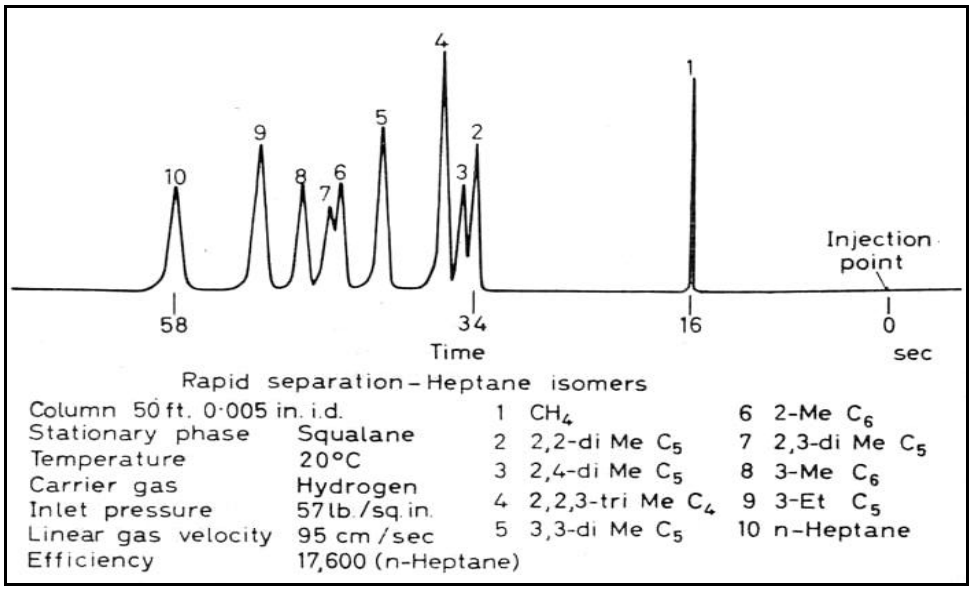

Figure 2. Rapid Separation of Heptane Isomers, (Desty, 1960)

Scott and Cumming[7] separated five components in five seconds. The five components (Figure 3) are pentanes and hexanes with n-pentane being the fourth peak. The first peak may be butane and the last peak is probably a hexane isomer. These compounds were separated on a 274 cm column with a 0.47 x 10^{-4} cm film thickness at a linear velocity of 28 cm/s.

Figure 3. Fast GC by Scott and Cumming, (1960)

Conditions: 274 cm x 0.47e10^{-4} cm d_f column, average linear carrier gas velocity - 28 cm/sec, peaks – pentanes and hexanes

Golay, in his capillary column patent, separated 5 components in 15 seconds on a 16 ft x 0.25 mm column coated with a Carbowax stationary phase. A micro-thermal conductivity detector was used in conjunction with an oscilloscope as a recorder. The 5 peaks present in the chromatogram are (Figure 4) air, acetone, carbon disulfide, chloroform and methylene chloride respectively.[8]

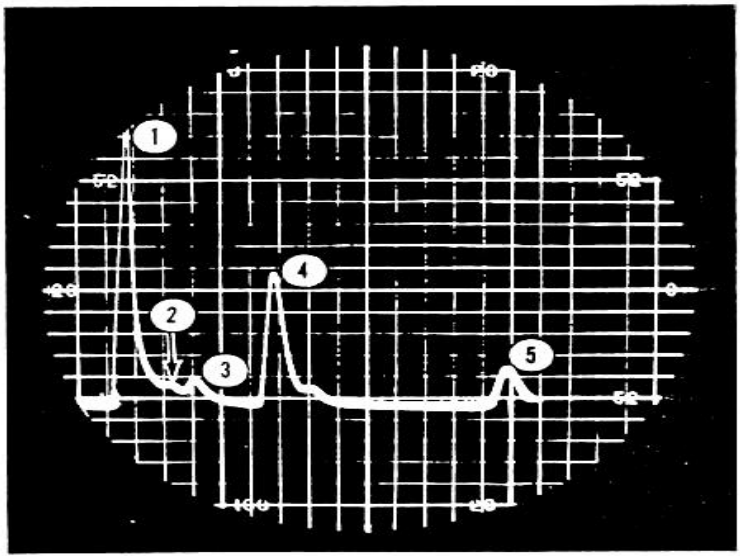

Figure 4. Fast GC by Golay

Conditions: 16 ft x 0.25 mm i.d. column, Carbowax stationary phase, micro-thermal conductivity detector, peaks – air, acetone, carbon disulfide, chloroform and methylene chloride

One of the fastest chromatograms ever performed was a separation of 4 peaks in 600 msec.[9] The headspace sample of four components, (n-pentane, n-hexane, n-heptane and toluene), was separated in 0.6 seconds on a 5 m x 0.32 mm i.d., 0.12 μm d_f column at an inlet pressure of 50 bar (Figure 5). This is an example of a chromatogram obtained under turbulent flow conditions. Turbulent flow is one way to decrease the analysis time. Turbulent flow occurs only at high velocities and requires high pressures. The transition from normal chromatographic laminar flow to turbulent flow occurs at a Reynolds number around 2300.[9] In turbulent flow, the flow profile is flattened which increases the diffusion coefficient and leads to less peak broadening in the mobile phase. In conclusion, the authors state that "the gain in analysis speed is insufficient to compensate for the larger pressure drop. The same gain can be obtained more easily under laminar flow conditions by using hydrogen as the carrier gas, and/or applying a vacuum at the column outlet and/or a reduction of the column diameter." Due to the impracticality of turbulent flow, it is not discussed further as a good means of doing fast GC.

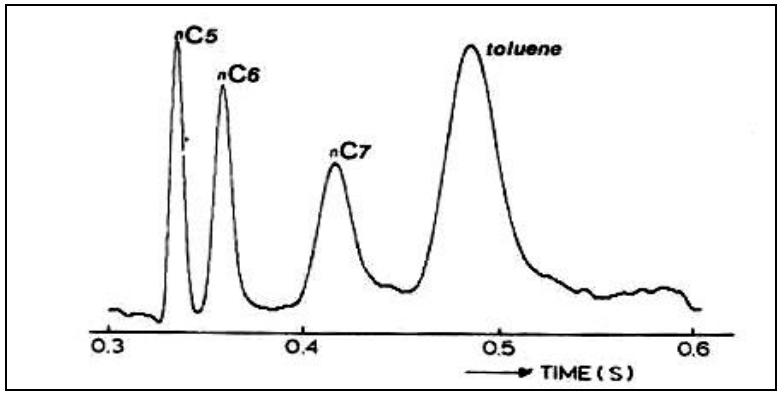

Figure 5. Turbulent Flow Chromatogram[9]

Conditions: 5 m x 0.32 mm i.d., 0.12 μm d_f column, inlet pressure of 50 bar, peaks – n-pentane, n-hexane, n-heptane, and toluene

The last chromatogram was very fast, four peaks in 0.6 seconds, but an even faster GC analysis was done using a packed column. Jonker[10] *et al*. separated methane, ethane, propane and butane in 0.15 s. The column was a 32 mm x 1.19 mm, column

packed with 10 μm particles of LiChrosorb Si-60. The analysis was done at 100 °C in 0.15 seconds (Figure 6).

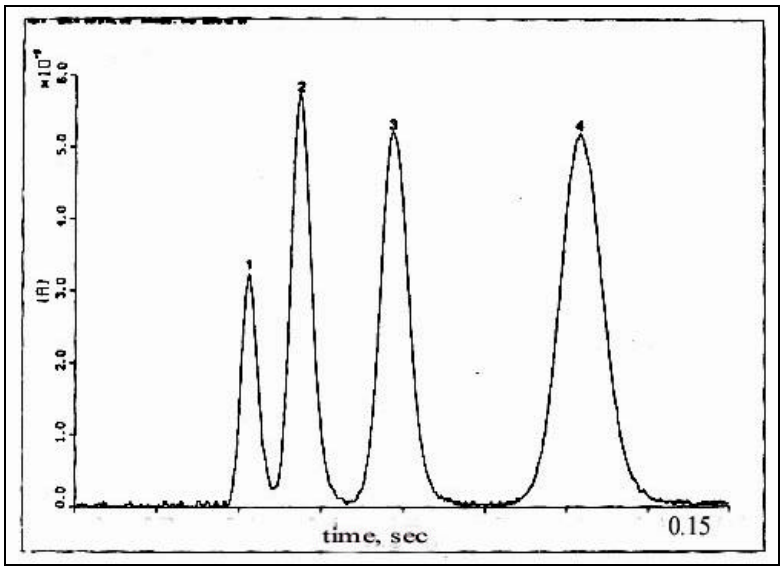

Figure 6. Fastest Published Chromatogram[10]

Conditions: 32 mm x 1.19 mm i.d. packed with 10 μm particles of LiChrosorb Si-60, 100 °C, peaks – methane, ethane, propane and butane

Using the WCOT columns, Rooney *et al.* were able to separate 90 components of a full range gasoline sample in three minutes.[11] This was done on a 10 m x 0.25 mm i.d. column, operated at a linear gas velocity of 50 cm/s and a temperature programming rate of 35 °C/min (Figure 7). At the time this chromatogram was published, the temperature programming rate and linear gas velocity were considered to be at the upper limits of the instruments capabilities. By today's standards, these values are low, and it seems likely that an even faster analysis could be performed.

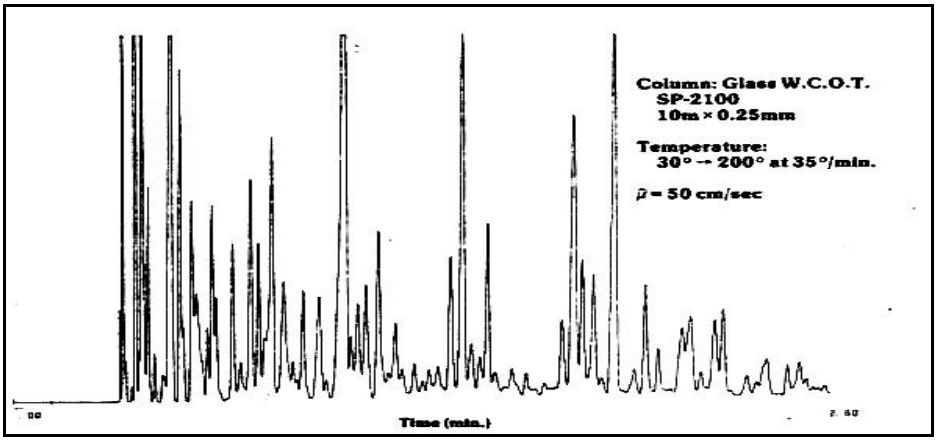

Figure 7. Rapid Separation of a Full Range Gasoline Sample, (Rooney, 1979)
Conditions: 10 m x 0.25 mm i.d., average linear gas velocity of 50 cm/s, temperature program of 30 °C to 200 °C at 35 °C/min

The capillary columns introduced by Golay offered higher resolution than the packed columns typically used at the time due to the longer lengths, thinner films and smaller internal diameters possible with these open tubular columns. As was just shown, these columns were able to perform analyses considered "impossible" by packed column standards. Some of the peak shapes in the examples shown are not ideal and this may contribute to lower precision in quantitative analyses. There is an absence of precision data for "fast GC' in the literature. Many peaks are tailing, and several peaks are not baseline resolved. These chromatographic issues raise the question as to what makes an acceptable chromatogram. The factors that make a chromatogram acceptable differ greatly, however, generally the answer is that it depends on the analysis being performed and the requirements of that analysis.

Some causes for the poor peak shapes seen in the previous chromatograms were slow injections, adsorption sites in the column, poorly designed injection ports, and slow detector response times. These problems needed to be minimized before high-speed separations could be fully exploited. These problems did not prevent chromatographers from continuing to pursue high-speed separations as was demonstrated in Figures 1-6. Despite their successes, fast GC work remained mostly in academic laboratories and was rarely applied to routine analyses. It appears that even though this early research in fast GC indicated its promising future, it was largely ignored by industry. Many researchers

still maintain this attitude even today, based on questions received from our presentations and publications on fast GC.

One logical application of fast GC would be in quality control laboratories or in routine analyses. In our fast paced society where virtually anything can be obtained instantly, it naturally follows that chromatographic results should be instantly obtainable as well. These fast measurements will allow chromatography to approach the capabilities of spectroscopy in its capabilities to do on-line monitoring and to provide "real-time" results. The capability of fast GC shows significant promise in production plants, where a lengthy sample turn around time in the quality control laboratory can be costly.

One final fast chromatogram to end the historical section was obtained by Reed and McNair in 1999.[12] A 1.9 second analysis of benzene, toluene and m-xylene is shown in Figure 8. A 1 m x 0.05 mm, 0.05 μm d_f column was used with hydrogen as the carrier gas at a split ratio of 2300:1 and a wet needle injection. This work was compared to a chromatogram published by Hewlett Packard in 1999, for the same analysis in 10 minutes.[13]

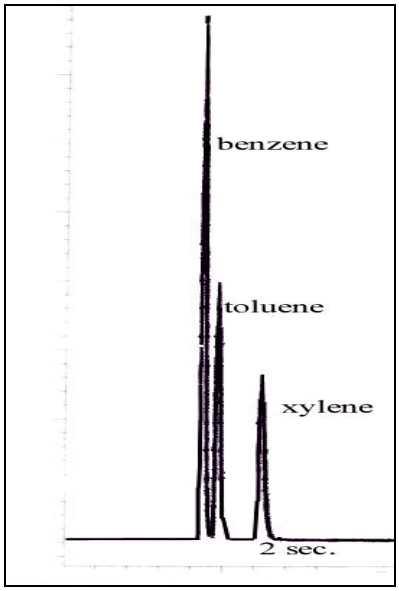

Figure 8. Fast Analysis of BTX

Conditions: 1 m x 0.05 mm i.d., 0.05 μm d_f, PE-1, 100% polydimethylsiloxane, hydrogen carrier gas, wet needle injection, split 2300:1, peaks – benzene, toluene and xylene

Background

The highlights of fast GC were discussed and illustrated in the historical section of this chapter. This section discusses in more detail, the progression of fast GC since the introduction of capillary columns. Fast GC incorporates many different aspects of GC and it implies modifications most parts of the gas chromatograph.

To begin, a definition of fast GC must be established. There are several facets of fast GC; one is "ultra-speed" GC and the other is "high-speed" GC, as opposed to "normal" GC. "Normal" GC and "high-speed" GC are accomplished with traditional instrumentation, or instrumentation commercially available in 1999. High-speed GC analyses are accomplished in minutes compared to the thirty to 60 minute analyses of "normal" GC. "Ultra-speed" analyses require specialized instrumentation, modified injection ports, ultra low volume detectors (less than 1.5 mL), fast data collection rates (greater than 200 Hz), and high pressure capabilities. "Ultra speed" GC analyses are accomplished in seconds.

Table 1. Subheadings of Fast GC

	Normal	**High-speed**	**Ultra-speed**
Time	30-60 minutes	minutes	seconds
Instrumentation	conventional	conventional	specialized

Very few laboratories are doing "ultra speed" analyses due to the lack of commercial instrumentation. The analyses that are considered "ultra-speed" GC today will move into the realm of "high-speed" GC tomorrow as new instrumentation and new technology are developed. This terminology is borrowed from G. Gaspar[14] and will be used in the remainder of this work. Fast GC in this text refers to high-speed GC, using commercially available instrumentation.

The instrumentation for fast GC consists of all the components that typically make up a gas chromatograph. These parts include a temperature controlled injection zone for sample introduction, an analytical column for separation of the analytes in a temperature controlled zone, a heated detection zone and a data handling system for

converting the analog signal from the detector into digital output. The band broadening of a peak is the summation of the broadening effects that occur in the injector, the column and the detector. In fast GC the column is generally much shorter so that the broadening affects that occur in the inlet and the detector become a larger proportion of the total band broadening compared to when the column is longer as in "normal GC". Our columns for fast GC are generally much shorter than conventional columns, 1 to 5 m compared to 15 to 50 m, with a smaller internal diameter, 0.05 to 0.2 mm compared to 0.25 to 0.32 mm, and coated with a thinner film, 0.1 to 0.25 μm compared to 0.25 to 1 μm. The logic and implications of the parameters will be discussed shortly.

Sources of band broadening in GC are described by equation 1 in terms of the peak variance. "Variance has the important property that the variance of a sum of independent quantities is equal to the sum of their variances."[15] Band broadening is an additive effect from all parts of the system.

$$\sigma_t^2 = \sigma_i^2 + \sigma_c^2 + \sigma_d^2 \qquad (1)$$

σ_t^2 =, total variance, s^2

σ_i^2 = the variance from the injector, s^2

σ_c^2 = the variance from the column, s^2

σ_d^2 = the variance from the detector, s^2

Since these terms are independent of each other, the variances are additive. The band broadening of a peak is important because it affects the efficiency of the column. The efficiency of the column is defined by eq. 2

$$N = \left(\frac{t_R}{s}\right)^2 \qquad (2)$$

N = plate number, a measure of the efficiency of the column

t_R = retention time of a peak in minutes

s = standard deviation of a peak in minutes

The broader the peak, the less efficient the column and the fewer number of peaks that can be separated within a certain time. Consequently, it is in the best interest of fast GC to minimize band broadening.

Injector

Sample introduction is an important step in fast GC. The broadening that occurs in the injector is due to the rate of injection, the rate of evaporation, and the rate of transfer of the sample from the inlet onto the column. Some chromatographers have used the hammer and syringe method to achieve very fast injections, with a large rate of syringe consumption. Small amounts of sample must be injected rapidly in narrow bands onto the analytical column. In this way the band broadening that occurs in the injection port is minimized. Generally autosamplers are used for sample introduction. However, there has been some work with fast GC and different types of sample introduction. One mode of sample introduction is by using "headspace". Headspace is defined in chromatography as the vapor phase above the sample, usually a solid or a solution. The headspace sampler minimizes or eliminates the solvent peak and allows for a faster analysis. In 1995, Russo[16] showed that headspace sample introduction could be combined with short microcapillary columns to decrease the time of analysis (Figure 9). A Petit-Grain, lemon essential oil was analyzed using a 3 m x 0.050 mm i.d., 0.18 μm d_f of SE-54 column, using hydrogen as the carrier gas at a linear gas velocity of 42 cm/sec. The oven temperature program was isothermal at 35 °C for 30 sec, programmed at 10 °C/min to 60 °C, held for 1.5 min, and then programmed at 2 °C/min until the analysis was complete (24 minutes). The analysis of essential oils typically requires 60 to 90 minutes.

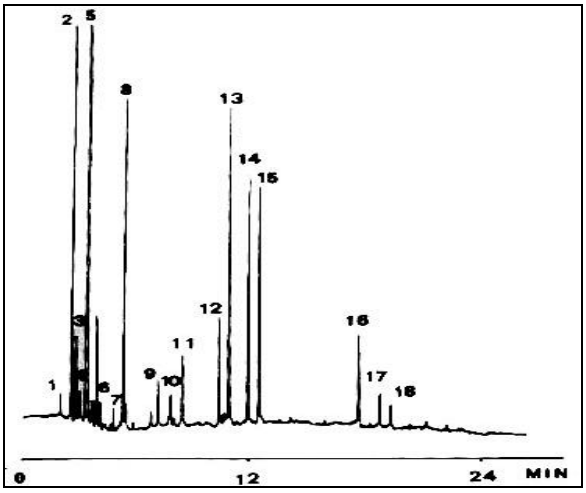

Figure 9. Fast Analysis of Lemon Essential Oil, (Russo, 1995)

Conditions: 3 m x 0.05 mm i.d., 0.18 μm d_f, stationary phase – SE-54, hydrogen carrier gas, oven temperature program – 35 °C for 30 s, programmed at 10 °C/min to 60 °C, held for 1.5 min., then programmed at 2 °C/min to completion

The numbered peaks in Figure 9 were quantitated by simple area percent.

The volume of the inlet and the gas flow rate through the inlet contribute to the broadening of the peaks. Even with a long column, the inlet effects can contribute significantly to the total broadening of the peaks. When the column is short, as it is often times in fast GC, the broadening that occurs in the inlet becomes a larger percentage of the total peak broadening and must be minimized as much as possible. Using smaller internal diameter liners can decrease the volume of the inlet. At the same volumetric flow rate (mL/min) this causes a faster carrier gas linear flow rate (cm/s) and sweeps the analytes onto the column faster. The importance of choosing the correct inlet liner dimensions to minimize band broadening in fast GC has been investigated by van Lieshout *et al*.[17] A 0.2 m x 0.32 mm column packed with 15 μm particles was used. This very short column revealed the effects of injector band broadening. They investigated 5, 1.23 and 0.7 mm i.d. liners. The conclusion was that the 1.23 mm liner was the best for fast GC using a 0.2 m x 0.32 mm i.d. column packed with 15 μm particles of C18. At low split ratios it is important to use a liner with a small i.d. At high split ratios where a large total flow rate is involved, a larger diameter liner can be used without significant band broadening.

Detector

The broadening of the peaks that occurs in the detector is due to the laminar carrier gas flow and the averaging of the detector signal over a gas volume that corresponds to the effective detector volume.[19] The detector time constant also contributes to band broadening. If the column is long, the broadening due to the detector volume is much smaller than the column volume. If the column is short, the broadening that occurs in the detector becomes a larger part of the total variance and often cannot be ignored. The detector must have a low volume to prevent band broadening and it must have a fast time constant to rapidly sample the narrow peaks produced when doing fast GC. Each peak must be defined by 10-12 data points, so that the peak is reproducible and reliable, and so that quantitative data can be obtained from the peak. The broadening due to the detector is more easily eliminated by instrument, electrometer, and data system re-design than the broadening due to the injection port. New micro detectors[18] and fast data systems are being introduced for fast GC.

Sample capacity of a column depends upon the mass of liquid phase in the column. Consequently, shorter columns, thinner films and smaller i.d. columns used in fast GC require smaller amounts of sample to be injected to prevent overloading of the column. This in turn causes the detection limits to be higher in fast GC. This is a problem when working with trace levels of analytes. In 1987, van Es[19] *et al.* looked at detection limits in fast GC. They discovered that the minimum detectable quantity for a mass flow sensitive detector (FID) is described by eq. 3 and for a concentration sensitive detector (ECD or TCD) without make-up gas it is described by eq. 4.

$$C_o(m) = \frac{2R_n\sqrt{F(k)}\sqrt{1+b^2}}{pSD_{m,o}bd_c} \qquad (3)$$

$$C_o(m) = \frac{4R_n\sqrt{1+b^2}}{Sb} \qquad (4)$$

$C_o(m)$ = minimum detectable quantity

R_n = noise of the detector, pA

S = sensitivity, pA/concentration

$D_{m,o}$ = diffusion of the analyte into the mobile phase, cm^2/s

k = capacity factor, dimensionless

d_c = internal diameter, cm

b = ratio of the band broadening in the injector to the band broadening in the column, dimensionless

To maintain low detection limits when operating under fast GC conditions, the equations just shown emphasize that it is imperative that the detector is in good working order with a low noise level and high sensitivity. Sensitivity of a detector is defined by the slope of the response versus concentration graph. For a mass flow sensitive detector, a smaller column i.d. will achieve a lower detection limit. This shows that efforts to decrease the analysis times often have other limitations. In the case of short columns, small internal diameters, and thin films, the capacity of the column is compromised, and this results in a higher detection limits.

Column

As the name implies, fast GC means faster analysis times. The analyte spends a small fraction of the time in the injector and the detector and the majority of the time is spent in the column. The analysis time can be mathematically described as shown in eq. 5.[20] Eq. 5 describes the analysis time in terms of column parameters; length, retention factor and the average linear carrier gas velocity.

$$t_R = \frac{L}{\bar{m}}(1+k) \tag{5}$$

t_R = retention time, s

L = length of the column, cm

$\bar{m}$ = average linear carrier gas velocity in cm/sec

k = retention factor (capacity factor), dimensionless

k is a dimensionless ratio of the time spent in the stationary phase, (t'_R), divided by the time spent in the mobile phase (t_o). $k = t'_R/t_o$. The retention time of a particular peak is

directly proportional to the length of the column, and inversely proportional to the average linear carrier gas velocity for an isothermal analysis. The column parameters that are changed when doing fast GC are the column length, internal diameter, film thickness, stationary phase type, temperature or temperature programming rate, or flow rate through the column. Manipulation of these parameters leads to two different cases. The first case is a faster analysis with some loss in resolution and the second case is a faster analysis with no loss in resolution.

For temperature programmed analyses, there are several ways to achieve faster analyses with less (but still acceptable) resolution. These ways include using shorter columns, increasing the carrier gas velocity, operating at higher column temperatures, using thinner films, using faster temperature programming rates, decreasing the solubility of solutes in the stationary phase or introducing selective stationary phases.

The second case is to maintain the original resolution and decrease the analysis time. Maintaining resolution while decreasing the analysis time is a more complicated way to do fast GC. The way to do achieve a faster analysis with the same resolution is by decreasing the internal diameter of the column.[21] Using hydrogen as the carrier gas or using a vacuum at the column outlet will also decrease the analysis time and maintain the original resolution, but with less dramatic effects. The effect of the i.d. on the retention time is shown mathematically in eq. 6 for a column with an internal diameter of less than 0.1 mm and a thin film.[21]

$$t_R = 16R^2\left(\frac{a}{a-1}\right)^2 \frac{(1+k)^3}{k^2}\frac{d_c}{\bar{m}} \qquad (6)$$

R = resolution, dimensionless,

a = selectivity, dimensionless,

k = retention factor, dimensionless

d_c = column diameter, cm

$\bar{m}$ = average linear gas velocity, cm/s

Published research on fast GC consists of a variety of studies. These studies focus on the parameters just mentioned. They include short columns, columns with thin

films of stationary phase, faster flow rates, vacuum at the column outlet, hydrogen as the carrier gas, faster column temperature programming rates or higher temperatures, small internal diameter columns, turbulent flow, packed columns and various selective stationary phases and column types. (References for these methods of fast GC are provided in Table 2.) Of the factors just mentioned, the major players are shorter columns, thinner films, faster column temperature programming rates, and smaller internal diameters. If the analysis is isothermal, then the use of hydrogen as a carrier gas is also a good choice to speed up the analysis. The next several pages will provide an overview of the various studies that have been done using fast GC, through the manipulation of the parameters just mentioned. The following table is a summary of the parameters of fast GC and their advantages and disadvantages.

Table 2: Parameters of Fast GC

Parameters	References	Advantages	Disadvantages
Length	21, 24	- TPGC - Lower Elution Temperatures	- Loss of Resolution - Lower Sample Capacity
Film Thickness	25, 26, 27	- Less diffusion in stationary phase	-Loss of resolution -Lower sample capacity
Temperature		- Sharpens late eluting peaks	- Loss of resolution
TPGC	31, 32, 34, 35	-Good for samples with wide range of boiling points -Increase peak heights	- Loss of resolution
Flow Rate A. Pressure B. Vacuum	37, 38, 39	-Higher linear gas velocities obtainable -Increased diffusion coefficient	- Loss of efficiency - Specialized Instrumentation - Specialized instrumentation
Carrier Gas	41	-H_2 preserves some resolution -N_2 gains efficiency	- Safety Factor for hydrogen - Loss of efficiency for N_2
Internal Diameter	44, 45, 46, 47	-Preserves Resolution	-High Pressure Drops -Low Sample Capacity
GC/GC Selectivity Other	53, 54	-Selectivity -Heartcutting, temperature	- Specialized instrumentation - Trial & Error method development
Multi-Capillary Columns	52	-Higher sample capacity -Lower minimum detectable concentration -Higher flow rates	-Easily broken -Difficult to manufacture well
Packed Columns	50, 51	-Increased sample capacity	-Loss of resolution -Not readily available

In addition to the advantages listed in Table 1, each parameter has the unwritten advantage of decreasing the analysis time.

Length

In an isothermal GC analysis, the retention time is proportional to the length of the column and the resolution is proportional to the square root of the length of the column. These relationships are shown in eq. 7[22] and eq. 8[23].

$$t_R = \frac{L}{\bar{m}}(1+k) \tag{7}$$

$$R = \left(\frac{a-1}{a}\right)\left(\frac{k}{k+1}\right)\left(\frac{\sqrt{L/H}}{4}\right) \tag{8}$$

t_R = retention time, s

L = column length, cm

k = retention factor, dimensionless

$\bar{m}$ = average linear carrier gas velocity, cm/sec

R = resolution, dimensionless

a = selectivity, dimensionless

H = plate height, cm

In an isothermal analysis, shorter columns are faster with less resolution when other parameters are held constant. Typical GC columns are anywhere from 10 to 100 m in length. Many times the length of the column is reduced in conjunction with the change of a second or third parameter as can be seen in various chromatograms presented in this thesis.

Decreasing the length is not always necessary to decrease the analysis time. Scott and Hazeldean[24] discovered that a longer column operated at higher velocities could yield a more rapid analysis than a shorter column operated at the optimum velocity with equivalent plate height and resolution. Generally, when doing fast GC the column length

will be reduced in conjunction with the modification of one or more of the other parameters described here.

Film Thickness

The retention time is related to the mass of liquid phase in the column as shown in equation 9. For a fixed internal diameter the retention time is proportional to the film thickness. For fast GC, thinner films will produce faster chromatograms. Eq. 9 describes this relationship between retention time and film thickness.[21]

$$t_R = \frac{L}{\bar{m}}\left(1 + \frac{2d_f K}{r}\right) \tag{9}$$

t_R = retention time, s

L = column length, cm

d_f = film thickness, cm

K = distribution constant, dimensionless

$\bar{m}$ = average linear carrier gas velocity, cm/s

r = radius of the column, cm

The effect of the film thickness on retention time can be seen in the following chromatograms (Figure 10).[25] Four 15 m x 0.3 mm i.d. columns are coated with various film thicknesses of SE-52. The same gasoline sample was analyzed on each column. The results of this change are seen in Figure 10.

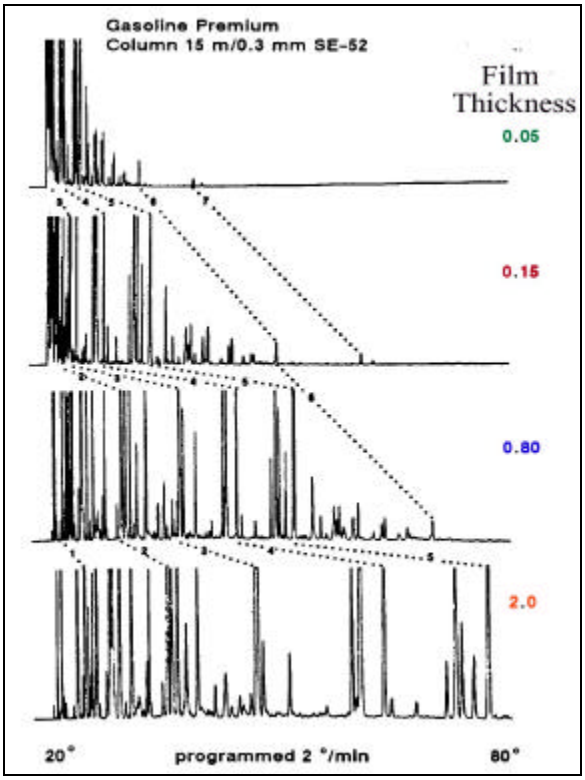

Figure 10. Effect of Film Thickness on Analysis Time[25]

Conditions: Gasoline analysis on a SE-52, 15 m x 0.3 mm i.d. column with varying film thicknesses, oven temperature program – 20 °C programmed at 2 °C/min to 80 °C

The thicker the film, the longer the analysis time. Film thickness is also often reduced in conjunction with the modification of other parameters. The film thickness affects the mass transfer in the stationary phase term of the Golay equation. Thinner films reduce mass transfer in the liquid phase and increase resolution. Leclercq[26], and Leclercq and Cramers[27] describe computer programs that can be used to determine the optimum performance of a capillary GC column under varying conditions, including the film thickness.

Temperature

GC analyses can be either isothermal or temperature programmed. Many samples, usually consisting of a few components, are handled isothermally. More complicated samples require temperature programming. Traditionally, the temperature is

raised by heating the oven air mass and cooled by forcing room air into an oven open to the atmosphere. Recently, resistive heating of the column has been developed as a way to heat the column. In this method, the column is wrapped in metal tubing that is resistively heated. The column is cooled by forcing room air into the oven. In our work, most samples require temperature programming and this thesis will deal mostly with temperature programmed analyses. To do a fast temperature programmed analysis the column temperature must be capable of rapidly changing.

The relationship between the column temperature and the partition coefficient of an analyte is defined by eq. 10.[28]

$$\log (K) = A/T_c + B \qquad (10)$$

K = partition coefficient, dimensionless

A and B = constants, K and dimensionless respectively

T_c = absolute column temperature, K

K is defined as the concentration of the analyte in the stationary phase divided by the concentration of the analyte in the mobile phase. The implication of equation 10 is that the higher the temperature, the smaller the value of K. This means the analyte will elute with a shorter retention time.

The same relationship exists between the selectivity, α, and the column temperature as well as between the retention factor, k and the column temperature. These relationships are valid only for isothermal GC. In temperature programming, the relationships are more complicated and in some cases unknown. In general, the selectivity, α, decreases with temperature, but cases of α increasing with increasing temperature have been reported.[29] The retention factor, k also decreases with an increase in temperature.

Temperature Programming

Temperature programming is used to analyze samples that contain analytes with a wide range of boiling points, as well as to clean out the column and avoid a buildup of

high boiling contaminants. The rate at which the column temperature changes affects the analysis time. Originally temperature programming rates ranged from 1 to 20 °C/min. These rates were determined by the power available, the large thermal mass of the early ovens and the packed metal columns that were commonly used. Currently, the upper temperature programming rate on most commercially available instruments is 50 to 100 °C/min. The rates available depend on the operating temperature. At higher temperatures more power is required, so the programming rates are slower. This situation is illustrated in Figure 11.[30]

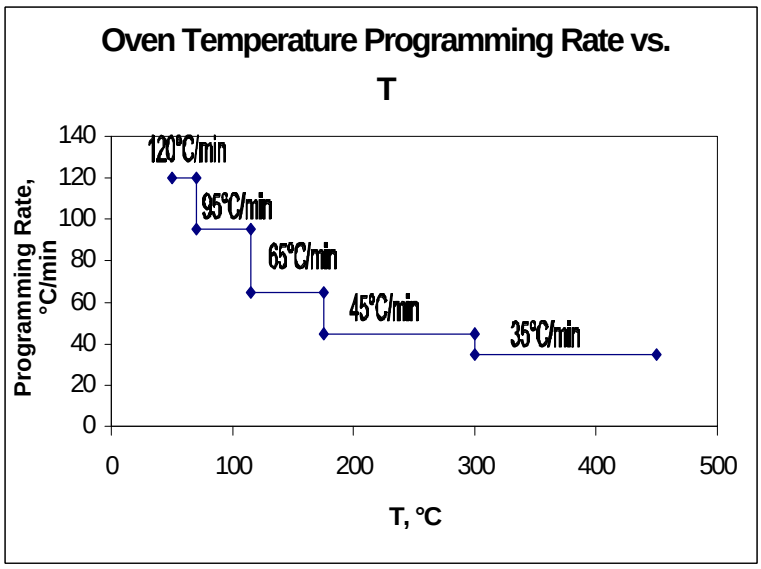

Figure 11. Effect of Operating Temperature on Programming Rate[30] (HP 6890)

From 70 °C to 115 °C, the 240 V HP model 6890 can program at 95 °C/min, but at 175 °C to 300 °C, the maximum temperature programming rate is 45 °C/min. The use of the fast programming rates has been investigated along with increased carrier gas flow rate for fast GC[31]. Fast temperature programming rates decreased the analysis time more than increasing the carrier gas flow rate. Large increases in the carrier gas flow rate caused poor resolution. Refer to the section on linear gas velocity (p. 24) for a more detailed explanation of this phenomenon.

Recently, new instrumentation[32] has been introduced that resistively heats a metal tubing that encloses the capillary column rather than heating the column oven with forced air. van Lieshout[33] *et al.* found this rapid temperature programming system to be "promising" for samples that are not too complex. The use of fast temperature programming for screening samples for drugs of interest was demonstrated by Williams *et al.*[34] Reed, *et al.*[35] compared conventional analyses to analyses done with fast temperature programming and found the precision of peak areas and heights in the fast temperature programming analyses to be as good as the conventional analyses. They also used fast temperature programming to do fast quantitative analyses. Dalluge[36] *et al.* analyzed polycyclic aromatic hydrocarbons, triazines and organophosphorus pesticides using fast temperature programming. They found good linearity between 10 pg and 5 ng and detection limits in the low picogram range for all compounds analyzed.

Linear Gas Velocity

The relationship between the average linear gas velocity, $\bar{m}$, and retention time was shown in equation 7 (p. 19). The analysis time is inversely proportional to the average linear gas velocity. H, plate height, is a asymmetric hyperbolic function of $\bar{m}$ (see Figure 12).

One means of increasing $\bar{m}$ while maintaining the same head pressure is by using a vacuum at the end of the capillary column. The use of a vacuum at the end of a capillary column increases the speed of analysis, due to an increase in the average linear carrier gas velocity. The retention time when using a vacuum at the column outlet is described by eq. 11.[37]

$$t_R = \frac{9t_{R,atm}}{8G} \tag{11}$$

t_R = retention time, min.

$t_{R,\,atm}$ = retention time under atmospheric pressure, min

G = ratio of the average atmospheric pressure to the average pressure under vacuum, dimensionless

The average pressure is calculated from the pressures at each point along the column. The lower outlet pressures of the vacuum leads to increased diffusivity of the solute in the gas phase, which in turn leads to increased optimum carrier gas velocities.[38] The effect of a vacuum at the column outlet on the plate height vs. linear gas velocity plot is shown in Figure 12. [38]

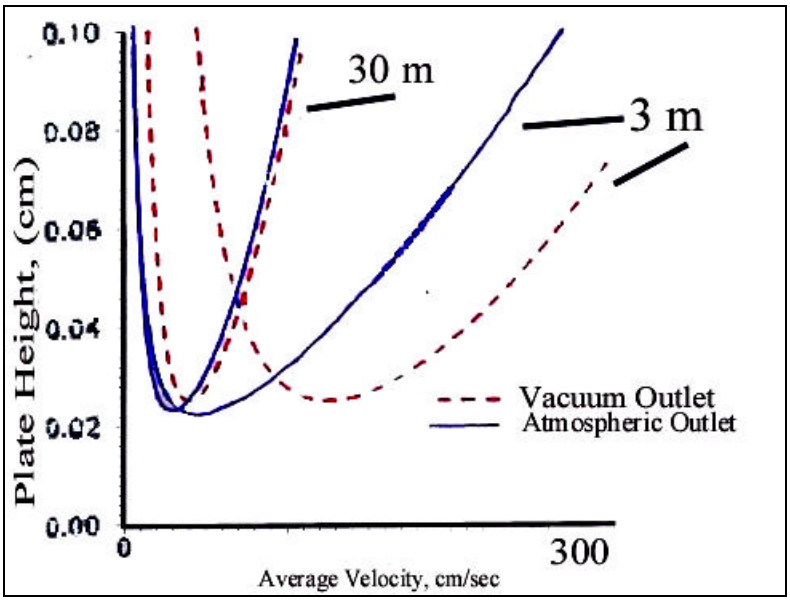

Figure 12. Effect of Vacuum on Golay Plot[38]

Conditions: 3 m or 30 m x 0.25 mm, DB-5, 0.25 μm d_f columns, helium carrier gas, 100 °C, k = 10

Figure 12 illustrates the effects of a vacuum at the column outlet on the Golay plot for both a 30 m and a 3 m column. The optimal velocities are shifted to higher values and the minimum plate heights are slightly increased. The shift to the higher plate heights is due to the gas decompression factor, which is 9/8 as shown in equation 11 (p. 24).[37] The effects of the vacuum for the shorter column are more dramatic since the lower pressure (vacuum) is experienced over a larger percentage of the column.

Giddings[39] was the first to show that the speed of analysis of capillary GC could be increased without the loss of resolution by operating a standard 0.3 mm internal diameter capillary column under vacuum. Hail and Yost[38] demonstrated the feasibility of using short columns with a vacuum at the column outlet. An ion-trap mass spectrometer

was used to improve the sensitivity over a quadrupole mass spectrometer in conjunction with high-speed GC.[40]

Type of Carrier Gas

The carrier gas also affects the analysis time, particularly in isothermal analyses. Hydrogen, helium and nitrogen are the most common carrier gases used. The effect of the carrier gas type on the Golay plot is shown in Figure 13.[41]

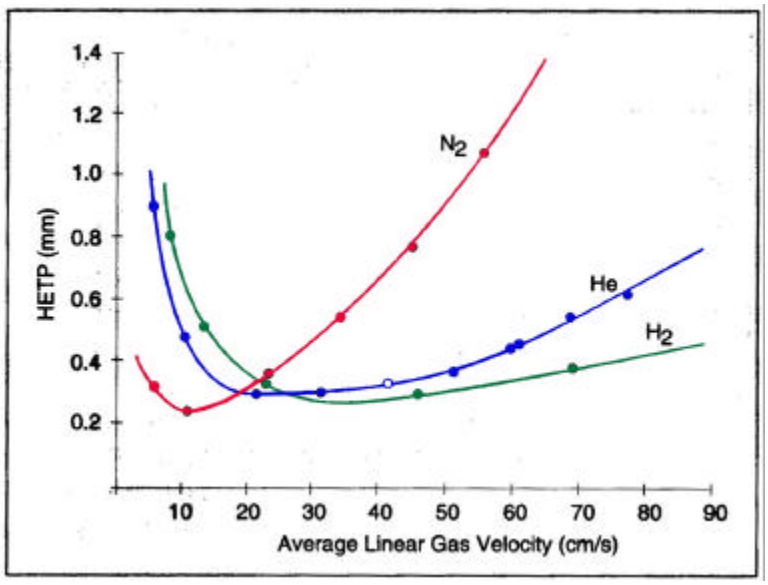

Figure 13. Effect of Carrier Gas on Golay Plot[41]

Conditions: n-heptadecane at 175 °C on a 25 m x 0.25 mm, OV-101 0.4 µm d_f column

The use of hydrogen as a carrier provides a faster analysis with almost equivalent resolution because the optimum linear carrier gas velocity is higher due to the higher diffusivity of hydrogen. At the optimal flow rates of 12, 20, 35 cm/sec for nitrogen, helium and hydrogen respectively, the analysis times would be 35/12, to 35/20 to 1 for nitrogen, helium and hydrogen respectively. Also, the slope of the Golay curve past the minimum is much shallower for hydrogen, which makes it less important to work at the optimum linear gas velocity to maintain a high efficiency. For example, using hydrogen at an average linear carrier gas velocity of 80 cm/sec would be 17 times faster than using

helium at its optimum average linear carrier gas velocity (20 cm/sec) with a 25% loss in efficiency. Consequently, a higher flow rate can be used for hydrogen than for helium or nitrogen, while maintaining the same plate height. The use of hydrogen is more prevalent in Europe than in the United States due to the higher cost of helium in Europe as well as the greater safety concerns about hydrogen in the United States. Nitrogen has a slightly higher efficiency at the optimal average linear gas velocity, but the price of the higher efficiency is a slow linear gas velocity and a steep curve past the minimum, which makes it important to work at the minimum, so there is no loss in efficiency. Helium is the carrier gas of choice for most chromatographers. For fast GC, hydrogen is only recommended if the analysis is isothermal.

Internal Diameter

The reduction of the internal diameter is reported to be a good means of reducing the analysis time while still maintaining resolution. An equation that relates retention time and the internal diameter of the column is shown below for columns with internal diameters of less than 0.1 mm and thin films.[21]

$$t_R = 16R^2\left(\frac{a}{a-1}\right)^2 \frac{(1+k)^3}{k^2}\frac{d_c}{\bar{m}} \qquad (12)$$

t_R = retention time, s

R = resolution, dimensionless

a = selectivity, dimensionless

k = retention factor, dimensionless

d_c = column diameter, cm

$\bar{m}$ = average linear carrier gas velocity, cm/s

Eq. 12 says that the analysis time is proportional to the internal diameter, provided all other factors remain constant. The smaller the i.d., the lower the minimum plate height and the shallower the curve. This means that a smaller i.d. column will be more efficient and it is possible to work at higher linear carrier gas velocities with less loss in efficiency.

There are two problems with the smaller the i.d., the large pressure drops across the column and the decreased sample capacity.

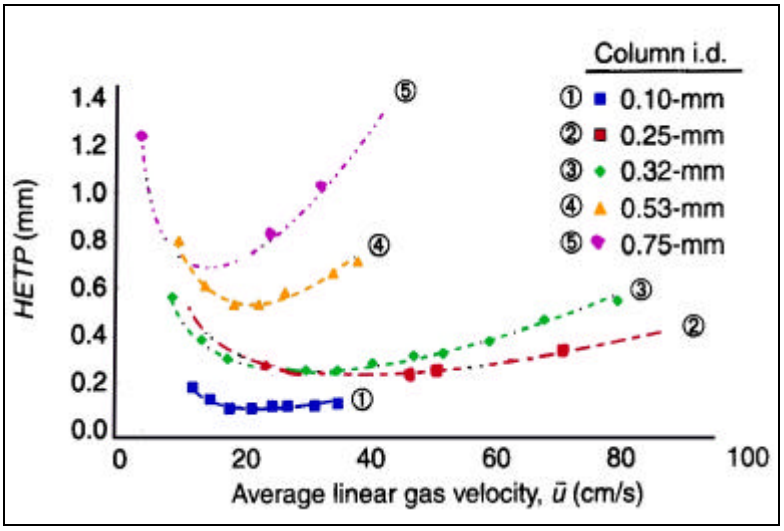

Figure 14. Effect of Internal Diameter on the Golay Plot[42]

Conditions: n-decane, helium carrier gas, see Table 3 for remainder of conditions

Figure 14 shows the effect of the column i.d. on the Golay plot.[42] Unfortunately, these plots were obtained under non-equivalent conditions. The film thicknesses were not equivalent (Table 3). The film was thicker on the larger i.d. columns and thinner on the small i.d. columns. If the film thickness were reduced on the larger i.d. columns, the plate height would be reduced from what is seen in Figure 14. However, the contribution of the film thickness, in general, to the total plate height has been reported to be less than 1%.[43]

Table 3. Conditions for Figure 14[42]

i.d., mm	L, m	d_f, μm	β	T_c, °C	k for C11	$\bar{m}_{opt}$, cm/s
0.10	25	0.09	278	110	1.63	20.0
0.25	25	0.25	250	110	1.81	38.5
0.32	25	0.26	308	110	1.47	30.2
0.53	25	5.5	24.1	130	9.69	15.0
0.75	30	1.03	170.5	130	1.28	20.5

In 1962, Desty[44] was the first to show that one effect of reducing the internal diameter was a decrease in the retention time. Gaspar[45] also demonstrated the effects of small internal diameters in 1977. A fluidic logic injection system was used to make it possible to rapidly switch gas flows and inject narrow bands of analyte. In Figure 15, a fast chromatogram of 13 hydrocarbons is shown[46]. The separation takes place on a 3 m x 0.030 mm i.d. column with a 0.06 μm film thickness of SE-30. There are three contributing factors to the fast analysis, a short column, a very small internal diameter, (which necessitated a high inlet pressure), and a thin film. The analysis was performed in 18 s. at 25 °C.

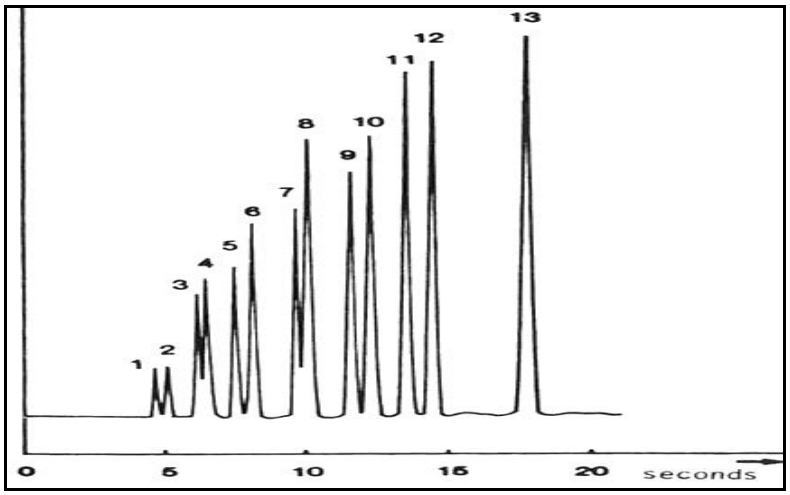

Figure 15. Fast Separation of Hydrocarbons on a Narrow Bore Column[46]

Conditions: 3 m x 0.03 mm i.d., 0.06 μm d_f, stationary phase – SE-30, 25 °C, fluidic logic injector

In 1986, Schutjes,[47] *et al.* developed a mathematical relationship between the inner diameter of a capillary column and the retention time of an analyte. It was shown that in an isothermal analysis the retention time is proportional to the column internal diameter. For temperature programmed GC at low pressure drops, retention time is proportional to the internal diameter squared and at high pressure drops retention time is proportional to the internal diameter. The data leading to the discovery of these relationships was collected using 30 and 50 μm internal diameter columns. Onuska[48] described the effects of the internal diameter reduction on the analysis of environmental toxicants. The focus in his study was on the actual preparation of the capillary column and not the analysis.

The reduction in the internal diameter with equivalent film thickness results in a reduced sample capacity of the capillary columns. This reduced sample capacity leads to higher detection limits, which creates a problem when doing trace analysis by fast GC. Splitless and on-column injection techniques help to increase the mass of sample injected onto the column. [49] An injection port liner with a smaller internal diameter (faster linear gas velocity at equivalent flow rates) decreased the splitless times as well. This allowed for a faster analysis with lower detection limits. Also, they found that the on-column injection required a pre-column in order to refocus the analytes. This increased the analysis time, but allowed for lower detection limits.

A result of internal diameter reduction is the increased pressure drop, which may create the need for specialized high pressure instrumentation. The reduction of the capillary column i.d. will reduce the analysis time; however, it will also increase the pressure drop across the column, which will be addressed in more detail in Chapter 3.

Turbulent Flow, Packed Columns and Specialty Columns

Turbulent flows, packed columns, and specialty columns are three additional means of doing fast GC. As was discussed earlier, turbulent flow requires specialized instrumentation for very high pressures without a significant gain in speed. Short packed columns for fast GC have also been investigated,[50,51] however they have not grown in use due to lack of availability and the difficulty in making them. Packed columns also

generate large pressure drops across the column. A multicapillary column was developed that consisted of over 900 capillaries bound together to make one column. van Deursen[52] *et al.* described the theory behind the multicapillary column and the constraints on its use for fast GC. Any variations in any of the 900 capillaries in terms of film thickness, internal diameter or length causes band broadening and diminishes any gains from the higher sample capacity, characteristics of the multicapillary column. Pressure tunable columns[53,54] have been investigated as a means of changing the selectivity of the columns. Two columns of different polarity are connected in series and a variable restrictor is placed at their junction so that the pressure can be adjusted. This pressure adjustment allows for more or less contribution from each column to control the selectivity, α, of the system. This method has shown promising results; however, it requires specialized instrumentation.

Sample preparation is also a part of fast GC and becomes an issue when fast analyses are performed routinely. A common issue raised when discussing fast GC is that the sample preparation is so time consuming that reducing the analysis time does not significantly effect the overall analysis time. As can be seen in Figure 16, sample preparation occupies 61% of the time a sample is handled. This study[55] was published in 1991 so we may expect some changes in the numbers; however, sample processing remains a significant portion of the handling time.

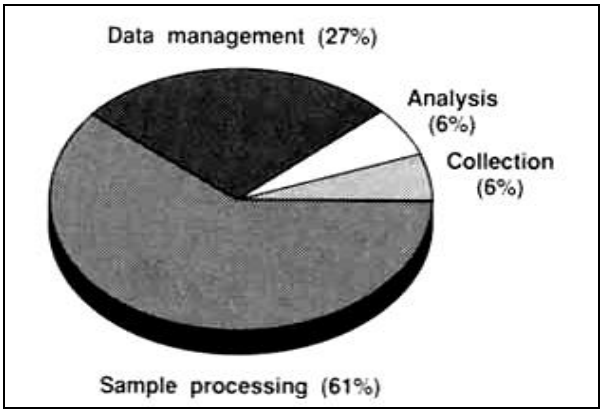

Figure 16. Handling Time of a Sample[55]

In the past the research on fast GC has been done mostly by academic researchers to demonstrate what was possible and was not necessarily what was practical. Now industry is demanding faster analysis times, and the instrumentation for fast GC is moving into the realm where it can be used routinely. The chromatography for fast GC is slowly being developed as the demand increases. Attention should now be focused on faster sample preparation methods. This is being done with solid phase extraction (SPE), solid phase micro-extraction (SPME), accelerated solvent extraction (ASE), supercritical fluid extraction (SFE) and other methods on the horizon. Several researchers who have reduced the sample preparation time include Current and Borgerding[56], Gorecki and Pawliszyn[57,58] and Leonard *et al.*[59] Current and Borgerding designed a high speed extraction system using a spray chamber. Volatile organic compounds were extracted from water and an injection was made every 45 seconds. Gorecki and Pawliszyn designed an injection system based on solid-phase microextraction(SPME). The analyte was desorbed rapidly from the fiber, but a two-minute exposure time was required to extract the analyte from the headspace of samples. Leonard *et al.* purged their samples and cryofocused them in the column. Extraction times of 20 seconds were shown, but the method was not shown to be repetitive.

At PittCon 1999, (Orlando, FL), fast GC was a popular topic. There were at least three symposia dedicated to fast GC. Interest in the theory and practice of fast GC is on the rise.

Chapter 3 – Theoretical Studies of Fast GC

Introduction

In 1979, Dandeneau[60] introduced fused silica columns, which made the WCOT columns more flexible, more reliable and easier to work with. Prior to this capillary columns were made of glass or stainless steel. Today most GC analyses are done using open tubular columns and not the original packed columns. At the Amsterdam[61] symposium in 1958, Golay introduced the WCOT columns as well as the theoretical description of the columns performance. The height equivalent to a theoretical plate height (HETP) model he presented was a modified version of the van Deemter equation. The van Deemter equation described the packed columns and the Golay equation modified the van Deemter equation to fit the new WCOT columns.

The van Deemter equation for packed columns is

$$H = A + B / \bar{m} + C * \bar{m} \qquad (13)$$

H = plate height, cm

A = eddy diffusion term, cm

B = molecular diffusion term, s/cm^2

$\bar{m}$ = average linear carrier gas velocity, cm/s

C = resistance to mass transfer term, s/cm^2

The van Deemter equation in its expanded form is shown in eq. 14.[62]

$$H = 2ld_p + \frac{2gD_g}{\bar{m}} + \left(\frac{8}{p^2} * \frac{k}{(k+1)^2} * \frac{d_f^2}{D_l} \right) * \bar{m} + \frac{wd_p^2 \bar{m}}{D_g} \qquad (14)$$

l = packing factor

d_p = particle diameter, cm

g = tortuosity factor

D_g = Einstein diffusion coefficient of the analyte in the mobile phase, cm^2/s

k = retention factor or capacity factor, dimensionless

d_f = film thickness, cm

D_l = diffusion coefficient of the analyte in the stationary phase, cm^2/s

w = obstruction factor for packed beds

d_p = particle diameter, cm

The A term describing the eddy diffusion through the packing material in the van Deemter equation was also no longer needed in the Golay equation for the open tubular columns. The tortuosity factor in the molecular diffusion term was no longer needed in the Golay equation. The particle diameter and the obstruction factor in the mass transfer term were also no longer needed. The mass transfer term was changed to fit open tubular columns in the Golay equation.

Golay Equation

The simplified Golay equation as we know it today is shown in eq. 15.

$$H = \frac{B}{\bar{m}} + C_m \bar{m} + C_L \bar{m} \tag{15}$$

C_m = resistance to mass transfer in the mobile phase, s/cm^2

C_L = resistance to mass transfer in the stationary phase, s/cm^2

All other terms are as previously defined following eq. 13.

The expanded version of the Golay equation is shown in eq. 16.[63]

$$H = \frac{2D_M}{\bar{m}} + \frac{(1+6k+11k^2)r_c^2\bar{m}}{24(1+k)^2 D_M} + \frac{2kd_f^2\bar{m}}{3(1+k)^2 D_s} \tag{16}$$

r_c = radius of the column, cm

D_m and D_s are equivalent to D_g and D_l respectively

All other terms are as previously defined following eq. 14.

The parameters in the Golay equation that are solely column dependent are the radius and the film thickness. By reducing each of these terms, the plate height, *H*, will be reduced, thereby generating greater efficiency. The average linear carrier gas velocity can also be changed to decrease *H* as much as possible.

When the rate equation,[64] (H vs. $\overline{m}$) is plotted, the curve goes through a minimum. A Golay plot, H vs. $\overline{m}$, is shown in Figure 17.[65] Both the original van Deemter and the Golay equations are asymmetric hyperbola equations with a minimum at $\sqrt{B/C}$. The minimum is at the optimum linear velocity. This velocity provides the smallest plate height and consequently, the largest efficiency. The contributions from the B term and the combination of the C terms ($C = C_m + C_L$) present in eq. 15 and eq. 16 are illustrated in the graph. At low linear velocities, B is the dominant term and at high linear velocities, C is the dominant term. The maximum efficiency is obtained when working at $\overline{m}_{\text{opt.}}$ Most work is done at higher than optimum linear gas velocities and some resolution is sacrificed to decrease the total analysis time. In fast GC the linear gas velocity is almost always set well above the optimum.

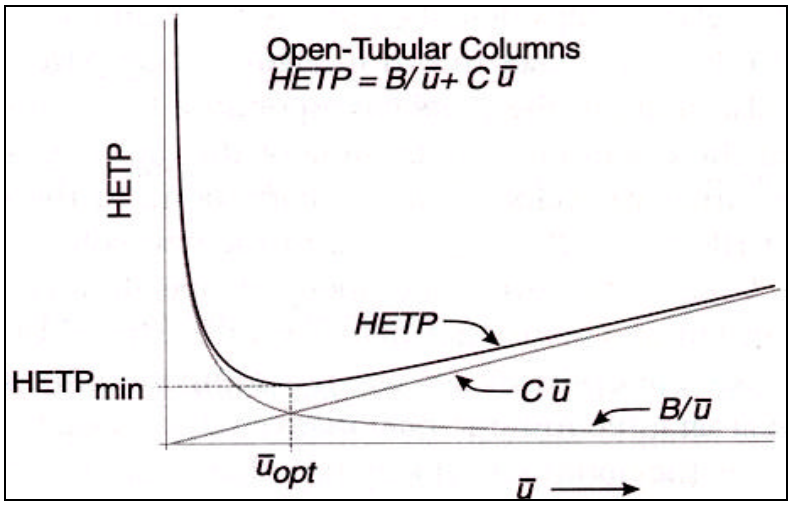

Figure 17. Golay Plot

The column radius and the film thickness are important parameters when doing fast GC. Decreasing the radius[66] and the film thickness[67] decrease the analysis time. (Recall eq. 6 and eq. 9). When the radius is decreased the pressure drop across the column increases. The pressure drop and the radius do not vary linearly, but they are related in a manner described by eq. 17.[68]

$$\Delta p * j' = \frac{8L * h * \bar{m}}{r_c^2} \qquad (17)$$

Dp = pressure drop across the column, psi

j' = pressure correction factor of Halasz, dimensionless

L = length of the column, cm

h = viscosity of the carrier gas, cP

$\bar{m}$ = average linear carrier gas velocity, cm/s

r_c = radius of the column, cm

The smaller the internal diameter the larger the pressure drop across the column. See Table 4.[69]

Table 4. Effect of Internal Diameter on Pressure Drop(psi)*

$\bar{m}$ **, cm/sec**	**0.10 mm**	**0.20 mm**	**0.25 mm**	**0.32 mm**	**0.53 mm**
20	52.8	13.2	8.5	5.2	1.9
30	79.2	19.8	12.7	7.7	2.8
40	106	26.4	16.9	10.3	3.8
50	123	33.0	21.1	12.9	4.7
60	158	39.6	25.3	15.5	5.6
70	185	46.2	29.6	18.1	6.6
80	211	52.8	33.8	20.6	7.5

*Assumes 25 m column, 100 °C, Helium carrier gas

This table shows the effects of the internal diameter on the pressure required to achieve various velocities. A 0.53 mm i.d. column requires only 7.5 psi to achieve a velocity of 80 cm/sec, but simply by reducing the i.d. to 0.10 mm a pressure of 211 psi is required to achieve the same velocity. These high pressures are impossible to generate with currently available instrumentation.

The affect of the pressure drop on the plate height is not taken into account in the Golay equation. Several years after Golay introduced his equation, Giddings modified the Golay equation, taking into consideration the compressibility of the mobile phase, as shown in eq. 18.[70]

$$\hat{h} = f \bullet \left(\frac{2D_m}{m_o} + \frac{\left(11 + 6k + 11k^2\right) d_c^2 m_o}{96(1+k)^2 D_m} \right) + \frac{2d_s^2 \overline{m}}{3(1+k)^2 D_s} \qquad (18)$$

All the terms in eq. 18 are the same as in eq. 14 and eq. 16 except *f*, which is the Giddings compressibility factor. *f* is a function of the outlet pressure, p_o and the inlet pressure, p_i. Even from this equation, it is not known how to optimize a column for the maximum efficiency under the high pressure drop conditions that are often used in fast GC.[71]

From 1997 to 1999 a series of papers were published by Blumberg[71,72,73,74] describing the effect of the pressure drop across a capillary column especially as it applies to fast GC, from a purely theoretical perspective. All other previous expressions of the rate equation expressed the plate height as a function of more than two pneumatic variables, $\overline{m}$ and μ_o.[71] Only two pneumatic parameters can be "mutually independent".[71] The Blumberg expression of the plate height was derived using only the average linear carrier gas velocity and the outlet velocity. An equation similar to the Golay equation was generated that is valid for all pressure drops. This equation simplifies to the Golay equation at low pressure drops assuming ideal carrier gas behavior and circular tubes as the columns. For high pressure drops, this new equation converges to eq. 19. The new equation will be called the Blumberg Equation. The Blumberg equation, valid for high pressure drops, is shown in equation 19.

$$H = B/\overline{m}^2 + C_1\overline{m}^2 + C_2\overline{m} \qquad (19)$$

H = height equivalent to a theoretical plate, cm

B = new molecular diffusion term, s/cm^2

C_1 = new resistance to mass transfer in the mobile phase term, s/cm^2

C_2 = resistance to mass transfer in the stationary phase term, s/cm^2

$\bar{m}$ = average linear carrier gas velocity, cm/s

The expanded form of eq. 19 is shown in eq. 20.

$$H = \frac{81 d_c^2 D_M p_o}{1024 h L} + \frac{G_1^2 L h}{D_M p_o} + \frac{2 k d_s^2}{3(1+k)^2 D_S} \tag{20}$$

where

$$G_1 = \left(\frac{1 + 6k + 11k^2}{3(1+k)^2} \right)^{1/2} \tag{21}$$

D_m = diffusion of the analyte in the mobile phase, cm^2/s

d_c = column diameter, cm

p_o = column outlet pressure, psi

L = length of the column, cm

h = viscosity of the carrier gas, cP

k = retention factor or capacity factor, dimensionless

d_s = stationary film thickness, cm

D_S = diffusion of the analyte in the stationary phase, cm^2/s

A comparison of the Golay equation and the Blumberg equation is given in Table 5. The table lists each of the terms from eq. 15 and eq. 19 in their expanded format to enable a comparison between the two equations.

Table 5. Comparison of Terms

	Golay Equation		Blumberg Equation	
Molecular Diffusion	$B/\bar{m}$	$2D_m$	$B/\bar{m}^2$	$\frac{81 d_c^2 D_m p_o}{1024 L h}$
Diffusion in Mobile Phase	$C_m * \bar{m}$	$\frac{r^2(1+6k+11k^2)}{24 D_g (1+k)^2}$	$C_1 * \bar{m}^2$	$\frac{Lh(1+6k+11k^2)}{D_m p_o 3(1+k)^2}$
Diffusion in Stationary Phase	$C_s * \bar{m}$	$\frac{2kd_f^2}{3(1+k)^2 D_l}$	$C_2 * \bar{m}$	$\frac{2kd_f^2}{3(1+k)^2 D_l}$

The differences between the two equations lie in the molecular diffusion term and the mass transfer in the mobile phase term. The differences in the molecular diffusion terms are coupled with the column i.d., the diffusion in the mobile phase, the outlet pressure, the column length, and the viscosity of the carrier gas. In addition there is a difference in the constants present in the Blumberg equation that are not in the Golay equation. The differences in the mass transfer in the mobile phase terms are coupled with the length of the column, the viscosity of the carrier gas, the outlet pressure and a new constant in the Blumberg equation, as well as the absence of a column radius term. The C_g term is also multiplied by $\bar{m}^2$ instead of simply $\bar{m}$.

There is no difference in the mass transfer in the stationary phase terms, C_s and C_2. From this comparison, it is seen that at high pressure drops the column length, the carrier gas viscosity and the average linear gas velocity play a larger role.

The reason for a modification of the Golay equation is that, according to Blumberg, no one has adequately taken into consideration the effect of high pressure drops across the column. The following series of equations is a partial derivation of the Blumberg equation.[71] Eq. 22 is the modified Golay equation valid for all pressure drops. This equation contains variables μ_o, $\bar{m}$, and $D_{m,}$ which either represent pneumatic conditions of the carrier gas or are functions of the pneumatic conditions. The two other

equations are used to describe more thoroughly the effects of the pneumatics of the system.

$$\hat{h} = f(P) \bullet \left(\frac{b}{m_o} + c_1 m_o \right) + c_2 \bar{m} \tag{22}$$

$$m_o = r\left(p_o, \bar{m}\right) \tag{23}$$

$$P = q\left(p_o, \bar{m}\right) \tag{24}$$

The b, c_1 and c_2 parameters are from the Golay equation. These terms were defined in eq. 16. The other terms are defined below.

$$f = f(P) = \frac{9\left(P^2+1\right)(P+1)^2}{8\left(P^2+P+1\right)^2} \tag{25}$$

where

$$P = \frac{p_i}{p_o} \tag{26}$$

p_i = pressure at the column inlet, psi

p_o = pressure at the column outlet, psi

From these definitions and equations, Blumberg derived the following equation to describe the plate height for an arbitrary pressure drop and film thickness.

$$\hat{h}\left(\bar{m}\right) = f\left(q\left(p_o, \bar{m}\right)\right) \bullet \left(\frac{b}{r\left(p_o, \bar{m}\right)} \right) + c_1 \bullet r\left(p_o, \bar{m}\right) + c_2 \bar{m} \tag{27}$$

The complexity of this equation for an arbitrary pressure drop comes from the transition from the low pressure region to the high pressure region. The simplification for the high pressure region arises because at high pressure drops, the outlet gas velocity, μ_o, becomes proportional to $\bar{m}^2$.[71] Several other conclusions[71] are drawn from a more detailed look at this equation.

1. The average linear carrier gas velocity needed to achieve the minimum plate height, $\bar{m}\min_H$, for a thin film column at high pressure drops, is inversely

proportional to the square root of the column plate capacity, $(N_c)^{½}$, regardless of the column diameter and the column length.

$$N_c = L/d_c \quad (28)$$

N_c = column plate capacity

L = length of the column

d_c = column diameter

2. The optimum average linear carrier gas velocity to achieve the minimum plate height, $\bar{m}\min_H$, of a thin film column under high pressure drops is proportional to the square root of the column temperature, $(T_c)^{1/2,}$ whereas for the low pressure drop it is proportional to $(T_c)^{1.75}$.

3. A column with a given i.d. and film thickness can act as a thick film column when it is short and as a thin film column when it is long and is under high pressure drops. When this happens due to the film thickness, the plate height of a long column can be substantially smaller than the shorter column even if both have the same i.d. and film thickness. The contribution of the film thickness to H diminishes with an increase in column length.

The second paper[72] by Blumberg discussing the theory of fast GC determines what can be done with a given column and carrier gas, while assuming that the improvement in the speed of analysis is obtained by maintaining a minimum resolution and consequently, a minimum efficiency. Scott and Hazeldean[24] found that a further reduction in retention time was possible if simultaneously, the gas velocity, $\bar{m}$, was increased as well as the column length. This allows for recovery of the lost efficiency and the new analysis time will be 5/8 of that corresponding to the efficiency-optimized velocity. However, they did not take into account the compressibility of the carrier gas in their study.

The Purnell criterion[75] states that the optimum speed of analysis corresponds to a minimum in the ratio of $H/\bar{m}$. His work also does not account for the compressibility of the carrier gas and leads to infinite gas velocity at the minimum in $H/\bar{m}$. Gaspar[14] applied the Purnell criterion to low pressure systems where the net efficiency is limited

by the instrumental contributions to the peak broadening and added an additional instrumental term to the Golay equation. However according to Blumberg, the increase in gas velocity has a more fundamental implication. Cramers, *et al.*[76,77] studied the Purnell criterion in conjunction with an arbitrary pressure drop. They stated that the lack of knowing the expression for the plate height as a direct function of $\overline{m}$ was the main barrier for the derivation of conclusive results. Recent computer software developments for symbolic manipulations of mathematical expressions help derive the Blumberg equation.

The conclusions in a more applicable way that were drawn by Blumberg in his papers are listed here.

1. There is a much larger role of the column length at high pressure conditions than at low pressure conditions. Column length affects the overall efficiency curve and also affects the value of the optimum linear carrier gas velocity. For thick film columns the length affects the contribution of the stationary phase to the overall efficiency plot.[71] Neither the original van Deemter nor the Golay equations discuss column length.
2. The speed of analysis in a speed optimized column can be 10% to 30% higher than the efficiency optimized column. If the gas velocity is higher than its speed-optimized value a substantial increase in the speed of analysis without loss of column efficiency can be achieved by cutting the column length and optimizing these conditions.[72]
3. H can be expressed in terms of the flow rate, F. A simplified expression of the speed optimized flow rate was found. At high pressure drops, the speed optimized flow rate is independent of the pressure drop, the length and the film thickness. The speed optimized flow (SOF) rate is described by eq. 29:

$$SOF = SOF_{100um} * 0.01 * d_c(\text{in } \mu m) \qquad (29)$$

where the $SOF_{100\mu m}$ is the speed optimized flow rate for a 100 μm i.d. column. For hydrogen the $SOF_{100\mu m}$ value is 1, helium is 0.8 and nitrogen is 0.25. These values are valid for any temperature.[73]

4.[74] The stationary phase thickness does not effect the column efficiency except when the column is both short and has a thick film, which means low pressure drops and the solutes have a retention factor of 0.3-0.4.

The previous paragraphs described the conclusions reached mathematically by Blumberg. The intent of the work in this chapter is to collect experimental data to determine the validity of the new theory.

Experimental

Data was obtained at pressures ranging from 15 psi to 150 psi for various columns. These columns included a: HP-5, 9 m x 0.1 mm, 0.17 μm d_f column; a HP-5, 9 m x 0.1 mm, 0.34 μm d_f column; a HP-5, 52 m x 0.2 mm, 0.33 μm d_f column; a HP-5, 13 m x 0.2 mm , 0.33 μm d_f column; and a PE-1, 9 m x 0.05 mm, 0.05 μm d_f column. The analyte used was 1.5 ppm solution of tridecane in hexane or a 0.1 % (v/v) solution of decane in hexane. Three injections were done at each condition so that an average and standard deviation could be determined. The peak areas and peak heights were tabulated and the standard deviation of the peak was calculated. The standard deviation of a peak is defined in eq. 30.

$$s = \frac{A}{H * 2.507} \tag{30}$$

A = area of a peak, pA*s

H = height of a peak, pA

The other two equations used in the determination of the plate height, H, are shown in eq. 31 and eq. 32.

$$N = \left(\frac{t_R}{s}\right)^2 \tag{31}$$

$$H = \frac{L}{N} \tag{32}$$

N = plate number or efficiency, dimensionless

t_R = retention time in minutes

s = standard deviation of the peak in minutes

H = plate height, mm

L = length of the column in mm

The hold-up time or t_o was calculated by injecting tap gas with the autosampler. $\bar{m}$ was calculated from eq. 33.

$$\bar{m} = L/t_o \quad (33)$$

$\bar{m}$ = average linear gas velocity, cm/s

L = column length, cm

t_o = hold-up time, s

From the plate height values and the average linear carrier gas velocities, a rate equation, H vs. $\bar{m}$ graph was prepared. The data points in the graph were fit with the Blumberg equation and the Golay equation using Kaleida Graph.[78] The GC conditions used to collect the data are listed in Table 6.

Table 6. GC Conditions

Parameter	Condition
Injector Temperature	250 °C
Carrier Gas	Helium
Oven Temperature	100 °C, 125 °C or 150 °C
Detector	Flame Ionization Detector
Detector Sampling Rate	100 Hz
Detector Temperature	300 °C

Results

First to be established was the reliability of the Pearson Correlation coefficient, R^2. This was done using two columns of different film thicknesses, 0.17 μm d_f and 0.34 μm d_f HP-5 with the same length, 1 m and the same internal diameter, 0.1 mm. These columns have low pressure drops so that the Golay equation should describe the data that is obtained from these columns. The data was obtained and fitted first with the Golay equation and then the Blumberg equation. The four graphs for these two capillary columns are shown in Figure 18 through Figure 21. The coefficient of determination, R^2, was calculated for each plot. The R^2 value describes the correlation between the line and the model, a value of 1.00 being a perfect fit.

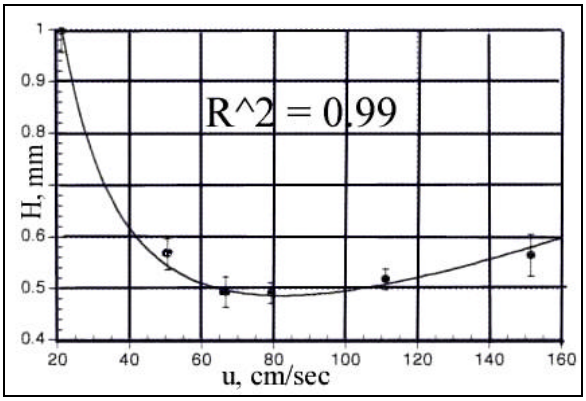

Figure 18. 1 m x 0.1 mm, 0.17 µm, Golay Fit

$H(\bar{m}) = 3.9(0.2)/\bar{m} + 0.002(8e\text{-}5) * \bar{m}$

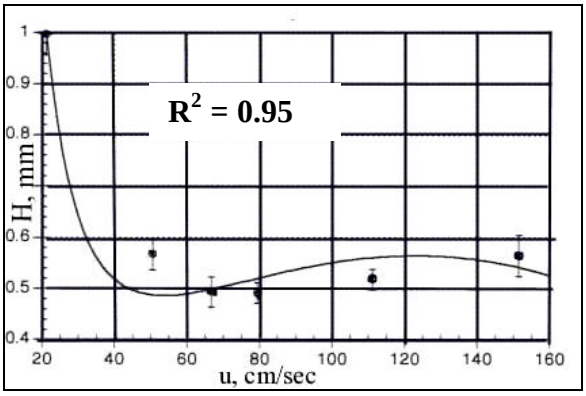

Figure 19. 1 m x 0.1 mm, 0.17 µm, Blumberg Fit

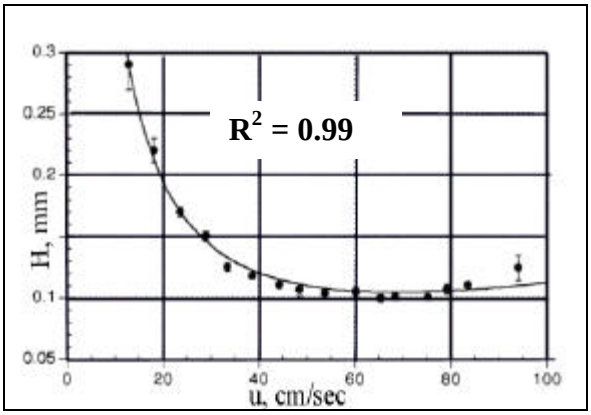

Figure 20. 1 m x 0.1 mm, 0.34 μm, Golay Fit

$H(\bar{m}) = 3.6(0.06)/\bar{m} + 8e\text{-}4(3e\text{-}5) * \bar{m}$

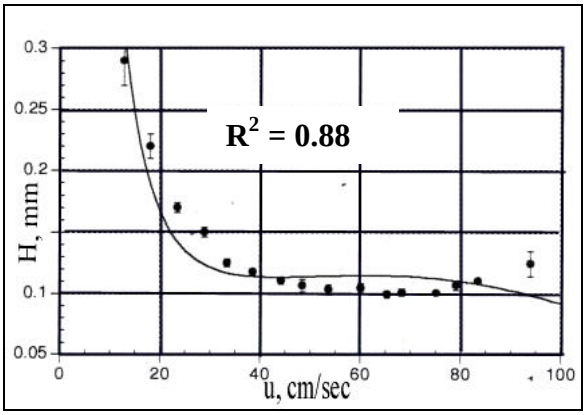

Figure 21. 1 m x 0.1 mm, 0.34 μm, Blumberg Fit

It can be seen from these graphs and the corresponding R^2 values that Golay equation fits well as is expected and the Blumberg equation does not fit as well, which is also mathematically predicted.

Next longer columns were tested. Data was collected over the range of pressures and once again fitted with both the Golay equation and the Blumberg equation. These graphs are shown in Figure 22 through Figure 25. Once again, each data point is an average of three runs with the corresponding error bars.

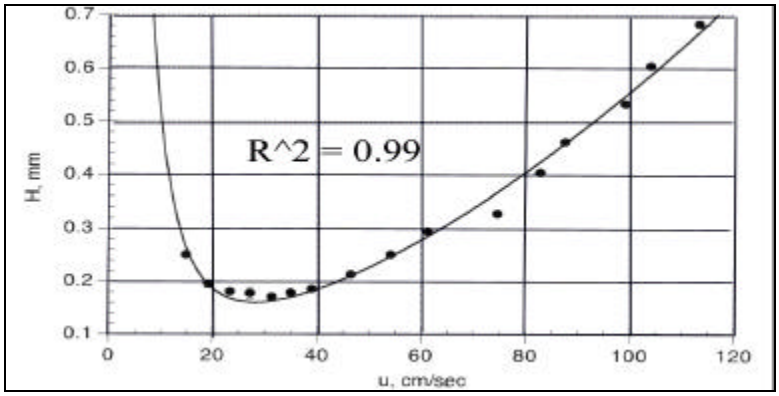

Figure 22. Blumberg Fit of 9 m x 0.1 mm, 0.17 μm d_f Column

$H(\bar{m}) = 49(4)/\bar{m}^2 + 3e\text{-}5(4e\text{-}6) * \bar{m}^2 + 3e\text{-}3(3e\text{-}4) * \bar{m}$

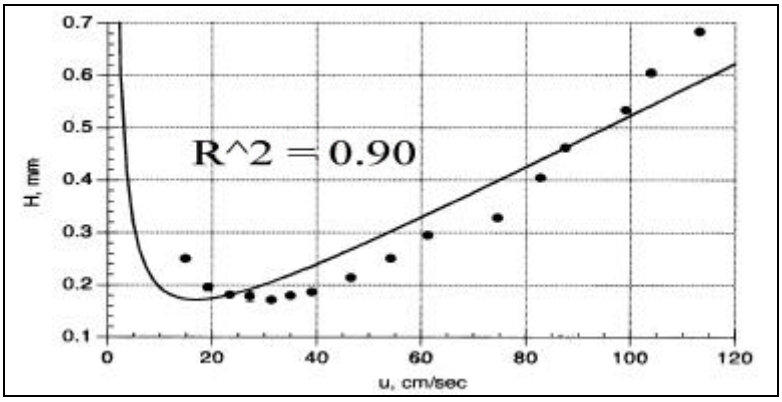

Figure 23. Golay Fit for 9 m x 0.1 mm, 0.17 μm d_f Column

For the first column the R^2 value is 0.99 for the Blumberg equation and 0.90 for the Golay equation. This indicates that the Blumberg equation is a slightly better fit than the Golay equation and mathematically describes more completely what is happening at the high pressure drops.

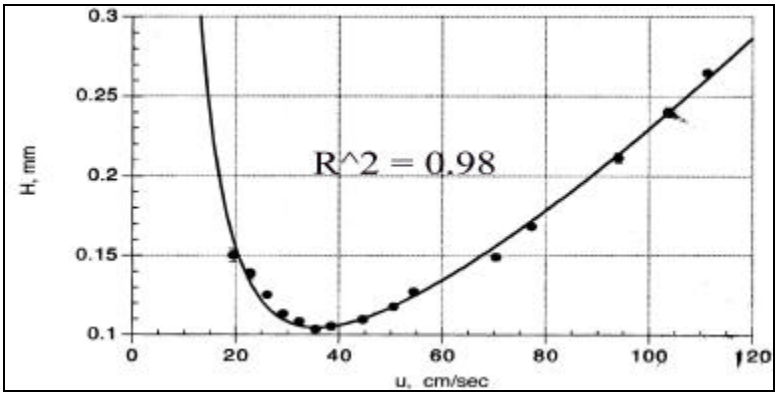

Figure 24. Blumberg Fit for 9 m x 0.1 mm, 0.34 μm d_f Column

$H(\bar{m}) = 45(2)/\bar{m}^2 + 6e\text{-}5(1e\text{-}5) * \bar{m}^2 + 3e\text{-}3(1e\text{-}4) * \bar{m}$

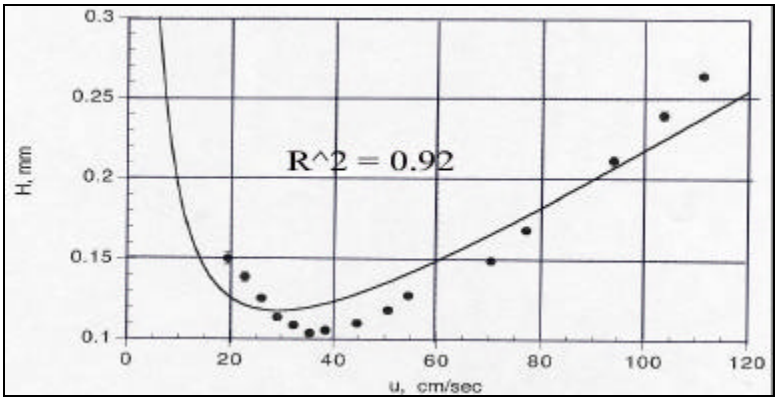

Figure 25. Golay Fit for 9 m x 0.1 mm, 0.34 μm d_f Column

For the second column the R^2 values range from 0.98 for the Blumberg equation to 0.92 for the Golay equation. Once again this would indicate that the Blumberg equation is a slightly better fit than the Golay equation. Table 7 is a summary of the R^2 values for the 0.1 mm columns.

Table 7. R^2 Values for 0.1 mm i.d. Columns

	Golay	Blumberg
9 m x 0.1 mm, 0.17 d_f	0.90	0.99
9 m x 0.1 mm, 0.34 d_f	0.92	0.98
1 m x 0.1 mm, 0.17 d_f	0.99	0.95
1 m x 0.1 mm, 0.34 d_f	0.99	0.88

The Blumberg model fits better than the Golay model, however, the important question is whether or not there is a statistically significant difference between the two fits. This was done by using form two of the t-test. The null hypothesis, H_o, is that there is no statistical difference between the R^2 values for the Golay fit and the Blumberg fit and the alternative hypothesis, H_1, was that there is a statistical difference between the fits. This was tested at the 95% confidence level using a two-tailed form two of the t-test.

Table 8. Statistical Analysis of 0.1 mm i.d. Columns

	t (calculated)	t (table)[79]	Conclusion
9 m x 0.1 mm, 0.17 d_f	22	2.78	$t_{calc} > t_{tab} \therefore$ reject $H_{o,}$ n = 6
9 m x 0.1 mm, 0.34 d_f	13	2.78	$t_{calc} > t_{tab} \therefore$ reject $H_{o,}$ n = 6

The conclusion from the statistical analysis is that there is a statistical difference between the R^2 values of the Golay and the Blumberg fits to the data points.

The data just shown was for 0.1 mm i.d. columns. The data shown in the next figures is from 0.2 mm i.d. columns of varying lengths. The effect of the length of the columns, which effects the pressure drop across the column, is demonstrated.

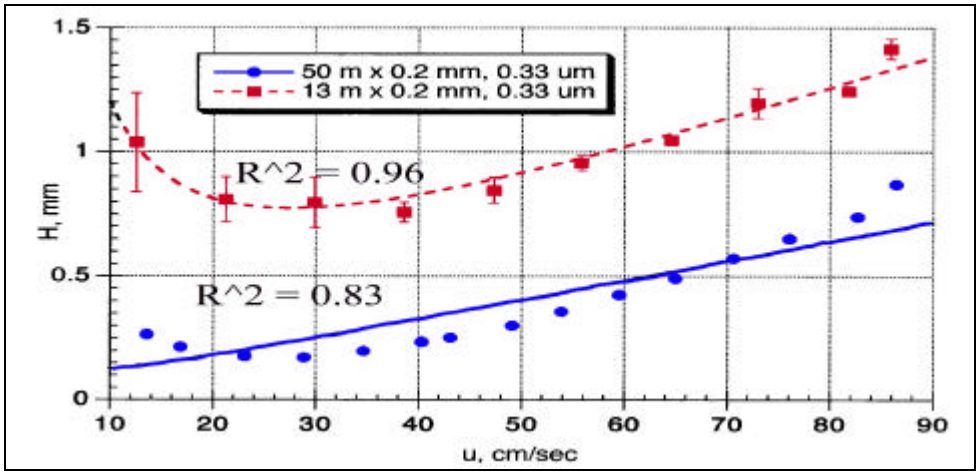

Figure 26. Golay Fit for 0.2 mm i.d. Columns (50 m and 13 m)

Conditions: 50 m x 0.2 mm i.d., 0.33 µm d_f, 13 m x 0.2 mm i.d., 0.33 µm d_f columns, 100 °C, helium carrier gas at 15 psi to 150 psi

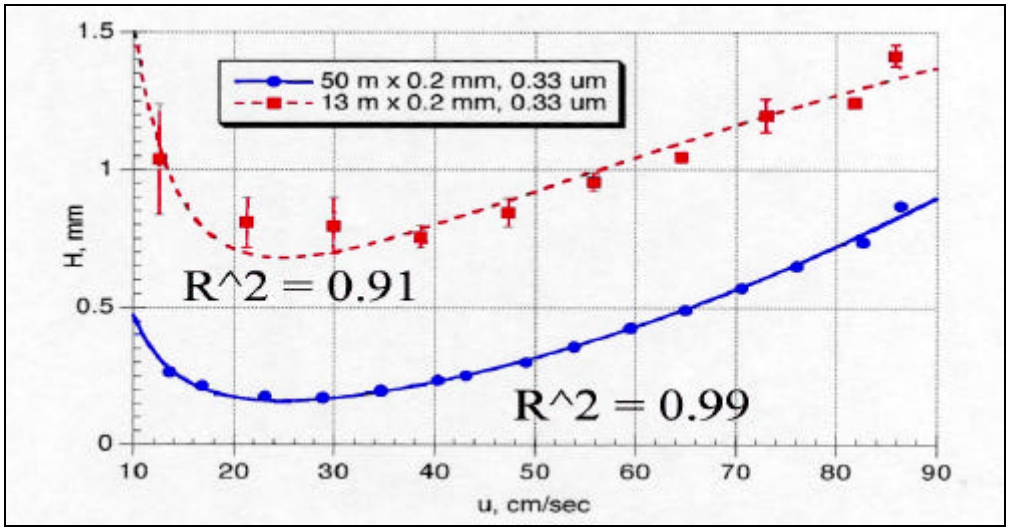

Figure 27. Blumberg Fit of 0.2 mm i.d. Columns (50 m and 13 m)

Conditions: 52 m x 0.2 mm i.d., 0.33 µm d_f, 13 m x 0.2 mm i.d., 0.33 µm d_f columns, 100 °C, helium carrier gas at 15 to 150 psi

In Figure 26 the data points for each of the columns is fit with the Golay equation. The R^2 value for the shorter column is 0.96, indicating a good fit and for the longer column it is 0.83, which indicates that the line does not fit the data points as well. The Blumberg equation, shown in Figure 27, fits the longer column with an R^2 value of 0.99, which is much better. The Blumberg equation also fits the shorter column with an R^2 value of

0.91, which is not poor, but it is worse than the Golay fit. Blumberg predicted that a long column with the same film thickness and i.d. under high pressure drop conditions, would behave like a short column with a thin film thickness and the short column would behave more like a column with a thick film. The experimental data shown in Figure 26 and Figure 27 support this. The longer column has a lower minimum plate height and the slope of the curve after the minimum is much shallower than for the shorter column.

Another difference mathematically predicted between the low pressure drop and the high pressure drop is the effect of the length of the column on the H vs. $\bar{m}$ curve. This is shown experimentally in Figure 28.

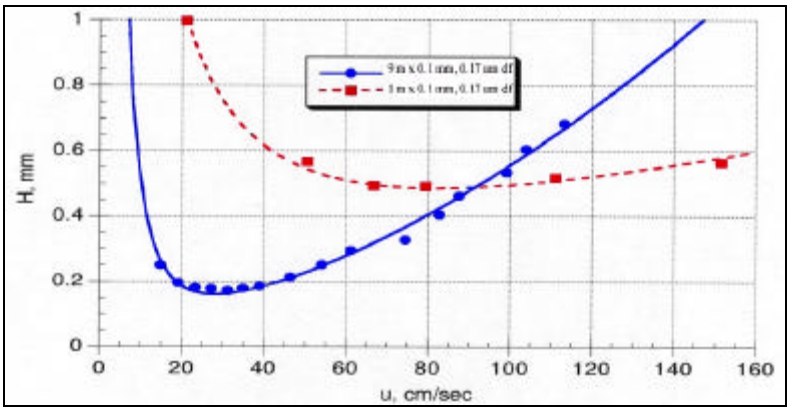

Figure 28. Effect of Length (9 m and 1 m)

Conditions: 9 m x 0.1 mm i.d., 0.17 µm d_f, 1 m x 0.1 mm i.d., 0.17 µm d_f, 100 °C, helium carrier gas at 15 to 150 psi, Golay fit for the 1 m column and Blumberg fit for the 9 m column

The minimum for the 9 m column is much sharper than the minimum for the 1 m column. This means that it is much more important to be working at the optimum linear velocity for a column operating under high pressure drops than a column operating under low pressure drops.

The optimum gas velocity, $\bar{m}\min_H$ of a thin film column under high pressure drops is proportional to $(T_c)^{1/2}$. Figure 29 is the Golay fit of the three temperature rate equation plots for the 52 m x 0.2 mm, 0.33 µm d_f column. In Figure 30 the Blumberg fit

for the H vs. $\bar{m}$ graph is shown for the 52 m x 0.2 mm, 0.33 µm d_f column at three temperatures. The temperatures chosen were 100 °C, 125 °C and 150 °C.

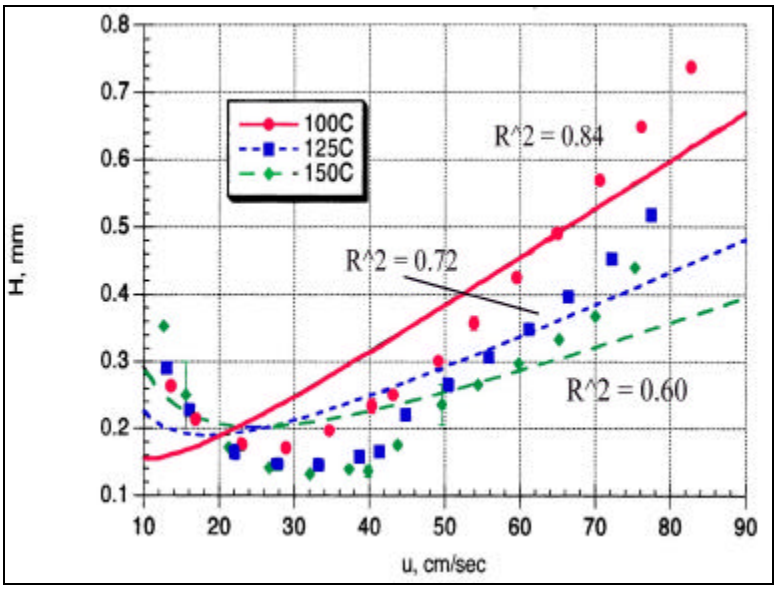

Figure 29. Effect of Temperature on Golay Plots

Conditions: 52 m x 0.2 mm i.d, 0.33 µm d_f, at 100 °C, 125 °C, 150 °C, head pressure – 15 to 150 psi

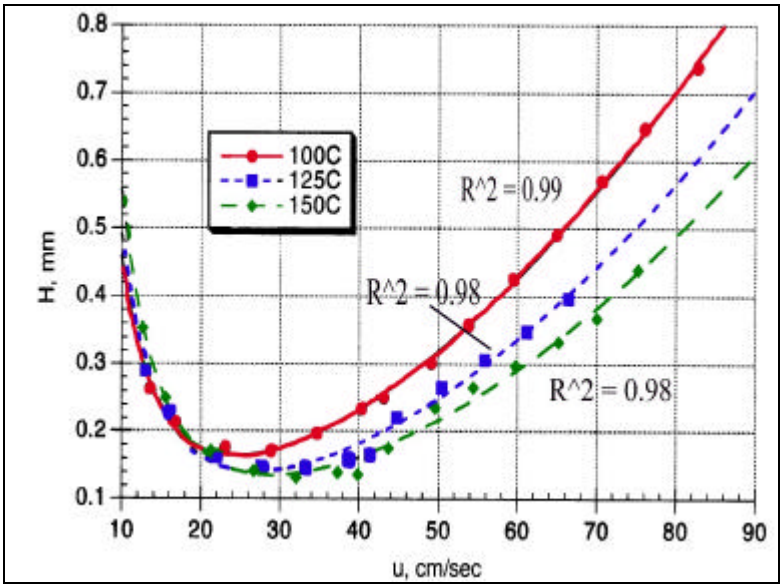

Figure 30. Effect of Temperature on Blumberg Plot

Conditions: 52 m x 0.2 mm i.d, 0.33 µm d_f, at 100 °C, 125 °C, 150 °C, helium carrier gas, 15 to 150 psi

$H(\overline{m})_{100\,°C} = 43(1)/\overline{m}^{2} + 9e\text{-}5(1e\text{-}6) * \overline{m}^{2} + 2e\text{-}3(2e\text{-}4) * \overline{m}$

$H(\overline{m})_{125\,°C} = 47(2)/\overline{m}^{2} + 8e\text{-}5(6e\text{-}6) * \overline{m}^{2} + 8e\text{-}4(4e\text{-}4) * \overline{m}$

$H(\overline{m})_{150\,°C} = 51(2)/\overline{m}^{2} + 7e\text{-}5(7e\text{-}6) * \overline{m}^{2} + 6e\text{-}4(4e\text{-}4) * \overline{m}$

The Golay plots shown in Figure 29 do not fit the data very well. It has been established earlier in this chapter that the Blumberg equation statistically fits the data from the high pressure drops better than the Golay equation. The minimum values for $\overline{m}$ were calculated to be 24 cm/sec, 27 cm/sec and 29 cm/sec for 100 °C, 125 °C and 150 °C respectively using the Blumberg equation. Recall that the optimum average linear gas velocity was predicted to be proportional to $T^{½}$. Using 24 cm/sec as the optimum for 100 °C and calculating the predicted temperatures for 125 °C and 150 °C leads to the following results (Table 9).

Table 9. Comparison of Predicted Temperatures vs. Actual Temperatures

Predicted Temperatures, °C	Actual Temperatures, °C	%Error
126	125	0.8
146	150	2

The errors between the predicted temperature and the actual temperature support the validity of the proposed Blumberg equation.

In the introduction it was mentioned that Giddings modified the Golay equation to account for the pressure drop across the column. This was necessary because the diffusion coefficient of the analyte in the gaseous mobile phase is inversely proportional to the pressure[80]. When the value of the diffusion coefficient is typically calculated the pressure is assumed to be atmospheric. This introduces error into the calculation. At low pressure drops, the error is small, but with increasing pressure drops, the error increases. The smaller i.d.s at the same lengths increase the pressure drop across the column. The effect of the pressure drop across the column on the velocity through the column is shown in Figure 31.[81]

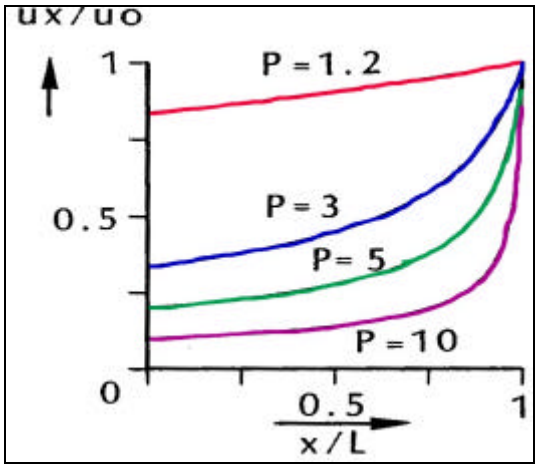

Figure 31. Carrier Gas Velocity Profile[81]

Figure 31 shows how the velocity (ux/uo) of the carrier gas through the column changes over the length of the column (x/L) depending on the pressure drop across the column. P is the ratio of the inlet pressure to the outlet pressure. At low pressure drops, the change is not very significant, but the higher the pressure drops, the larger the change in velocity over the length of the column. The equation that Giddings developed is shown in equation 18. We wanted to compare the fit of the Giddings equation to that of the Blumberg equation. To do this, it was necessary to plot H vs. μ_o instead of H vs. $\bar{m}$. μ_o is calculated with the eq. 34.[82]

$$m_o = \frac{\overline{m}}{j} \tag{34}$$

μ_o = the linear gas velocity at the outlet of the column, cm/s

$\overline{m}$ = average linear carrier gas velocity, cm/s

j = carrier gas compressibility correction factor described by James and Martin[83], dimensionless

j is calculated from eq. 35

$$j = \frac{3\left(P^2 - 1\right)}{2\left(P^3 - 1\right)} \tag{35}$$

where

$P = p_i/p_o$

p_i = pressure at the inlet, psi

p_o = pressure at the outlet, psi

j was calculated from eq. 35 and from those values, μ_o was calculated. Figure 32 is a plot of H vs. μ_o of the data obtained with the 52 m column at the three different temperatures tested. The data was fitted with the Giddings modified Golay equation.

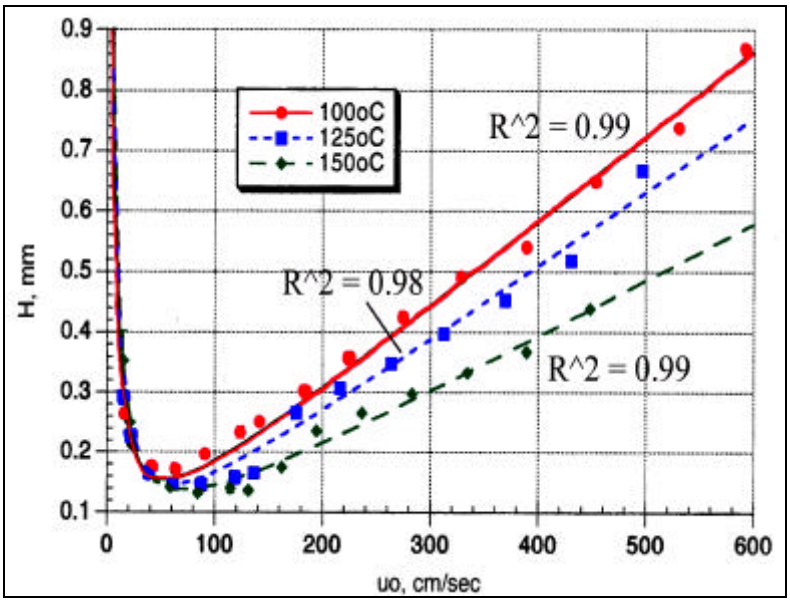

Figure 32. H vs. μ_o Plot

Conditions: 52 m x 0.2 mm i.d, 0.33 µm d_f, at 100 °C, 125 °C, 150 °C, head pressure – 15 to 150 psi

It can be seen in Figure 32 that the R^2 values for the Giddings modified equation fit to the H vs. μ_o data higher than the R^2 values for the Golay fit to the H vs. $\bar{m}$ data (Table 10).

Table 10. R^2 Values for Various HETP Plots

	Golay H vs. $\bar{m}$	**Blumberg H vs. $\bar{m}$**	**Giddings H vs. μ_o**	**Blumberg H vs. μ_o**
100 °C	0.84	0.99	0.99	0.97
125 °C	0.72	0.98	0.98	0.94
150 °C	0.60	0.98	0.99	0.91

Table 10 indicates that for the H vs. $\bar{m}$ plots, the Blumberg equation fits the data better than the Golay equation. The statistical analysis is shown in Table 11. Table 10 also indicates that the Giddings modified Golay equation fits the data better than the Blumberg equation for the H vs. μ_o plots. The statistical analysis is shown in Table 12. The H vs. $\bar{m}$ data was statistically evaluated using a two-tailed form two of the t-test at

the 95% confidence level. Again, H_o was that there is no statistical difference between the Blumberg and Golay fits and H_1 was that there is a statistical difference (Table 11).

Table 11. Statistical Analysis of the Temperature Effects (H vs. $\bar{m}$)

	t (calculated)	t (table)[79]	Conclusions
100 °C	39	2.78	$t_{calc} > t_{tab}$, $\therefore$ reject H_o, (n=6)
125 °C	88	2.78	$t_{calc} > t_{tab}$, $\therefore$ reject H_o, (n=6)
150 °C	13	2.78	$t_{calc} > t_{tab}$, $\therefore$ reject H_o, (n=6)

The conclusion is that there is a statistical difference between the fits of the Golay equation and the Blumberg equation at all three of the temperatures evaluated using the H vs. $\bar{m}$ data.

The H vs. μ_o data was statistically evaluated using a two-tailed form two of the t-test at the 95% confidence level. Again, H_o was that there is no statistical difference between the Blumberg and Golay fits and H_1 was that there is a statistical difference.

Table 12. Statistical Analysis of the Temperature Effects (H vs. μ_o)

	t (calculated)	t (table)[79]	Conclusions
100 °C	11	2.78	$t_{calc} > t_{tab}$, $\therefore$ reject H_o, (n=6)
125 °C	77	2.78	$t_{calc} > t_{tab}$, $\therefore$ reject H_o, (n=6)
150 °C	5	2.78	$t_{calc} > t_{tab}$, $\therefore$ reject H_o, (n=6)

The conclusion is that there is a statistical difference between the fits of the Giddings modified Golay equation and the Blumberg equation at all three of the temperatures evaluated using the H vs. μ_o data. In conclusion, the Blumberg equation is a fundamental modification of the original Golay equation so that it fits the typical H vs. $\bar{m}$ rate equation data. The modified Giddings equation requires different data to be obtained and

plotted in order to achieve a good fit of the data and is a better fit than the Blumberg equation.

Another conclusion arrived at by Blumberg was that the film thickness does not affect the shapes of the curves. We know that the effect of the film thickness on the total plate height decreases with a decrease in the film thickness due to the smaller contribution of mass transfer in the liquid phase. According to Schutjes, "from published values for the diffusion coefficients of n-alkanes in the gaseous phase and in the stationary phase it is concluded, that the stationary phase contribution is normally less than 1%. For columns with a large pressure gradient the importance of the C_s term will be even less, due to the decreased value of the" pressure correction factor.[43] Two columns were evaluated for the effect of the column i.d. A plot of H vs. $\overline{m}$ for various internal diameters is shown in Figure 33.

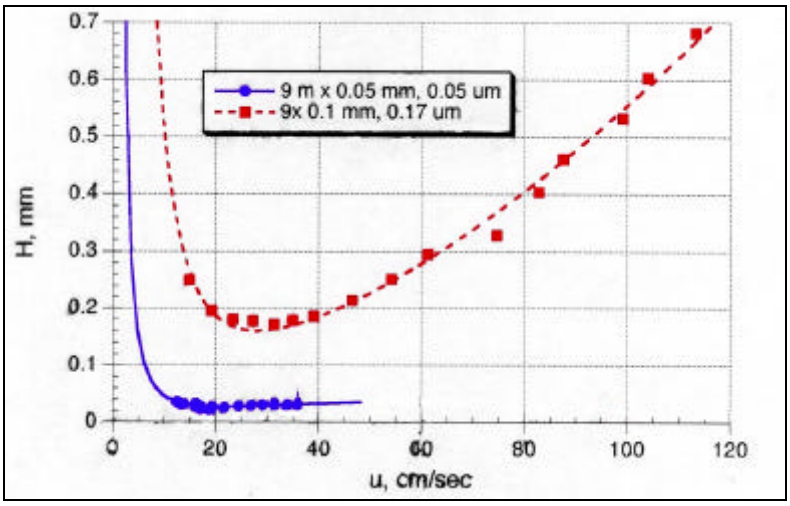

Figure 33. Effect of i.d. on Blumberg Plot

Conditions: 9 m x 0.05 mm i.d., 0.05 µm d_f, 9 m x 0.1 mm, 0.17 µm d_f, 100 °C

The curve with the largest minimum plate height, H, is for a 0.1 mm i.d. column and the curve below that one, with a much smaller minimum plate height is for a 0.05 mm i.d. column. The optimum linear gas velocity was calculated to be 28 cm/sec for the 0.1 mm i.d. column and 21 cm/sec for the 0.05 mm i.d. column. The column plate capacity, N_c, is 90,000 for the 0.1 mm i.d. column and 180,000 for the 0.05 mm i.d. column. Using the

values for the 0.1 mm column and calculating N_c for the 0.05 mm i.d. column leads to a 12% error in the experimental value compared to the mathematically predicted value. Typically it is predicted from the original Golay equation that the larger the i.d., the larger the minimum plate height and the steeper the curve after the minimum. This means that the larger the i.d., the more important it becomes to work at the optimum linear gas velocity. This is seen in the graph above. Blumberg predicts that there should not be very much of an effect on the rate equation plot from the i.d. at high pressure drops, however, this was not seen in this work.

As already mentioned, working with the very small i.d. columns leads to very large pressue drops and limited velocities obtainable with conventional instrumentation. The other problem is that the sample capacity is greatly decreased when working with small diameter columns.

Conclusions

It has been determined that the proposed equation describing the mathematics of fast GC under high pressure drop conditions has an improved fit over the conventional Golay equation fit. However if H vs. μ_o is plotted rather the H vs. $\bar{m}$, the Giddings modified Golay equation gives a fit, R^2 values greater than 0.90, that is statistically better than the Blumberg equation. The predicted effect of the length on the shape of the graph was seen as shown in Figure 28. The predicted effect of a long column under high pressure drop conditions acting as a thin film column was seen in Figure 27. The effect of changing the temperature was evaluated and the minimum velocities for the rate equation curves calculated. The predicted relationship between the temperature and the optimum velocities was compared to the experimental data and shown to differ by only 2%. However, the predicted minimal effect of the i.d. on the rate equation plot was not seen.

In conclusion, the proposed Blumberg equation offers a statistically better fit than the traditional Golay equation under high pressure drop conditions for the H vs. $\bar{m}$ plots. The Giddings modified Golay equation fits the H vs. μ_o data statistically better than the

Blumberg equation. The Giddings modified equation fits the data. The work here shows that the Blumberg equation explains the experimental data when working with the average linear carrier gas velocity, but not when working with the outlet velocity. Statistically, the Golay equation still shows correlation with the data; however, the Blumberg equation has a statistically better correlation.

Chapter 4 - Fast GC by Fast Temperature Programming Using Resistive Heating

Background

In 1961 Giddings published his theory of temperature programmed gas chromatography (TPGC).[84] Originally only isothermal chromatography was done due to the lack of ovens and temperature programmers with reproducible heating rates. One main advantage of TPGC is to separate mixtures that contain analytes with a wide range of boiling points. The first published[85] temperature programmed chromatogram is shown in Figure 34. It was obtained by Griffiths *et al.* and published in 1952.[86]

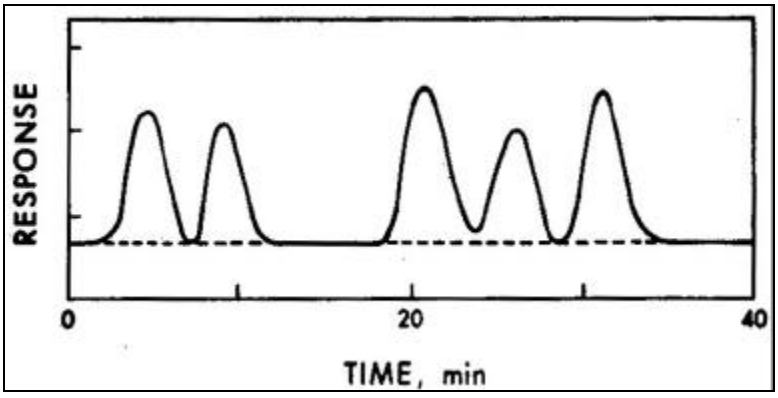

Figure 34. First Published Temperature Programmed Chromatogram, (1952)

Conditions: temperature program – 0 °C programmed at 1.25 °C/min to 50 °C, peaks – isopropyl chloride, n-propyl chloride, n-butyl chloride, chloroform, and ethylene dichloride

This chromatogram of isopropyl chloride, n-propyl chloride, n-butyl chloride, chloroform and ethylene dichloride was obtained using a tricresyl phosphate column. The temperature program was a linear rate of 1.25 °C/min from 0 °C to 50 °C. This programming rate is slower than the rates typically used today. The peaks are very wide, which is a product of the column, injector and detector technology of the time. Today it is possible to program much faster and produce much narrower peaks. Temperature programming in the early days of chromatography used large forced air ovens to heat and

cool packed metal columns. This led to the use of slow programming rates. Over the years the ovens have become smaller, capillary columns have been introduced, and technology has advanced. This has led to faster temperature programming rates, but the upper limit is still 100 °C/min for most commercial systems as of early 1999.

Resistive heating of the column has been an attractive means of heating the column, but it has been difficult to implement well, until recently. One of the first studies was to investigating resistive heating of the analytical column, rather than using the conventional forced air heating was done in 1984.[87] Later, a GC probe was used with an open tubular aluminum-clad capillary column in connection with mass spectrometry.[88] The aluminum allowed the column to be resistively heated. Due to the low thermal mass of aluminum it could be heated and cooled faster than traditional columns. Another method of resistive heating was to coat capillary columns with a conductive film, to achieve very fast analyses.[89] An example is shown below.[90]

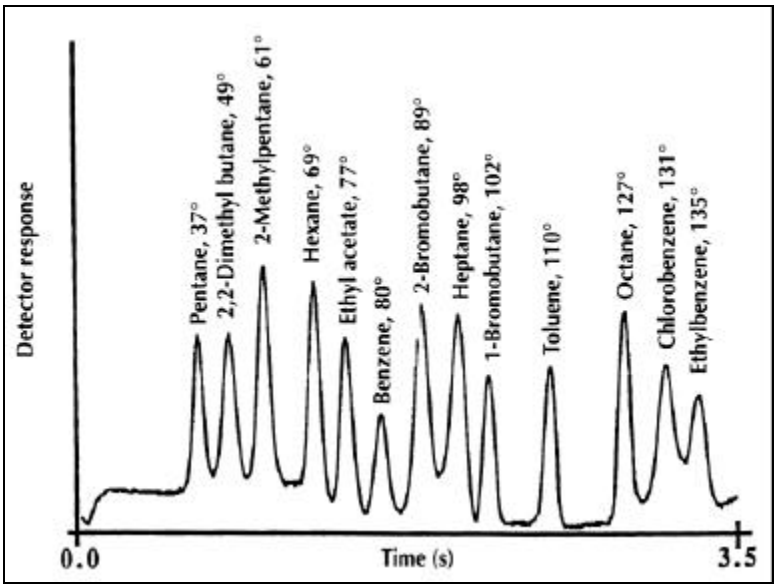

Figure 35. Fast Analysis Using Coated Capillary Columns

Conditions: 84 cm x 0.1 mm i.d., 0.2 μm d_f, heated with an electrically conductive paint coated on the column

This chromatogram was obtained on a SE-30 column, 84 cm x 100 μm, 0.2 μm d_f. The column was coated with an electrically conductive paint. There was a temperature gradient for the column both in time and in space. Thirteen components were separated

in 3.5 seconds, although some were not baseline resolved. Ehrmann[91] *et al.* used a metal tube to enclose a capillary column in order to avoid some of the problems with uneven heating and limited column life encountered when coating the column with a conductive film. This means of fast temperature programming is similar to the commercially available system used in this study.

When developing a TPGC method, several temperature parameters must be decided: the initial temperature, T_o, the final temperature, T_f, and the programming rate, β. The use of β in conjunction with temperature programming is consistent with the early work of Giddings. The initial and final temperatures can be readily determined by knowing the boiling points of the components in the sample, or by running a trial chromatogram and finding the capacity factors of the peaks. The programming rate is more difficult to establish, but generally a slow rate will result in better resolution and a slower analysis time. In order to do fast GC, the techniques of reducing column length, film thickness, and internal diameter as well as using higher flow rates, turbulent flow and vacuum at the column outlet have all been investigated. Only a few groups have studied fast temperature programming rates. This may have been due to the lack of commercially available instrumentation. Fast temperature programming has only recently been more recognized as a means of doing fast GC. The temperature effects on an analysis are significant and can effect the analysis time much more than the flow rate or the column length.[92] To double the flow rate will cut the analysis time in half, to cut the column length in half will decrease the analysis time by a half; and raising the column temperature 120 °C will approximately reduce the analysis time to 1/16 of the original value. The purpose of this chapter is to explore very fast temperature programming rates and the effects of these rates on various chromatographic parameters.

The parameters needed to predict what will yield the maximum separability of compounds depend on two quantities, the retention temperature or time and the peak spreading or the effective plate height. The separation of two peaks is defined by Giddings[84] in terms of F, shown in eq. 36.

$$F = \frac{(t_2 - t_1)^2}{8(s_2 + s_1)^2} \tag{36}$$

F = separability factor, dimensionless

t_2 and t_1 = retention times of peaks two and one respectively, minutes

s_2 and s_1 = variances of peaks two and one respectively, minutes

Giddings drew several conclusions[84] concerning the effects of various chromatographic parameters when working under TPGC conditions.

1. F is shown to increase with length under all conditions. At low velocities F is proportional to L and at high velocities F is proportional to L^b where b is the relative enthalpy of activation for liquid diffusion. The value for b is approximately 0.35 for small molecules and less for larger solutes.

An increase in β, or the temperature programming rate, always leads to an increase in the retention temperature, T_R and the significant temperature, T' and this causes the separability to decrease. (T_R is the temperature at which elution of the peak maximum occurs. T' is the isothermal temperature that would lead to the same amount of peak spreading and the same degree of separability as obtained with a programmed run. It is usually about 40 °C less than the elution temperature.) This decrease in separation should not be a large effect since T_R increases slowly with changes in β. The analysis time is nearly inversely proportional to β. Some data is shown below. (Table 13).

Table 13. Effect of Programming Rate on Elution Temperature

Conditions: Rtx-5, 5 m x 0.32 mm, 0.25 μm d_f, Helium at 4.2 mL/min, 1 μL split 82:1, T_o = 60 °C, decane in hexane

β, °C/min	**T_R, °C**
48	84
60	87
80	93
120	104
240	127
480	163
960	223
1200	255

2. An increase in carrier gas velocity will reduce the analysis time, once again with only small effects. "Efforts to reduce analysis time by increasing velocity are therefore rather futile and only impair resolution".[84]
3. An increase in T_o, or the initial temperature by ΔT, will reduce the analysis time by a factor of $\beta\Delta T$. Adjust T_o for the requirements of the low boiling components of the sample. T_o does not affect the retention temperature of compounds eluting about 60 °C above T_o, so lower T_o to optimize the resolution of the early eluting peaks. If the early eluting peaks are well resolved increase T_o until R is adequate.

The exact mathematics of TPGC is rather complicated. A simplified version is presented below. A step-function is used to describe the peak velocity increase as the peak moves through the column. This step function is shown in Figure 36[93]. The smooth curve describes the actual velocity of the peak through the column. It can be seen that the largest changes in velocity (the biggest steps) are in the later sections of the analysis (higher temperatures). The mathematics for temperature programming and the calculation of the smooth curve have been published[94,95,96], but a detailed treatment is beyond the scope of this work. The simplified model depicted here in Figure 36 was introduced by Giddings in 1962[93].

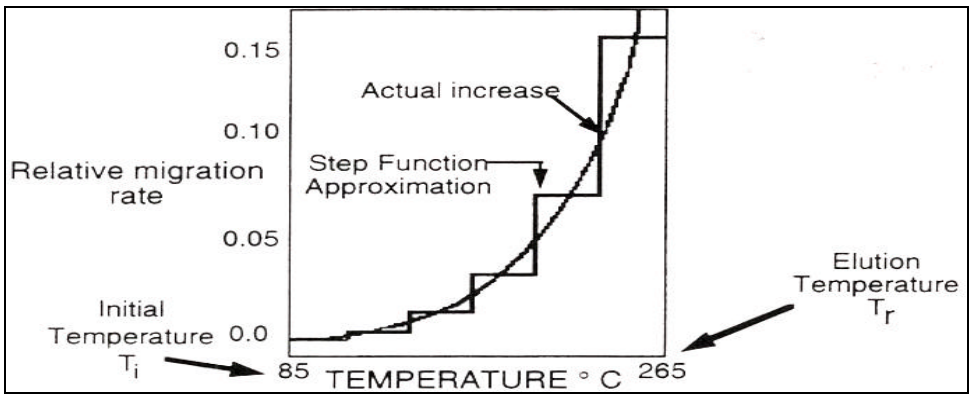

Figure 36. Step Function Approximation for Temperature Programmed GC

In Figure 36, the movement of the peak through the column is described. The smooth line is the actual movement of the peak through the column and the line labeled "Step Function Approximation" is the line used to approximate the smooth line. The step

function approximation assumes that the peak moves at the same rate throughout a 30 °C interval and then makes a sudden change. In actuality there is a continuous change in the peak velocity. Figure 36 also shows the difference in relative migration rate between the first two steps and the last two steps. The majority of the peak movement occurs in the final portion of the analysis. 50% of the peak movement occurs in the final step, and 75% of the movement in the final two steps.

The rate at which the velocity increases is related to the ability of the solute to vaporize into the gas phase.[97] A good approximation is that the relative migration rate is proportional to the vapor pressure, which is exponentially related to the temperature.[97] This relationship can be described by the integrated Clausius-Clapeyron equation, (eq 37).[97]

$$\ln \frac{P_2}{P_1} = \frac{\Delta H (T_2 - T_1)}{R T_1 T_2} \qquad (37)$$

P_2 = final pressure, psi

P_1 = initial pressure, psi

DH = heat of vaporization, J/mol

T_2 = final temperature, K

T_1 = initial temperature, K

R = gas constant, J/mol*K

If the change in temperature required to double the vapor pressure, or to cut the retention time in half, is calculated, several assumptions must be made. Using a column temperature of 227 °C (500 K), and assuming that Troutons rule is valid ($\Delta H/T = 23$ for hydrocarbons) then the ΔT required to double the vapor pressure is 30 °C. If other column temperatures are chosen the ΔT values change.

In TPGC, the analytes are put onto a cold column all compounds are effectively frozen at the head of the column. As the column temperature increases each analyte finds a temperature where its vapor pressure is sufficient to initiate movement through the column. Separations occur throughout the column, however, most of the movement through the column occurs in the final 30 °C interval before the elution temperature, T_R.

In a similar schematic as Figure 36, Figure 37[93] illustrates the movement of the analyte through the column.

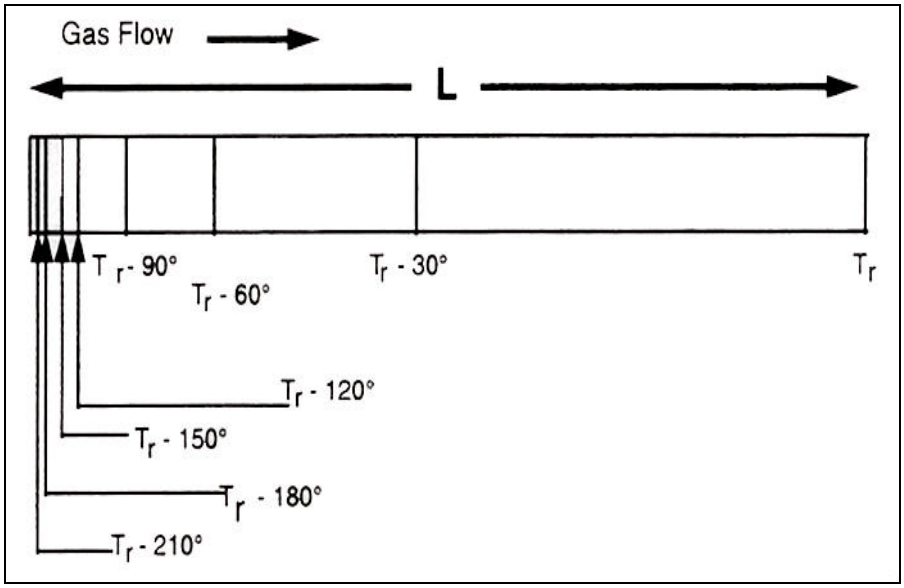

Figure 37. Peak Migration Through the Column

L is the length of the column, the peak travels through the column from left to right finally eluting at temperature T_r. If the distance traveled in the last 30 °C segment is x, the preceding cooler segments are ½ x, ¼ x, 1/8 x etc. This series approaches 2 as the limit.[93] Thirty degrees prior to the elution temperature the peak is only half way through the column at a temperature of T_r –30 °C. This demonstrates the fact that 50% of the movement of the analyte occurs in the last 30 °C temperature change and 75% in the last two steps.

If T_o is too high the more volatile analytes are not initially frozen on the column and the R-value at the end of the column will approach one and the last part of the column may actually hinder the separation rather than help it. R is the fraction of the solute that is in the vapor state. R is defined by eq. 38.[93]

$$R = ae^{-\Delta H / RT} \tag{38}$$

where a is defined by eq. 39[93]

$$a = \frac{A_m}{A_s} e^{\Delta S / R} \tag{39}$$

A_m = area of the mobile phase, cm^2

A_s = area of the stationary phase, cm^2

DS = entropy change for a solute going from liquid to gas phase

R = gas constant, J/mol*K

T = temperature, K

DH = enthalpy change in solute going from liquid to gas phase, J/mol

βt_o should not exceed 10 °C for close adherence to theory and should not be above 20 to 30 °C for a good separation. t_o is the hold-up time of the system; β is the programming rate.

In a linear temperature programmed rate with an isothermal portion at the end, a compound that elutes in the isothermal portion is described in two different steps, the TPGC portion and the isothermal portion. Eq. 40 describes the temperature programmed portion of the analysis and eq. 41 describes the isothermal portion of the analysis.

$$\frac{z_1}{L} = \frac{(r/F)^*_{T1}}{r/F} \tag{40}$$

z/L = fraction of the column traveled in the temperature programmed portion of t he run

r = heating rate, °C/min

F = is the flow rate, mL/min

$(r/F)^*_{T1}$ is the hypothetical program that would give complete elution at T_1

The remainder of the column is traveled isothermally according to eq. 41.

$$\frac{1-(r/F)^*_{T1}}{r/F} \tag{41}$$

It is common practice and recommended practice to use flow rates that are significantly above the optimum. This permits relatively high heating rates without

raising r/F excessively. However, the analysis time is usually decreased more by an increase in the heating rate rather than by an increase in the flow rate (Recall page 63). The use of increased temperature programming rates rather than increased flow rates becomes even more important when using the mass spectrometer as a detector. Evidence for this statement will be shown later in this chapter.

Experimental I

The experimental work for this part of the thesis involved the following instrumentation. The instrumentation includes a Hewlett Packard (Little Falls, DE), model 5890 GC equipped with an HP 7673 autosampler and a Thermedics Detection (Chelmsford, MA) EZFlash™ attachment. The EZFlash™ resistively heats the analytical column. The analytical column is placed inside of a metal tubing by Thermedics. Prior to an analysis, the GC oven temperature is set and allowed to equilibrate. The resistance is calibrated at this temperature. The remainder of the parameters are described in Table 14.

Table 14. Experimental Parameters for EZFlash™ Work

Parameters	Experimental Conditions
Injection Port	250 °C
Split Ratio	82:1
Flow Rate/Linear Gas Velocity	4.2 mL/min helium, 87 cm/sec
Column	Rtx-5, 5 m x 0.32 mm, 0.25 μm d_f
Detector	Flame Ionization Detector, 325 °C
Autosampler	1 μL injections

The sample was a 0.1% mixture of decane, tetradecane, octadecane, docosane, hexacosane and triacontane in hexane. The temperature program began at 60 °C and ended at 300 °C with programming rates of 48, 60, 80, 120, 240, 960, and 1200 °C/min. The sample was analyzed three times at each temperature programming rate. Peak areas,

retention times and peak heights were collected, averaged and the standard deviations calculated.

Results I

It has long been known that the analysis time for hydrocarbons can be significantly reduced by increasing the temperature programming rate. Figure 38 is a summary of the retention times at the various programming rates and the %RSDs of the retention times in parentheses, n = 3.

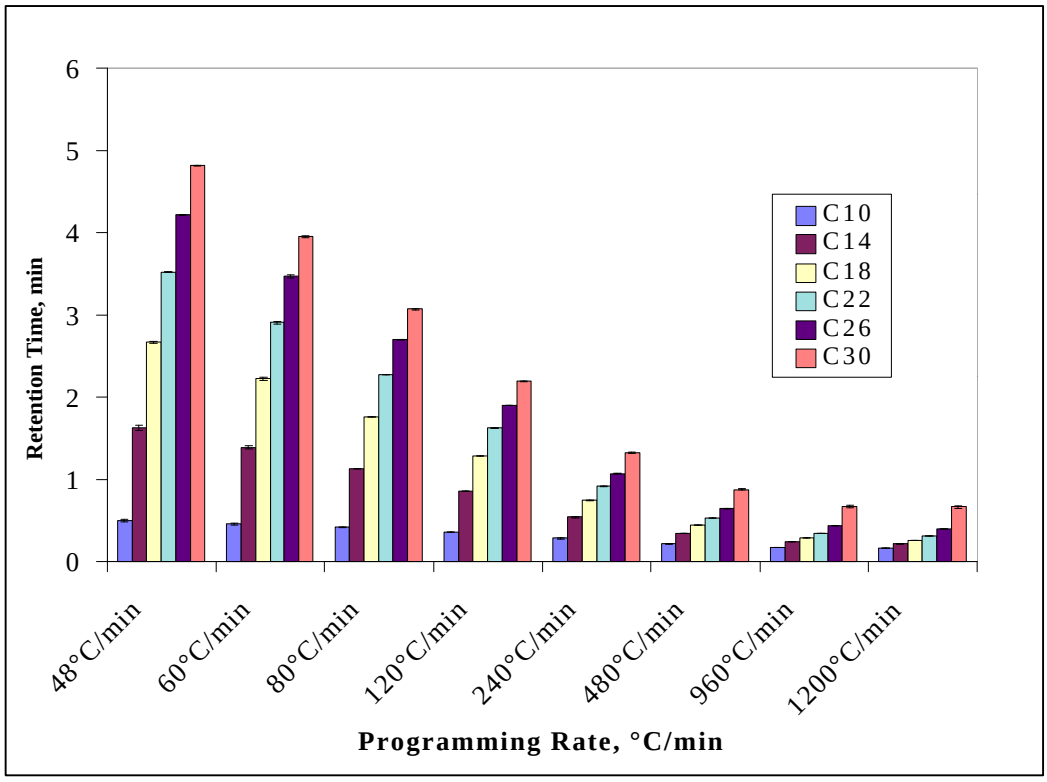

Figure 38. Effect of Temperature Programming on Retention Time

GC Conditions listed in Table 14.

Table 15. Average Retention Times (%RSDs)

GC Conditions listed in Table 14, n = 3.

	48 °C/min	*60 °C/min*	*80 °C/min*	*120 °C/min*	*240 °C/min*	*480 °C/min*	*960 °C/min*	*1200 °C/min*
C10	0.498**(3.2)**	0.456**(1.5)**	0.416**(0.50)**	0.364**(0.48)**	0.281**(1.3)**	0.214**(0.54)**	0.170**(0.34)**	0.163**(0.35)**
C14	1.627**(1.6)**	1.389**(1.3)**	1.130**(0.18)**	0.859**(0.12)**	0.539**(0.75)**	0.344**(0.29)**	0.234**(0.25)**	0.214**(0.47)**
C18	2.668**(0.62)**	2.227**(0.80)**	1.761**(0.06)**	1.280**(0.05)**	0.749**(0.60)**	0.448**(0.22)**	0.288**(0.0)**	0.259**(0.45)**
C22	3.520**(0.11)**	2.905**(0.64)**	2.270**(0.05)**	1.621**(0.04)**	0.918**(0.49)**	0.533**(0.11)**	0.343**(0.0)**	0.310**(0.19)**
C26	4.218**(0.12)**	3.470**(0.50)**	2.696**(0.06)**	1.905**(0.06)**	1.067**(0.61)**	0.643**(0.27)**	0.434**(0.23)**	0.403**(0.14)**
C30	4.820**(0.10)**	3.955**(0.37)**	3.068**(0.06)**	2.194**(0.14)**	1.323**(0.94)**	0.876**(0.54)**	0.670**(1.9)**	0.661**(2.1)**

It can be seen from Figure 38 that the reproducibility of the retention times is good with a %RSD of less than 1% for all but seven of the data points. Note also, the eight fold decrease in analysis time from 4.820 min at 48 °C/min to 0.661 min at 1200 °C/min. Obviously raising the programming rate is an easy way to reduce the analysis times.

A concern of potential users of fast GC systems is that the reproducibility of the retention times and peak areas for very fast analyses will be compromised. The F-test can be used to show that the precision of the fastest temperature programming rate (1200 °C/min) is not statistically different than the slowest temperature programming rate (48 °C/min) (Table 16). A one-tailed F-test at the 95% confidence level was used with 5 degrees of freedom in each sample set. The ratio of the standard deviations to the retention times was used in the F-test so that the results of the F-test would not be skewed by the orders of magnitude difference in the values being tested. H_o is that here is no statistical difference in the precision at the two different programming rates and H_1 is that the precision for fastest temperature programming rate is statistically worse than the precision of the slowest programming rate. The data show no significant difference

Table 16. *F*-test on %RSDs of Retention Times at Various Programming Rates

Avg. std. dev. of 48 °C/min	Avg. std. dev. of 1200 °C/min	Statistical Analysis
0.00950	0.00619	$f_{calc} = 2.35 < f_{crit} = 5.05$[79] ∴ no statistical difference

The mean results and the %RSDs for peak areas for the same experiment are shown in Table 17.

Table 17. Average Peak Areas (%RSDs)

GC Conditions listed in Table 14, n = 3.

	48 °C/min	*60 °C/min*	*80 °C/min*	*120 °C/min*	*240 °C/min*	*480 °C/min*	*960 °C/min*	*1200 °C/min*
C10	70240**(1.9)**	70078**(1.6)**	70159**(2.6)**	69199**(4.6)**	72745**(2.2)**	68636**(5.3)**	64118**(3.6)**	64089**(2.5)**
C14	84786**(1.9)**	84979**(0.2)**	84882**(1.7)**	84222**(4.5)**	87814**(2.0)**	82391**(5.0)**	76533**(3.0)**	75557**(2.5)**
C18	88236(**2.6)**	88316**(1.0)**	88276**(1.2)**	86647**(4.7)**	90060**(2.0)**	83945**(4.2)**	77740**(2.9)**	76226**(3.0)**
C22	87527**(3.1)**	87214**(1.9)**	87371**(1.0)**	84858**(4.4)**	88242**(1.8)**	81916**(4.4)**	75141**(2.4)**	73475**(3.1)**
C26	92311**(3.6)**	91898**(2.3)**	92105**(1.0)**	89162**(4.0)**	92153**(2.1)**	83822**(4.3)**	76132**(2.1)**	74073**(3.1)**
C30	95551**(4.0)**	95032**(2.4)**	95292**(1.3)**	92115**(3.5)**	94882**(1.9)**	84106**(4.1)**	74038**(1.1)**	72054**(3.3)**

To better illustrate the results, the averages and the standard deviations for C10, C18 and C30 are plotted in Figure 39.

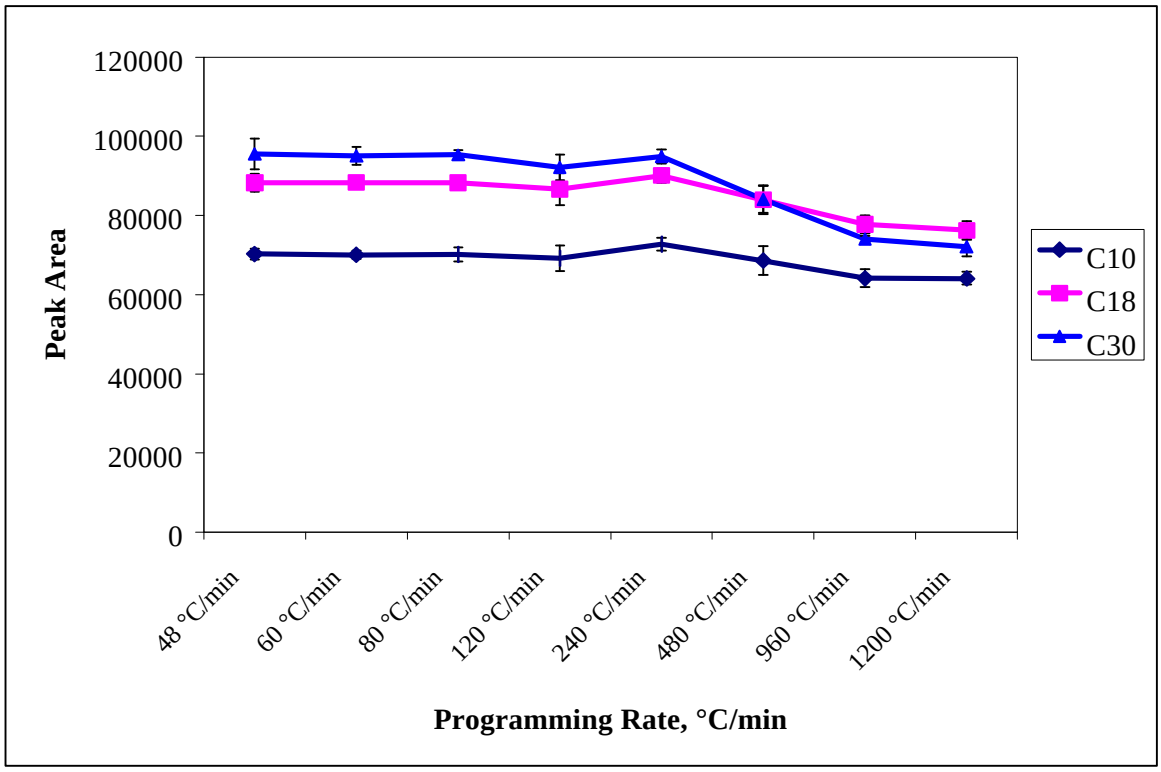

Figure 39. Effect of Temperature Programming Rates on Peak Area

GC Conditions listed in Table 14.

In Figure 39 a trend can be seen. The peak areas remain constant up to 240 °C/min and then decrease slightly. The areas can be shown to be statistically different by using form two of the t-test at the 95% confidence level. (Table 18). H_o is that the areas are statistically the same, H_1 is that the areas are statistically different.

Table 18. Form 2 of the t-test, Comparison of Programming Rates

	48 °C/min	**1200 °C/min**
Mean	8.64×10^4	7.26×10^4
Std. Dev.	8.80×10^3	4.47×10^3
$Sp = 6961$, $\nu = 10$, $t_{calc.} = 3.45$, $t_{crit} = 2.23^{79}$, $t_{calc} > t_{crit}$ **$\therefore$ There is a statistical difference**		

There is no known good explanation for the decrease in the peak areas at this time. The decrease may be a result of the slow data sampling rate used to record the fast peaks. It

was not possible to sample any faster than 20 Hz (FID), which may be too slow. The effect of the data sampling rate will be investigated further later in this chapter.

The next parameter to be evaluated was the peak height. The average results and the %RSDs in parentheses of the peak heights are shown in Table 19.

Table 19. Average Peak Heights(%RSDs)

GC Conditions listed in Table 14, n = 3.

	48 °C/min	*60 °C/min*	*80 °C/min*	*120 °C/min*	*240 °C/min*	*480 °C/min*	*960 °C/min*	*1200 °C/min*
C10	1.2e5**(0.52)**	1.3e5**(4.3)**	1.6e5**(1.4)**	196582**(1.8)**	2.8e5**(4.8)**	3.5e5**(1.8)**	3.6e5**(1.8)**	3.6e5**(2.7)**
C14	90987**(2.9)**	1.1e5**(0.61)**	1.4e5**(1.8)**	1.9e5**(0.75)**	3.2e5**(2.6)**	4.2e5**(4.8)**	4.5e5**(3.6)**	4.5e5**(2.6)**
C18	77193**(3.1)**	93498**(1.2)**	1.2e5**(1.2)**	1.6e5**(0.54)**	3.0e5**(2.6)**	4.0e5**(4.2)**	4.2e5**(2.7)**	4.2e5**(3.0)**
C22	60654**(3.5)**	72583**(1.5)**	9.5e4**(2.0)**	1.3e5**(0.57)**	2.5e5**(2.4)**	3.3e5**(3.6)**	3.2e5**(2.2)**	3.1e5**(3.3)**
C26	48108**(4.3)**	57352**(3.0)**	7.5e4**(0.58)**	1.0e5**(0.24)**	1.5e5**(2.3)**	1.5e5**(1.5)**	1.3e5**(0.75)**	1.2e5**2.4**)
C30	36808**(3.5)**	44057**(0.74)**	50658**(3.2)**	46333**(1.5)**	42835**(6.0)**	41209**(3.9)**	22795**(34)**	19953**(24)**

To better illustrate the results, the averages and standard deviations are plotted in Figure 40.

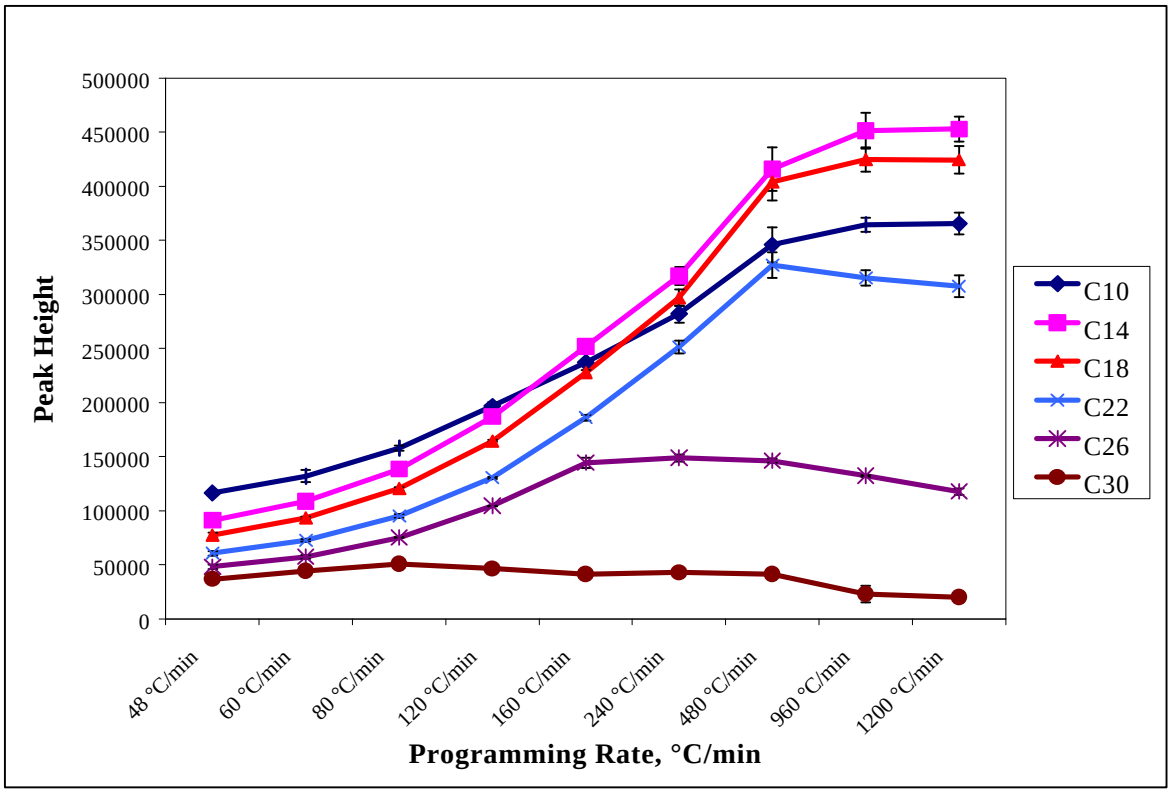

Figure 40. Effect of Temperature Programming on Peak Height

GC Conditions listed in Table 14.

Figure 40 illustrates the trend in the peak heights as the temperature programming rate increases. For C10 through C18, the peak heights increase over the entire range of programming rates. For C22, the peak height increases up to 480 °C/min and then begins to decrease slowly. For C26, a similar result is seen. In this case the peak height only increases slowly until 160 °C/min then remains steady until 480 °C/min and finally decreases slowly. For C30, the peak heights seem to remain constant at the low temperature programming rates and then begin to decrease at the higher temperature programming rates. Keep in mind that the C30 peak does not elute during the temperature programmed portion of the analysis, but during the isothermal portion, thus explaining most of its behavior. The percent increases in the peak heights of the various analytes, at the various temperature programming rate from 48 °C/min to 1200 °C/min, are shown in Table 20.

Table 20. Percent Increase of Peak Height from 48 °C/min to 1200 °C/min

GC Conditions listed in Table 14.

Peak	% Increase in Peak Height
C10	3.1
C14	5.0
C18	5.5
C22	5.1
C26	2.4
C30	0.5

Table 20 shows the improvement in peak height that is gained by increasing the temperature programming rate. At the same time, resolution is lost, and this may or may not be acceptable. The resolution in these analyses will be discussed later in this chapter. The increase in the peak height indicates that it would be possible to inject less sample at the higher programming rates and maintain the same signal to noise ratio. It also indicates that when working at trace levels, the signals in the chromatogram would increase if faster temperature programming rates are used. This is however, dependent on achieving acceptable resolution.

One other point to notice from Table 19 is that the %RSDs for the peak heights of C30 at the fastest two temperature programming rates are very high, 34% and 24% respectively. This indicates that it is possible to program at too fast a rate for the higher molecular weight compounds. Peak integration parameters may need to be adjusted for the broader peaks eluting in the isothermal portion of the chromatograph. These results are to be expected for isothermal results; see the peak areas in Figure 39, which indicate good quantitative data.

The peak widths are an important parameter for determining how many peaks can be fit into a certain amount of time. The peak widths at half height were also evaluated and the results are tabulated in Table 21 and shown graphically in Figure 41.

Table 21. Effect of Temperature Programming Rates on Peak Width (%RSD)

GC Conditions listed in Table 14, n = 3, peak width at half height.

	48 °C/min	*60 °C/min*	*80 °C/min*	*120 °C/min*	*240 °C/min*	*480 °C/min*	*960 °C/min*	*1200 °C/min*
C10	0.009**(6.2)**	0.008**(6.9)**	0.007**(0.0)**	0.006**(10.2)**	0.004**(0.0)**	0.003**(0.0)**	0.003**(0.0)**	0.003**(0.0)**
C14	0.015**(3.9)**	0.012**(0.0)**	0.010**(0.0)**	0.007**(0.0)**	0.004**(0.0)**	0.003**(0.0)**	0.003**(0.0)**	0.003**(17)**
C18	0.018**(3.3)**	0.015**(0.0)**	0.011**(5.1)**	0.008**(0.0)**	0.005**(0.0)**	0.003**(0.0)**	0.003**(0.0)**	0.003**(0.0)**
C22	0.022**(2.6)**	0.019**(3.1)**	0.014**(4.0)**	0.010**(0.0)**	0.005**(10.8)**	0.004**(0.0)**	0.004**(0.0)**	0.004**(0.0)**
C26	0.030**(1.9)**	0.025**(0.0)**	0.019**(0.0)**	0.013**(0.0)**	0.010**(6.0)**	0.009**(0.0)**	0.009**(0.0)**	0.010**(0.0)**
C30	0.039**(2.6)**	0.034**(1.7)**	0.029**(5.2)**	0.030**(3.3)**	0.034**(4.5)**	0.032**(3.6)**	0.051**(44)**	0.051**(21)**

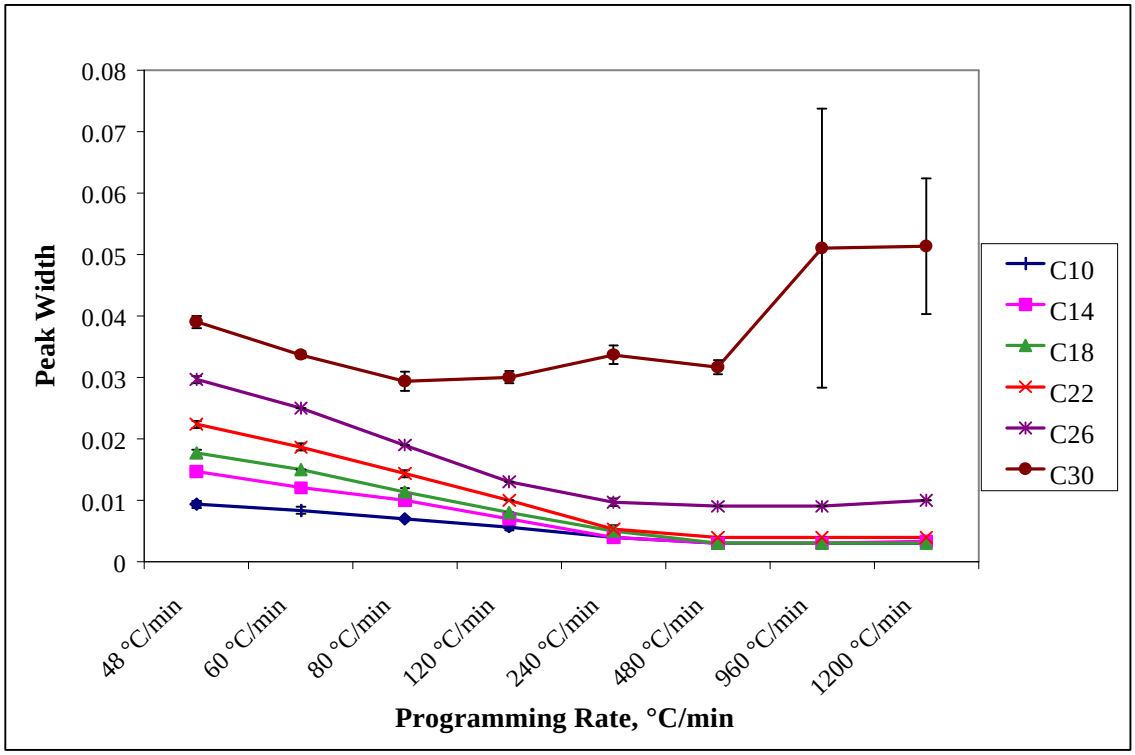

Figure 41. Effect of Temperature Programming Rate on Peak Width

GC Conditions listed in Table 14. Peak width measured at half height.

The results shown in Figure 29 show that the peak widths decrease for all compounds, except C30, as the programming rate increases. This decrease in peak width would be consistent with a shorter residence time in the column as well as a hotter

column temperature that helps narrow the peaks. The peak widths for C30 decrease initially and then begin to increase. For the last two temperature programming rates, the standard deviations of the peak widths are very large. Since C30 elutes only after the temperature programming portion of the analysis maybe there was too much time for diffusion in the mobile phase before it reached the detector. The column reached 300 °C in 12 seconds and the C30 peak eluted at 40 seconds. See the discussion of the elution temperatures in the next several paragraphs. At these fast temperature programming rates, it would be better to use a shorter column to analyze C30. The Giddings R value approaches 1.0 at the end of the column and hinders the separation.

The elution temperatures were compared at each of the programming rates and these results are tabulated in Table 22 and shown graphically in Figure 42. These values were calculated from the retention time, the initial temperature and the programming rate.

Table 22. Effect of Temperature Programming Rate on Elution Temperatures

GC Conditions listed in Table 14, n = 3.

	48 °C/min	*60 °C/min*	*80 °C/min*	*120 °C/min*	*240 °C/min*	*480 °C/min*	*960 °C/min*	*1200 °C/min*
C10	83.9	87.4	93.2	104	127	163	223	255
C14	138	143	150	163	189	225	285	300
C18	188	194	201	214	240	275	300	300
C22	229	234	242	255	280	300*	300*	300*
C26	262	268	276	289	300*	300*	300*	300*
C30	291	297	300*	300*	300*	300*	300*	300*

*peaks eluting isothermally

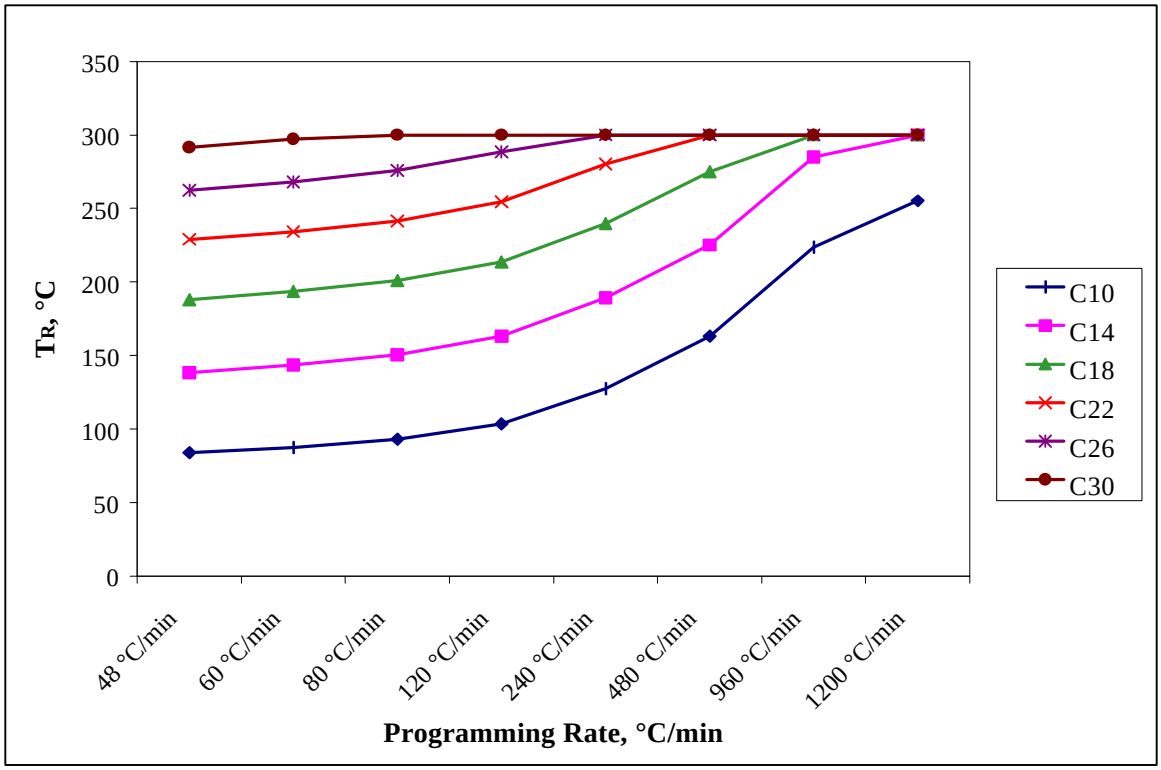

Figure 42. Effect of Temperature Programming Rate on Elution Temperature

GC Conditions listed in Table 14.

The next parameter of interest is the resolution, R. R is defined by eq. 42.[98]

$$R = \frac{2(t_2 - t_1)}{w_{b1} + w_{b2}} \tag{42}$$

R = resolution, dimensionless

t_2, t_1 = retention times of peaks 2 and 1 respectively, minutes

w_{b1}, w_{b2} = peak width at the base for peaks 1 and 2 respectively, minutes

Without resolution it is not possible to quantitate the peaks. The resolution results are tabulated in Table 23 and plotted in Figure 43.

Table 23. Effect of Temperature Programming on Resolution (%RSDs)

GC Conditions listed in Table 14, n = 3.

	48 °C/min	*60 °C/min*	*80 °C/min*	*120 °C/min*	*240 °C/min*	*480 °C/min*	*960 °C/min*	*1200 °C/min*
Peak 1-2	55.4**(2.7)**	54.0**(1.2)**	49.4**(0.0)**	46.0**(2.1)**	37.9**(0.1)**	25.4**(0.1)**	12.5**(0.0)**	9.59**(0.9)**
Peak 2-3	37.9**(0.3)**	36.5**(0.1)**	34.8**(0.9)**	33.0**(0.0)**	27.4**(0.1)**	20.4**(0.0)**	10.5**(0.1)**	8.50**(0.6)**
Peak 3-4	25.1**(0.3)**	23.7**(0.5)**	23.4**(1.0)**	22.3**(0.0)**	19.3**(1.0)**	14.3**(0.1)**	9.24**(0.0)**	8.46**(0.1)**
Peak 4-5	15.8**(0.0)**	15.2**(0.2)**	15.0**(0.3)**	14.5**(0.1)**	11.7**(0.7)**	9.92**(0.1)**	8.23**(0.1)**	7.81**(0.0)**
Peak 5-6	10.3**(0.2)**	9.73**(0.0)**	9.05**(0.3)**	7.91**(0.2)**	6.95**(0.3)**	6.75**(0.2)**	4.98**(1.4)**	5.04**(0.6)**

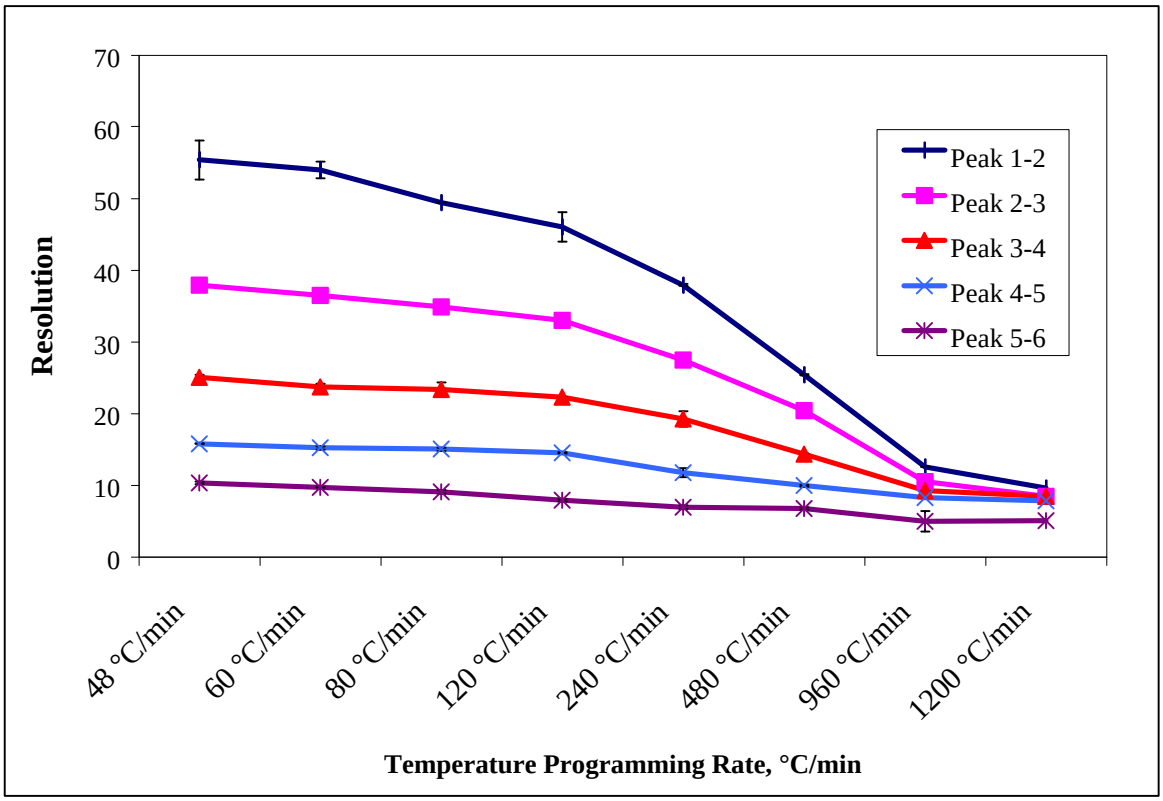

Figure 43. Effect of Temperature Programming Rates on Resolution

GC Conditions listed in Table 14.

The minimum resolution required for quantitation is 1.5, baseline resolution. As can be seen by the tabulated values all of the peak pairs more than meet this requirement.

With the resolutions listed in Table 23 how many peaks can fit between each of these peak pairs? There is another measure of column efficiency, called the Trennzahl. The Trennzahl defines the number of peaks that can fit between two alkanes. Trennzahl is also called the separation number, SN, which is one of the few terms that can be used to describe the column performance in a TPGC analysis.[99] It is defined by the following equation.

$$SN = \frac{t_{R(z+1)} - t_{R(z)}}{w_{h(z)} + w_{h(z+1)}} - 1 \qquad (43)$$

$t_{R(z+1)}$ = larger alkane, minutes

t_{Rz} = smaller alkane, minutes

w_{hz} = width at half height of the smaller alkane, minutes

$w_{h(z+1)}$ = width at half height of the larger alkane, minutes

Eq. 43 calculates the number of peaks that can be resolved with a resolution of 1.2 between two consecutive peaks.[99] It is normally used for alkanes. A graph of the Trennzahl vs. the temperature programming rate is shown in Figure 44 for the alkane sample discussed earlier.

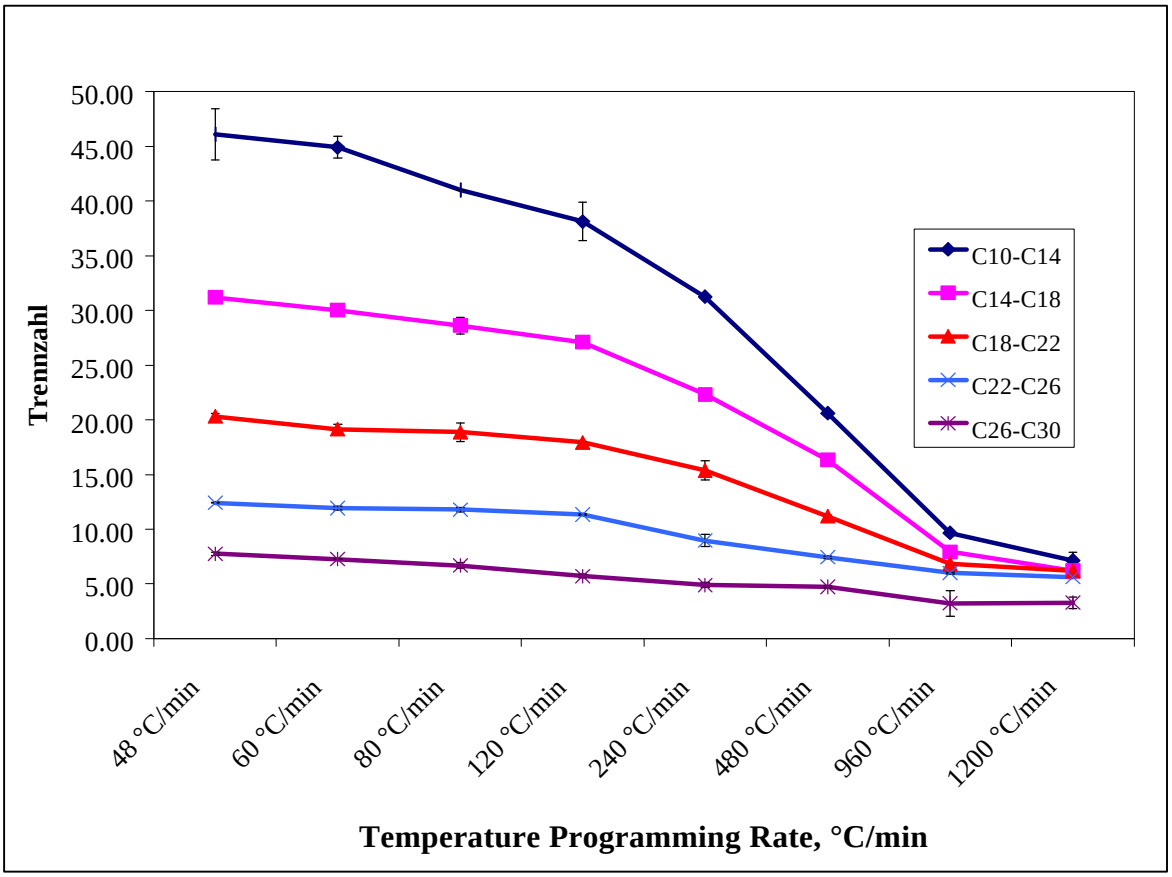

Figure 44. Effect of Temperature Programming Rate on the Trennzahl Number
GC Conditions listed in Table 14.

For the lower carbon numbers at the lower temperature programming rates, a large number of peaks with a resolution of 1.2 could fit between them, as the programming rate increases, the Trennzahl number decreases rapidly. For the higher carbon numbers there is not a large change in Trennzahl number over the range of temperature programming rates studied. The Trennzahl shows that even at the fastest temperature programming rate, all of the consecutive alkanes could fit between the two peaks. For example, C11, C12 and C13 could fit between C10 and C14 when programming at 1200 °C/min with a resolution of at least 1.2.

The final parameter evaluated was the plate number of the column. The plate number was calculated using eq. 44.[100]

$$N = 5.54\left(\frac{t_R}{w_{1/2}}\right)^2 \qquad (44)$$

N = efficiency of the column, dimensionless

t_R = retention time , minutes

$w_{1/2}$ = peak width at half height, minutes

The results are shown graphically in Figure 45.

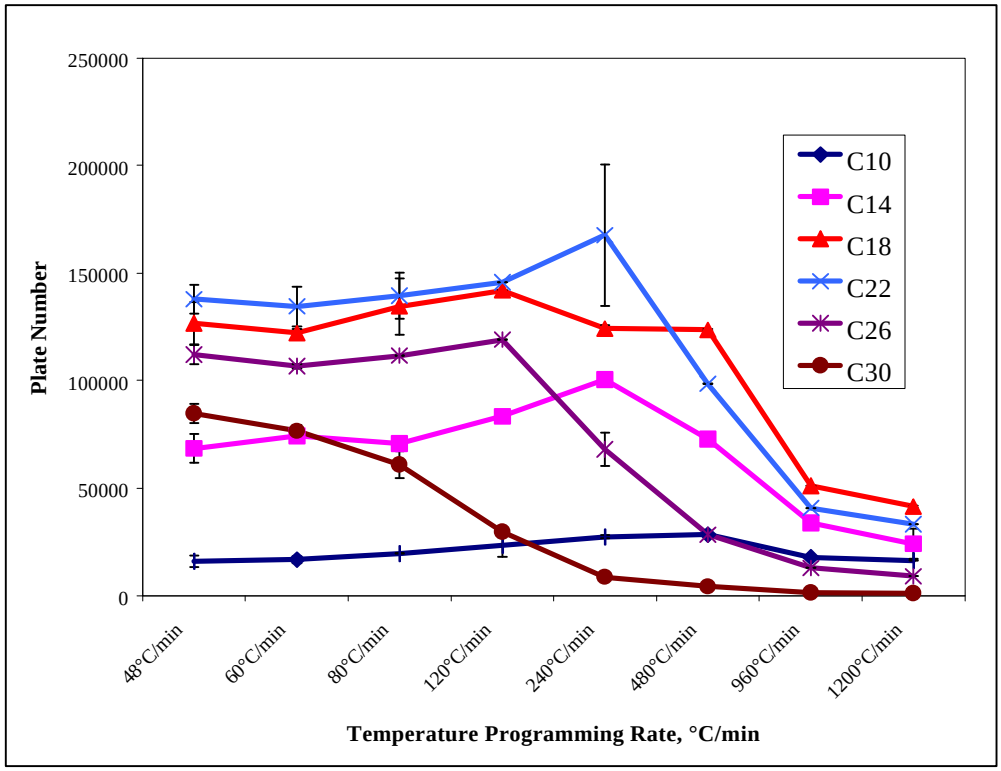

Figure 45. Effect of Temperature Programming Rate on Plate Number, (N)

GC Conditions listed in Table 14.

The general trend is that the efficiency of the column remains fairly constant for each compound at the lower programming rates and the efficiency decreases at the temperature programming rates, except for C10 where the efficiency actually increases slightly.

Sample chromatograms of programming rates of 48 °C/min and 1200 °C/min are shown below in Figure 46 and Figure 47.

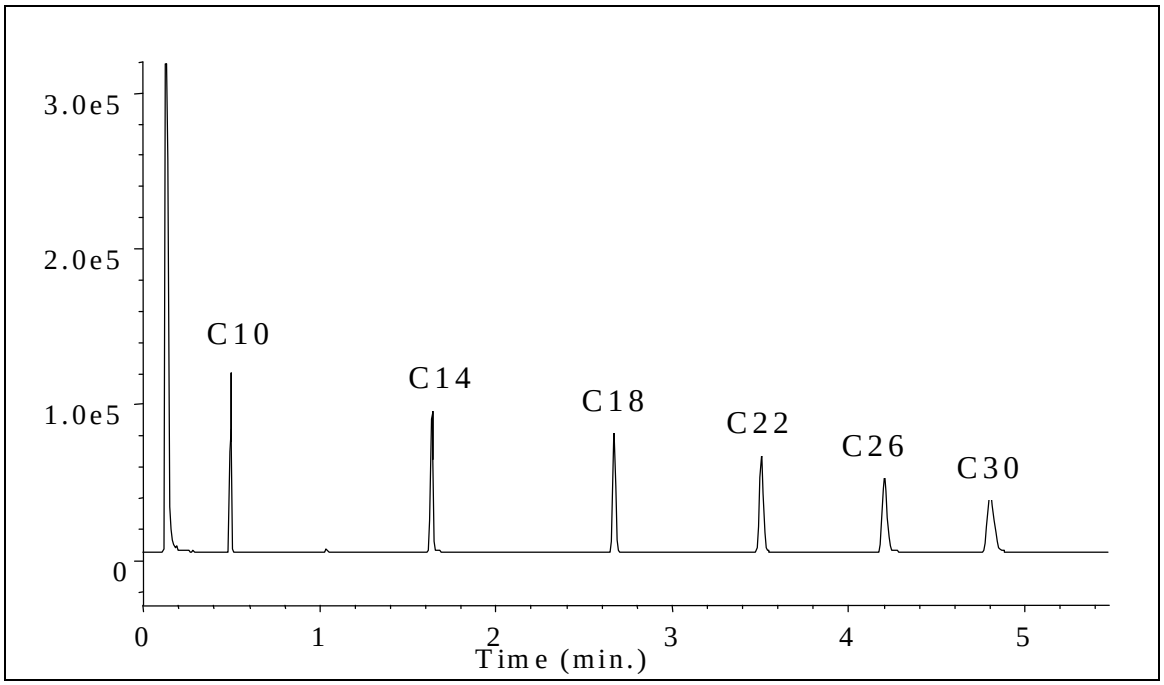

Figure 46. 48 °C/min Temperature Programming Rate

Conditions: Rtx-5, 5 m x 0.32 mm i.d., 0.25 µm d_f, helium at 4.2 mL/min, 1 µL, split 87:1

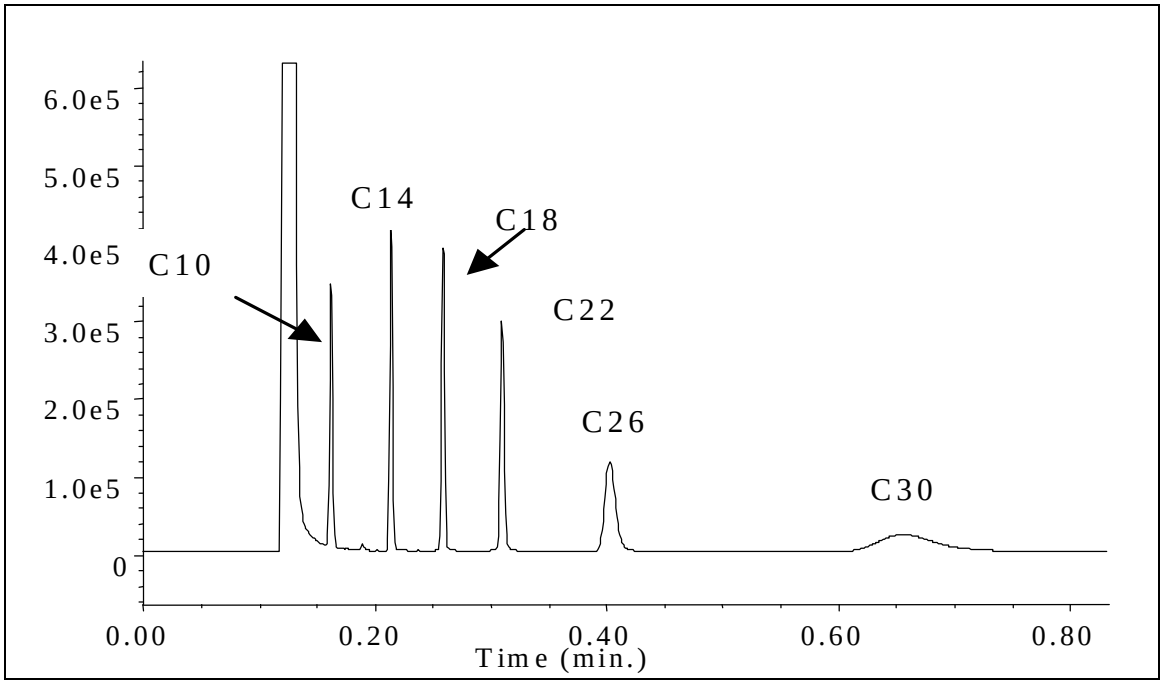

Figure 47. 1200 °C Temperature Programming

Conditions: Rtx-5, 5m x 0.32 mm i.d., 0.25 µm d_f, helium at 4.2 mL/min, 1 µL, split 87:1

In Figure 47 the broad peak shape of C30 illustrates the fact that most of the separation occurs isothermally at 300 °C. In this portion of the experimental work the effects of fast temperature programming on various chromatographic parameters has been shown. No unusual results have been found. In light of this work, the use of fast temperature programming is encouraged whenever possible. With a wide range of boiling points it is possible to program to fast with a given length of column. The column length must be reduced or the temperature programming rate decreased to obtain acceptable peak shapes.

Experimental II

The second part of this work compares results obtained on various GC systems. The systems used for this work were a HP (Wilmington, DE), model 6890 GC, a PE (Norwalk, CT), Autosystem XL, and an HP model 5890 GC equipped with an EZFlash™ attachment from Thermedics (Chelmsford, MA). The results were obtained over the past three years in our research group. Some of this work has recently been published by Reed *et al.*[35]

Results II

The first sample investigated was a normal alkane mixture sample, nonane through heptadecane. The traditional chromatograms shown below were obtained by a research group member who had run the sample and developed a good method from his or her perspective. No claim of speed optimization was made for some of these methods. The first chromatogram, (Figure 48), was obtained by Dr. Marisa Bonilla while working on an industrial project in our laboratory in 1996. The column used was an HP-5, 15 m x 0.25 mm i.d., 0.25 μm d_f. The analysis time was 10 minutes.

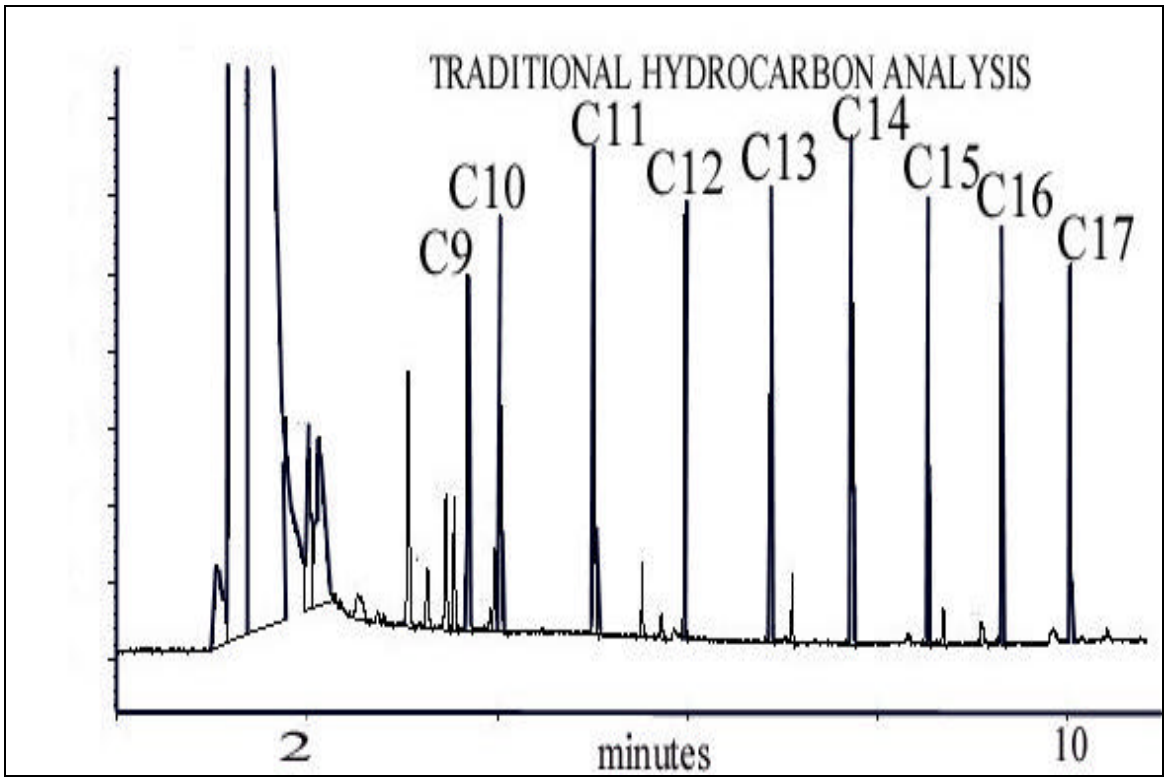

Figure 48. Traditional Hydrocarbon Analysis

Conditions: HP-5, 15 m x 0.25 mm i.d., 0.25 μm d_f, helium carrier gas

The next chromatogram (Figure 49) was obtained by Karen Clark-Baker while working on her Masters thesis, in 1996.[101] The column used was a 1 m x 0.1 mm i.d., 0.17 μm d_f. She was able to reduce the analysis time of the alkane mixture shown in Figure 49 to less than 1 minute by using a shorter column, smaller i.d. and thinner film as well as faster temperature programming rates and higher split ratios. The temperature program used was the maximum possible when using the HP model 6890, 240 V GC system. The temperature program was 85 °C for 0.1 min, 95 °C/min to 115 °C, 65 °C/min to 150 °C.

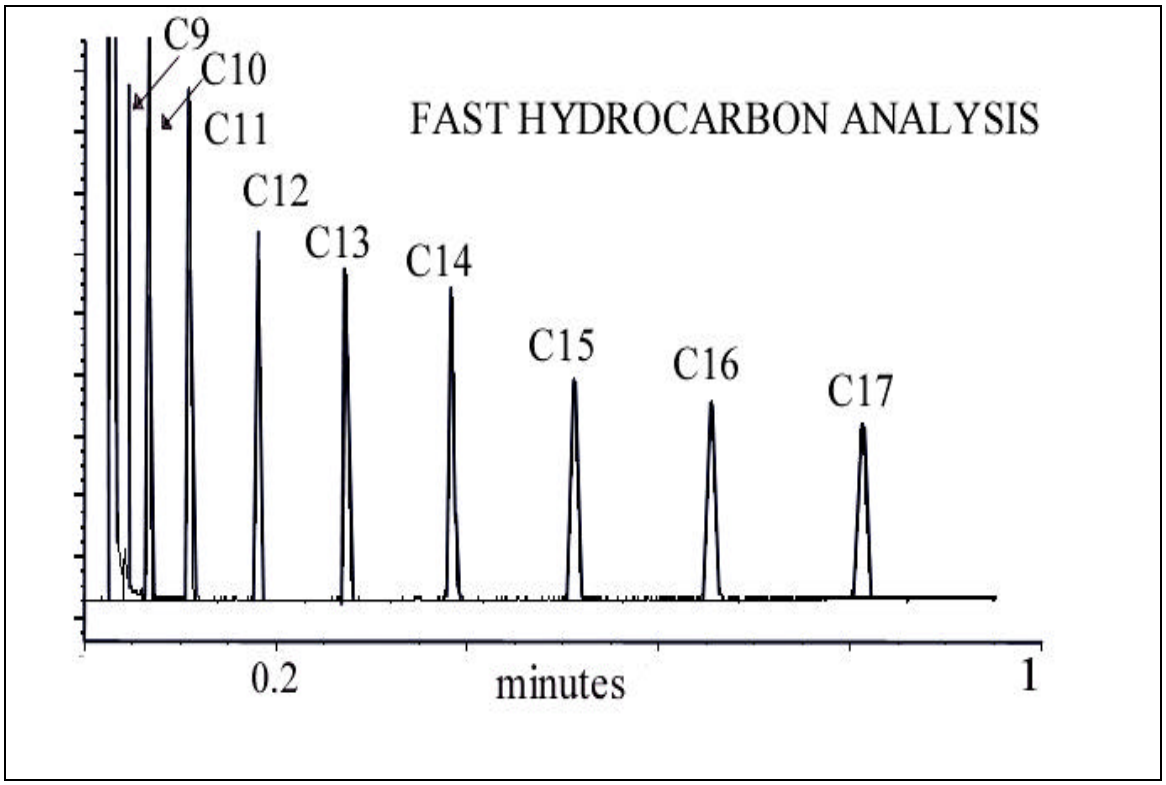

Figure 49. Fast Analysis of Hydrocarbons Using a Conventional System, (95 °C/min)

Conditions: HP-5, 1 m x 0.1 mm i.d., 0.17 μm d_f, oven temperature program – 85 °C for 0.1 min, programmed at 95 °C/min to 115 °C, then 65 °C/min to 150 °C

The space between the peaks, especially the higher molecular weight peaks is evidence for the need to have faster temperature programming rates. That was the limiting factor for the analysis speed for the chromatogram shown in Figure 49.

The next chromatogram (Figure 50) was obtained using an HP 5890 GC equipped with an EZFlash™ from Thermedics, 1999. The column is a Rtx-5, 5 m x 0.32 mm i.d., 0.25 μm d_f. The analysis time is less than 10 seconds, a dramatic decrease in the analysis time. This decrease was brought about mostly by the increased temperature programming rates and not by flow rate and not with column dimensions such as film thickness and internal diameter. The length was reduced to 5 m and the temperature program used was 60 °C, then 1152 °C/min. to 300 °C.

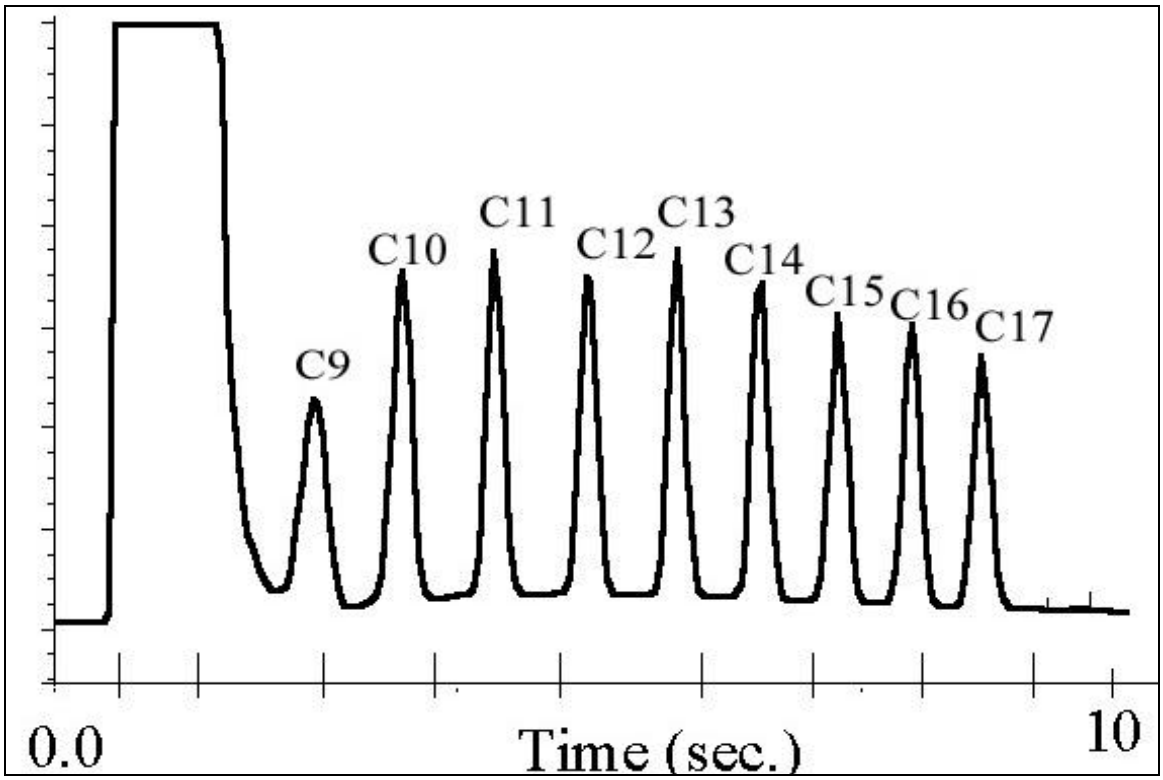

Figure 50. Hydrocarbon Analysis Using Fast Oven Temperature Programming (1152 °C/min)

Conditions: Rtx-5, 5 m x 0.32 mm i.d., 0.25 μm d_f, helium carrier gas, oven temperature program – 60 °C programmed at 1152 °C to 300 °C

The data for the retention times and the resolution for all three chromatograms is shown in Table 24.

Table 24. Comparison of Retention Times and Resolution for Three Different Systems

	RETENTION TIMES, MIN			RESOLUTION		
	Fig 50	Fig 49	Fig 48	Fig 50	Fig 49	Fig 48
C9	0.040	0.046	3.102		4.87	8.40
C10	0.054	0.067	4.073	2.33	5.08	23.82
C11	0.068	0.109	5.063	2.93	8.38	27.81
C12	0.083	0.181	6.018	2.93	11.40	28.08
C13	0.097	0.274	6.924	2.80	12.37	26.97
C14	0.110	0.384	7.780	2.60	12.67	26.55
C15	0.122	0.512	8.590	2.40	12.39	24.74
C16	0.133	0.654	9.358	2.27	11.31	23.87
C17	0.144	0.812	10.086	2.13	11.02	22.17

It can be seen that there is about a 10 fold decrease in analysis time from the analysis in Figure 48 to the fast analysis shown in Figure 49 and about a 100 fold decrease in analysis time for the rapid temperature programming analysis shown in Figure 50. The resolution decreases from an average of 23 for Figure 48, to an average of 10 for Figure 49 and to an average of 2.2 for Figure 50. The peaks in the chromatogram shown in Figure 50 are not as Gaussian as Figure 48 and Figure 49. At the very fast temperature programming rates less reproducibility was seen in the peak areas and widths as was shown in the first part of this chapter. This may be due to the rate of data collection. The maximum collection rate was 20 Hz for the FID used to obtain the data in Figure 50. The significance of the data rate will be discussed in more detail, later in this chapter.

The next standard analyzed was a polycyclic aromatic hydrocarbon (PAH) sample. The list of compounds is shown in Table 25.

Table 25. List of PAHs

Compound #	Name
1	Naphthalene
2	Acenaphthalene
3	Acenaphthene
4	Fluorene
5	Phenanthrene
6	Anthracene
7	Fluoranthene
8	Pyrene
9	Benzo(a)anthracene
10	Chrysene
11	Benzo(b)fluoranthene
12	Benzo(k)fluoranthene
13	Benzo(a)pyrene
14	Indeno(1,2,3-cd)pyrene
15	Benzo(ghi)perylene
16	Dibenzo(ah)anthracene

This sample is a typical environmental sample for EPA method 610. The critical pairs as far as resolution is concerned and as defined by the EPA are peak pairs 5 and 6, 9 and 10 and 14 and 15. Peaks 11 and 12 are defined as a non-critical peak pair. The first chromatogram (Figure 51) was published by Dr. Yuwen Wang in his Ph.D. thesis, 1997.[102] The chromatogram was obtained using a PE-1, 30 m x 0.25 mm, 0.25 μm d_f column. The analysis time was 35 minutes.

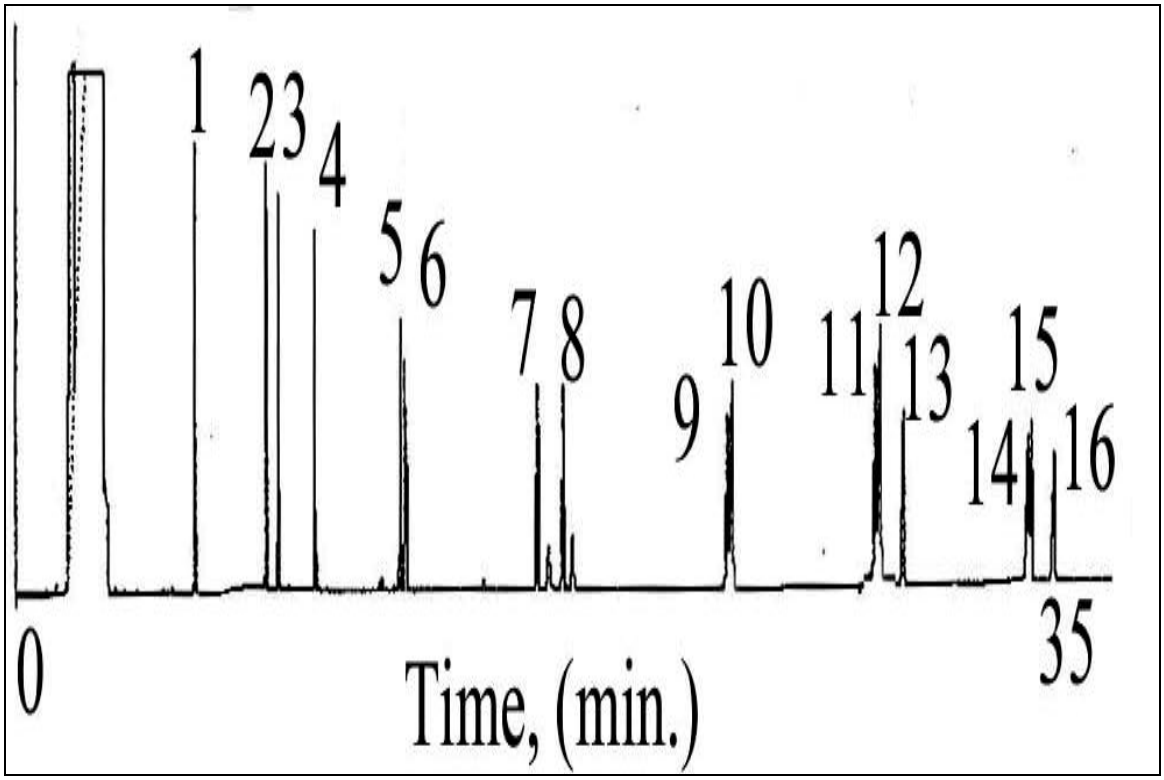

Figure 51. Conventional Analysis of PAHs

Conditions: PE-1, 30 m x 0.25 mm i.d., 0.25 μm d_f, helium carrier gas, see peak identity in Table 25

It is evident in this chromatogram that the critical pairs mentioned earlier are difficult to resolve.

A faster analysis of this PAH sample (Figure 52) was attempted by Karen Clark-Baker, while working on her Masters thesis in 1996, with a conventional system using an HP-5, 1 m x 0.1 mm, 0.17 μm d_f column.

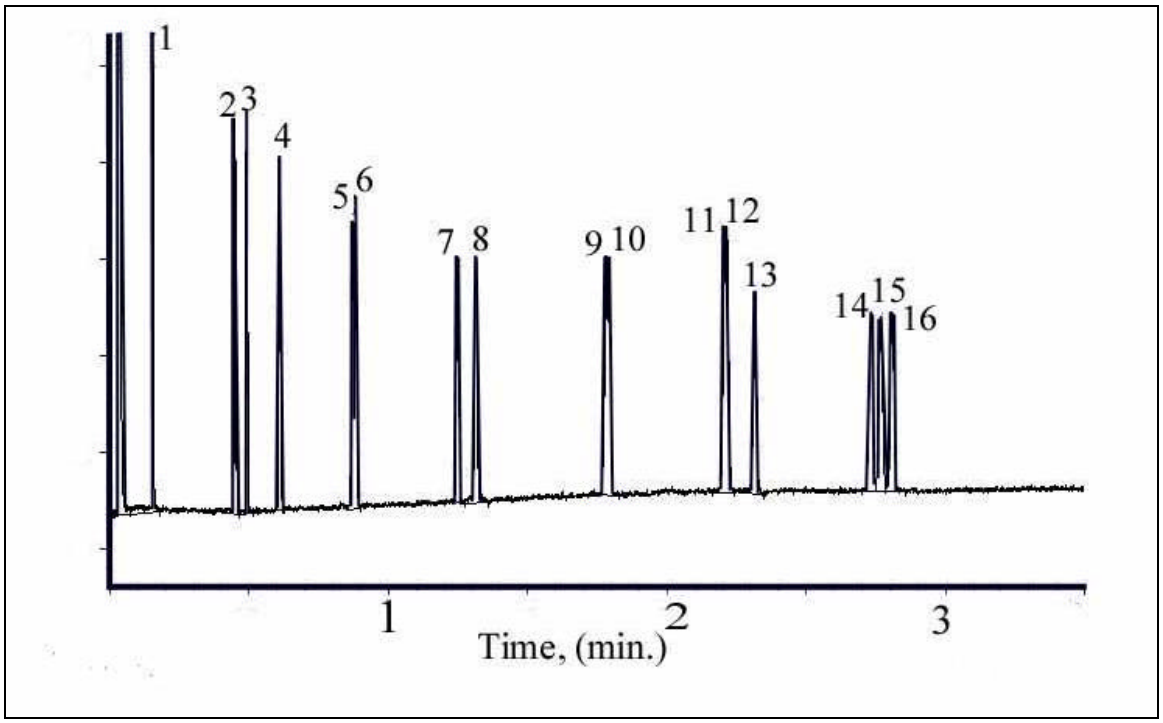

Figure 52. Fast Analysis of PAH Sample Using a Conventional System

Conditions: HP-5, 1 m x 0.1 mm x 0.17 μm d_f, see list for peak identity in Table 25

It can be seen that the analysis time was significantly reduced, however, the resolution between the critical peak pairs did not improve, in fact, the resolution between the critical pairs decreased for all but one of the critical pairs (Table 26).

Finally, the same PAH sample was analyzed using the EZFlash™ system, (Figure 53).

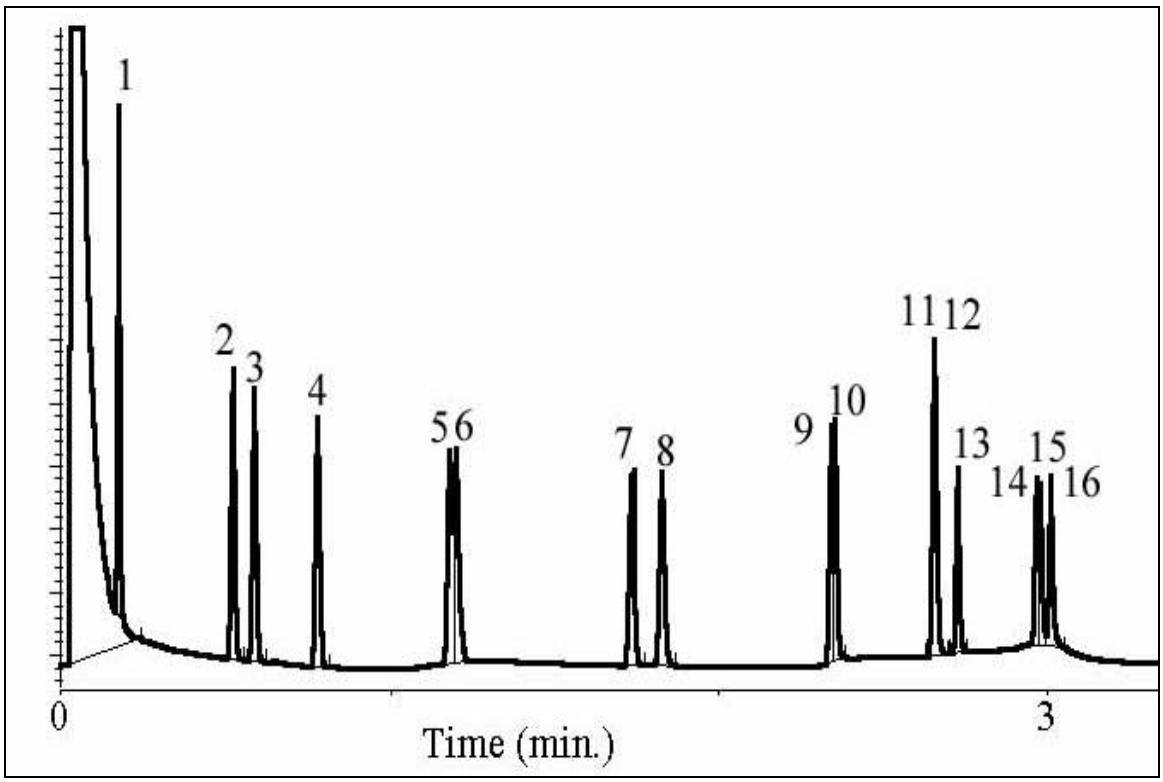

Figure 53. EZFlash™ Analysis of a PAH Sample

Conditions: 3 minute analysis using a Rtx-5, 5 m x 0.32 mm, 0.25 µm d_f column, initial temperature - 100 °C, programmed at 50 °C/min. to 250 °C, then 325 °C/min to 325 °C, held 0.3 min., 0.5 µL injection, split 60:1, see list of peak identities in Table 25

The EZFlash™ analysis time was much faster than Figure 51, but the same as Figure 52. The resolution was the same as the resolution achieved with the fast analysis on a conventional system (Figure 52). A tabulated comparison of the retention times and the resolutions for the three different methods of analyses for the PAHs is shown in Table 26.

Table 26. Polycyclic Aromatic Hydrocarbons, Comparison of Methods

	Retention Time, (min)			Resolution		
	Fig 53	Fig 52	Fig 51	Fig 53	Fig 52	Fig 51
1	0.18	0.16	6.15			
2	0.53	0.45	8.66	24.49	39.95	52.93
3	0.60	0.49	9.91	3.39	4.45	7.99
4	0.79	0.61	10.41	9.17	11.55	22.90
5	1.19	0.87	13.43	17.87	21.62	43.50
6	1.21	0.88	13.63	0.81	0.95	2.37
7	1.74	1.25	18.27	21.97	26.47	54.81
8	1.83	1.32	19.14	3.68	4.33	9.25
9	2.34	1.78	24.79	23.72	16.20	48.29
10	2.35		24.96	0.55	N.R.	1.26
11	2.66	2.22	29.67	14.54	10.75	35.40
12			29.79	N.R.	N.R.	1.02
13	2.73	2.32	30.89	3.50	3.33	9.45
14	2.97	2.73	35.25	15.09	16.21	30.32
15	2.98	2.77	35.37	0.63	1.39	0.85
16	3.01	2.81	36.18	1.89	1.65	5.71

*N.R. – not resolved

This sample involved critical pairs. The critical peak pairs are shown in entries 6, 10, and 15 of Table 26. The retention time was reduced from 36 minutes for the conventional analysis (Figure 51) to 3 minutes for the fast analysis (Figure 52) with a conventional system and for the analysis with the EZFlash™ (Figure 53). This is a reduction of 10 fold in the analysis time. The resolutions for the critical pairs on the conventional system are not good, two values are below 1.5 (baseline resolution). For the faster analyses, the resolutions are generally worse except for Figure 52 (line 15) where the resolution actually increases for the fast analysis on the conventional system. It has been proposed that this is due to the fact that the analysis was done with a different stationary phase (HP-1 rather than HP-5) which may have shown more selectivity.

The PAH sample is different from the hydrocarbon sample discussed earlier. The hydrocarbon analysis time was decreased while maintaining acceptable resolution for all peaks in the analysis. This was not possible for the PAH sample. Does this negate any value that fast programming can provide for the analysis? In most cases, no. For an

environmental sample, of which PAHs are an example, doing fast analyses for screening work could bring about great savings in time. There are often many samples to be run to confirm the presence or absence of a certain set of compounds. By doing an analysis in three minutes, it could quickly be determined if the sample needed further attention or not. The other possibility with a sample like the PAH sample where there is a problem of resolution is to use the mass spectrometer as the detector in the selected ion monitoring (SIM) mode to achieve the remainder of the resolution needed.

Using the mass spectrometer also introduces a means to increase the analysis speed due to the column outlet being under vacuum conditions rather than atmospheric pressure (Chapter 2). Two problems with using the mass spectrometer are that the sensitivity of the mass spectrometer can be reduced when using an increased flow rate (due to the vacuum pump speed limitations) and the relatively slow scan rate of benchtop quadroupoles (less than 10 scans/second). If it is desirable to operate the system in the SIM mode, it is important to ensure that the compounds that are partially co-eluting have ions characteristic of each peak, but ions that do not appear in the partially co-eluting peak. This is a problem in the PAH sample. The first critical pair has ions that are identical to one another, however the last critical pair does not and it is possible to use SIM to fully quantitate these two peaks.

The next few figures are examples of PAH analyses obtained using the mass spectrometer. Figure 54 was obtained using a standard method of analysis[103] except that helium was used as the carrier gas at 1 mL/min and the mass spectrometer was used as the detector scanning from 40 to 500 amu.

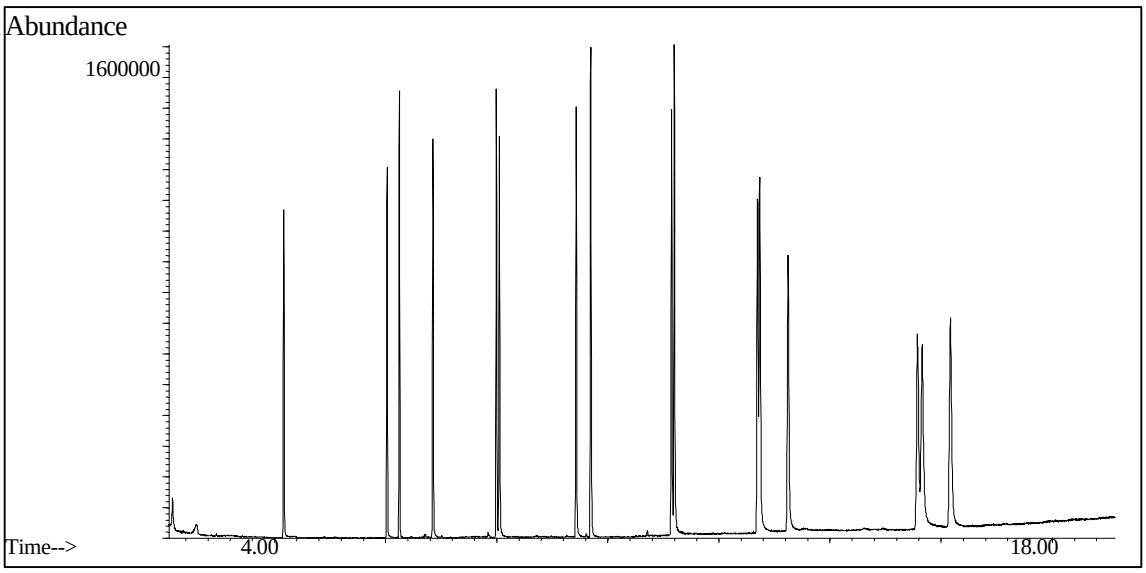

Figure 54. Standard Analysis of PAH Sample

Conditions: HP-5, 30 m x 0.25 mm, 0.25 μm, 1 μL, split 25:1, oven - 80 °C for 1 min., 20 °C/min to 280 °C, 2.5 °C/min to 300 °C, Helium at 1 mL/min, mass spectrometer – scan 40 to 500 amu

The peak height of the largest peak is around 1,600,000. To decrease the analysis time, the temperature programming rate and the initial temperature were increased. The TIC for this analysis is shown in Figure 55.

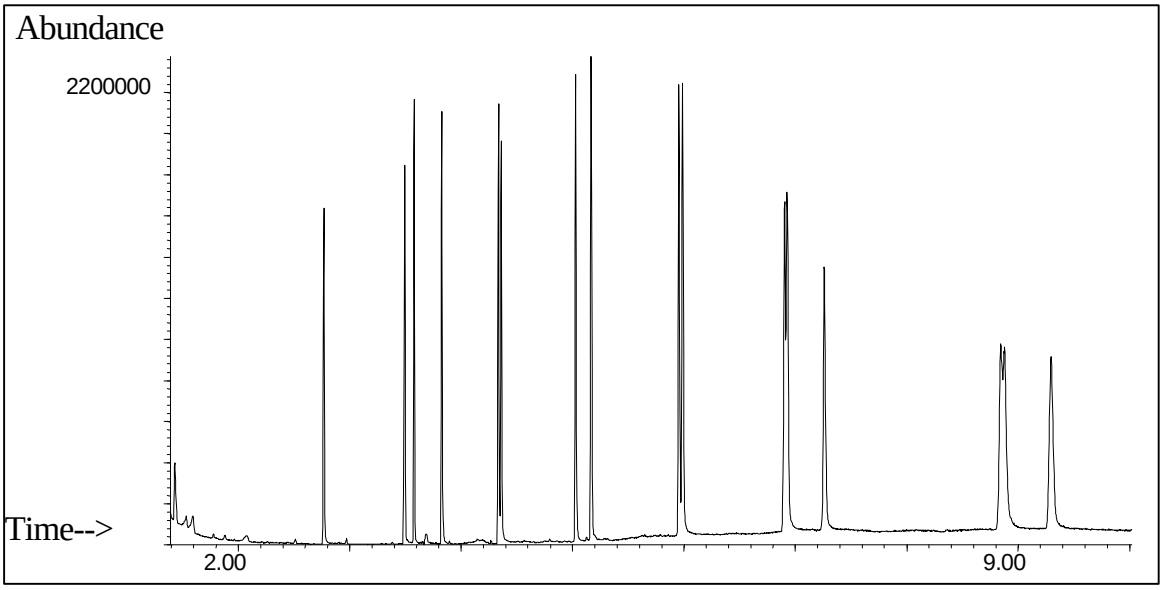

Figure 55. Increased Temperature Programming Rate PAH Analysis

Conditions: Same as Figure 54, but oven – 100 °C, 45 °C/min to 300 °C

The peak height of the largest peak is around 2,200,000, which is an increase from the previous analysis. The analysis time has also decreased from 17 min to 9.5 min., along with an expected decrease in the resolution of some peaks. Because the peak heights have increased it would be possible to inject a smaller amount of sample and maintain the signal to noise ratio seen in Figure 54 and increase the resolution of the peaks. Figure 55 is the same conditions as Figure 54, but the flow rate is doubled.

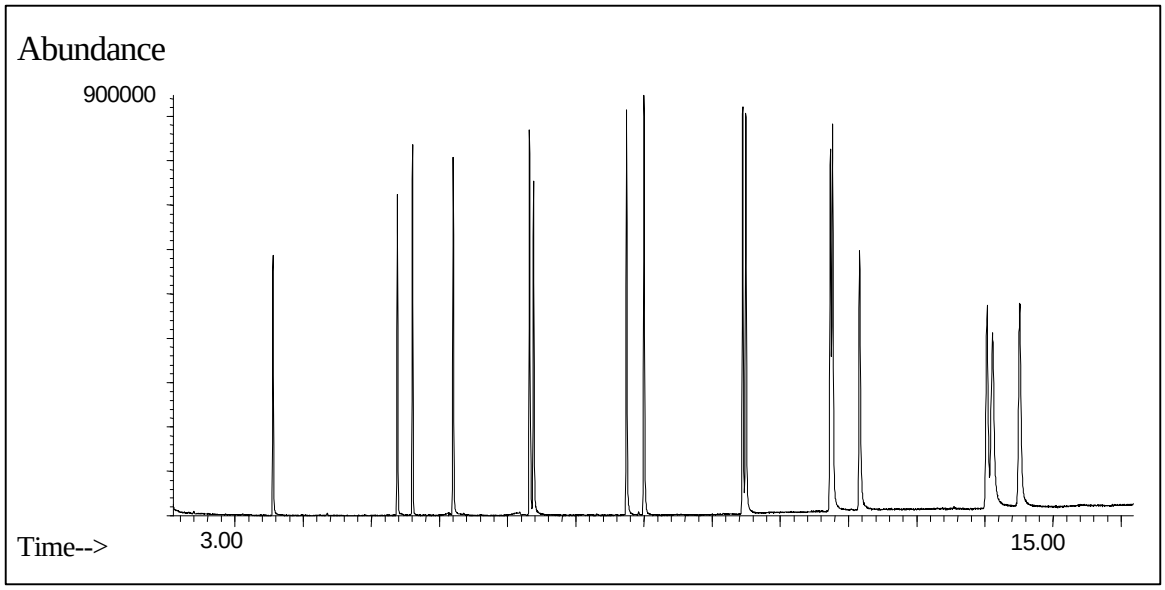

Figure 56. Increased Flow Rate Analysis of the PAH Sample

Conditions: Same as Figure 55, but the flow rate is 2 mL/min

When the flow rate is doubled, the largest peak has an abundance of 900,000, which is almost half of what was seen in Figure 54. The analysis time was decreased by about 1.5 minutes from Figure 54. The peaks are still not all well resolved, although they are better resolved than with the fast temperature programming. The conclusion to be drawn from the last three figures is that temperature programming is the best method to decrease the analysis time with the mass spectrometer rather than increasing the flow rate. Increasing the flow rate does decrease the analysis time slightly, but leads to decreased sensitivity.

The effect of the data collection rate was evaluated to investigate its effect on fast GC. A sample of benzene, toluene, ortho, meta, and para-xylene, and ethylbenzene was analyzed on the HP model 6890 GC. This instrument has data collection rates of 5, 10, 20, 50, 100 and 200 Hz. The column was an HP-5, 1 m x 0.1 mm, 0.1 μm d_f. The

temperature was 30 °C, with a flow rate of 1 mL/min of helium. The FID was used as the detector. 1 µL of sample was injected with the autosampler at a split ratio of 599:1. An overlay of the benzene peak at 4 different data collection rates is shown in Figure 57.

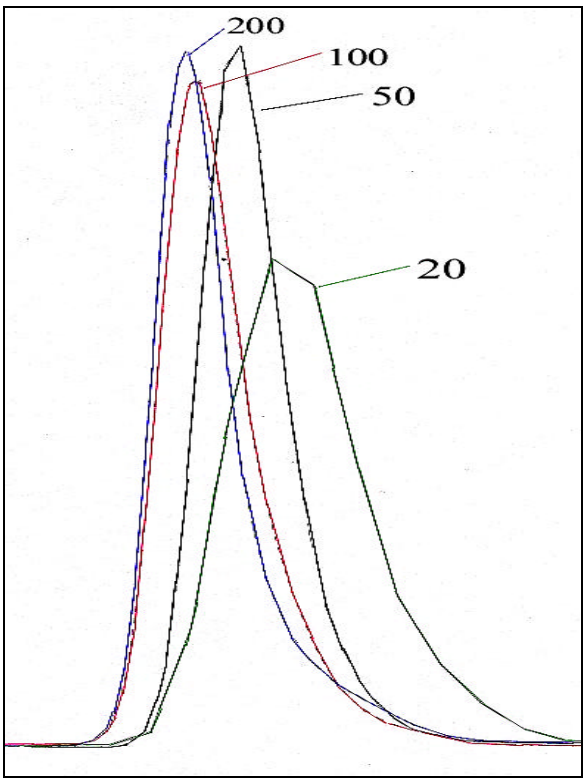

Figure 57. Effect of Data Collection Rate on Peak Shape

Conditions: HP-5, 1 m x 0.1 mm, 0.17 µm d_f, 30C, helium at 1 mL/min, 1 µL split 599:1

It appears that the data collection rate at 20 Hz significantly affects the peak shape. It is much shorter and choppier than the peaks obtained using 50, 100 or 200 Hz. Comparing the peak heights at the various data collection rates graphically demonstrate this effect. (Figure 58). There is little difference between 50, 100 and 200 Hz sampling rates

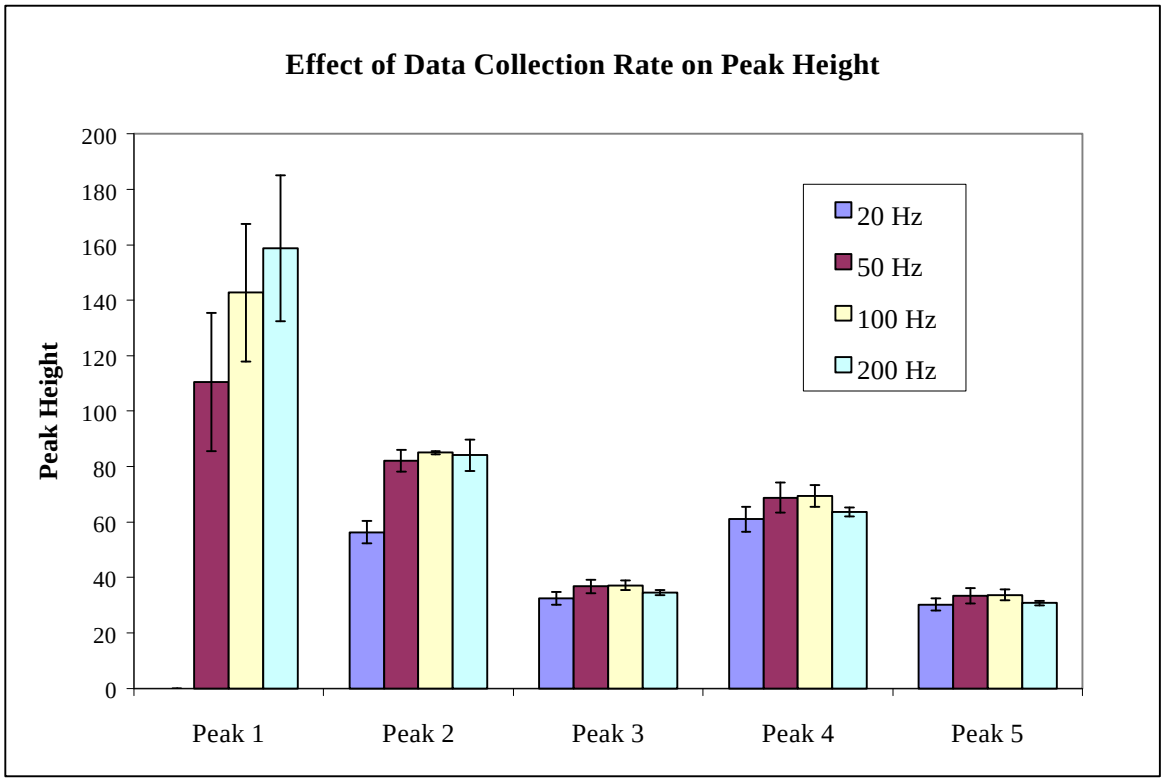

Figure 58. Effect of Data Collection Rate on Peak Height

Conditions: same as Figure 57. peaks – benzene, toluene, ethylbenzene, m and p-xylene co-eluting and o-xylene

No data was available for Peak 1 at 20 Hz. Probably peak 1 was co-eluting with the solvent. For the remainder of the peaks, the peak height increases slightly with sampling frequency except for 200 Hz, which is slightly lower than 100 Hz. Statistically only peak 2 is different in peak height from 20 to 50 Hz. The remainder of the peaks are statistically the same at the 95% confidence level using the 2-tailed, form 2 of the *t*-test. H_o is that the peak areas are not statistically different and H_1 is that the peak areas are statistically different (Table 27).

Table 27. Statistical Analysis of Peak 2 Heights at Various Data Collection Rates

Data is for peak 2 in Figure 58. (n = 6)

Sampling Rate, Hz	Statistical Analysis
20 to 50	$t_{calc} = 7.97 > t_{tab} = 2.78$, $\therefore$reject H_o
50 to 100	$t_{calc} = 1.25 < t_{tab} = 2.78$, $\therefore$accept H_o
100 to 200	$t_{calc} = 0.27 < t_{tab} = 2.78$, $\therefore$accept H_o

The results shown in Table 27 are for peak 2. Similar results are found for the remainder of the peaks. A statistical difference is found from 20 to 50 Hz, however from 50 to 100 Hz and from 100 to 200 Hz there is no statistical difference. Graphically, the results show a small increase in peak height, but it is not a statistically different. It is also important that the peaks showing the significant differences from 20 to 50 Hz are at the lowest retention times (peaks 1 and 2). This indicates that analysis times in seconds must be done with a data collection rate of 50 Hz or greater. This suggests that Figure 50 may look different if the data was collected at 50 Hz rather than 20 Hz. Unfortunately, it was not possible to repeat this experiment due to a broken column.

Similar results are found for the peak areas. The peak areas appear to increase from 20 Hz to 50 Hz and then decrease for 100 and 200 Hz. These changes are seen graphically; however, none of the numbers are statistically different at the 95% confidence level.

The effects of the data collection rate on the resolution are also similar. There is a slight increase in the resolution from 20 Hz to 50 Hz to 100 Hz and 20 200 Hz for peak pairs 2-3, 3-4 and 4-5. For peak pair 2-3, there is a statistically significant increase from 20 Hz to 50 Hz at the 95% confidence interval. Once again, indicating that the shorter the retention times, the more important it becomes to use a fast data rate.

Conclusions

In this chapter temperature programming has been shown to be a good way for decreasing the analysis time. This parameter has been ignored in many studies, but it offers valuable time savings with some added benefits. It is important to ensure that the

data collection rate is fast enough for peaks with low retention times in order to ensure good reproducibility of all peak parameters. It has been shown that using fast temperature programming is a better way than using faster flow rates to decrease the analysis times. This is particularly valid for the mass spectrometer where faster flow rates dilute the sample and result in higher detection limits. Temperature programming rates can reach a magnitude where they actually decrease the usefulness of the chromatographic results (i.e. poor precision, and loss of resolution). Temperature programming may offer a fast way to do screening of samples as was shown with the PAH sample. Finally, fast temperature programming offers benefits with sample capacity issues that can not be obtained when using smaller internal diameters. Shorter columns with typical internal diameters and film thicknesses can be used, without much loss in sample capacity.

Temperature programming is a good way to do fast GC analyses and should be utilized more than it is currently.

Chapter 5 - Applications of Fast GC

Introduction

In Chapters 3 and 4, the effects of the reduced internal diameter and the use of fast temperature programming rates were discussed. These are fundamental aspects of fast GC. This chapter presents research on some applications of fast GC. Fast GC analyses must be demonstrated to be reliable and rugged for more complex samples. Complex samples often introduce sample preparation problems. A major criticism of fast GC, heard from practicing chromatographers, is that it does not matter if the analysis time is decreased from 45 minutes to 5 minutes if it still takes 2 hours to prepare the sample for the analysis. First, it is true that sample preparation has a long way to go to reach the capabilities of fast GC. Secondly, even if your sample preparation remains lengthy, a faster analysis will yield some benefits. These benefits include the capability of analyzing the sample multiple times in the same time period, which would make it possible to better determine the analytical results and the error involved in the measurement. It would also allow more time to run standards and to prepare better calibration curves.

The objective of this chapter is to show that a fast analysis and a fast sample preparation method could be developed that provided quantitative data for a "real-world" sample while maintaining the integrity of the analysis. These results will help demonstrate the applicability and validity of fast GC. The analysis that was chosen to demonstrate the applicability and the validity of fast GC, is the analysis of 2,6-di-(tert-butyl)-4-methylphenol, commonly known as butylated hydroxytoluene or BHT, in chewing gums and breakfast cereals. The sample preparation method used was microwave assisted extraction (MAE).

BHT

BHT is an antioxidant that is added to various food products, food packaging, oils, and soaps. BHT is controlled by the FDA as a food additive and preservative. The maximum concentration of BHT in food products with a moderate to high fat content is 0.02% of the fat content. The limit for foods containing small amounts of fat is 50 ppm.[104] The FDA classifies BHT as a generally-recognized-as-a-safe compound (GRAS compound) in low dosages. However, some studies[105,106] have found correlations between BHT and some health problems. In these studies large quantities of BHT were given to the test subjects. In addition, the International Agency for Research on Cancer, part of the World Organization of Health (WHO) considers BHT to be carcinogenic, due to the ability of the chemical to accumulate in the body. Regardless of its debatable toxicological effects, as a food additive, it is required that its concentration is controlled and that a method of analysis exists to quantitatively analyze the food product for the compound.

Methods

Currently many of the methods, including the Association of Official Analytical Chemists (AOAC) methods, for the analysis of BHT in food samples require a lengthy extraction process involving large quantities of organic solvents. The official AOAC chromatographic analyses are done on a packed GC column or by HPLC. Very few of the published methods use capillary GC. One study that uses a capillary GC analysis method is by Greenberg, *et al.*[107] They converted a packed column GC method to a capillary column GC method for the analysis of BHT in chewing gum. The sample preparation method was a 16 hour solvent extraction with shaking and the GC analysis time was over 60 minutes. Manura[108] used a short path thermal desorption instrument as the sample preparation method followed by a 30 minute capillary GC analysis for BHT in chewing gum and breakfast cereals. Thermal desorption as the sample preparation method significantly decreased the sample preparation time to about 15 minutes per sample. Thermal desorption improved the sample preparation time problem, however,

was is only possible to desorb one sample at a time and each desorption took about 10 minutes plus the time involved in preparing the sample. A sample preparation method that could extract multiple samples simultaneously would decrease the sample preparation time even further. A method that meets this criterion is microwave assisted extraction (MAE). MAE is an extraction method that uses microwave energy as the heat source for the extraction. The MES model 1000 from CEM Microwave Innovators, (Matthews, NC) is a closed system that allows up to 12 extractions simultaneously.

Microwave Extraction[109]

Microwave extraction is based on the interaction between microwaves and the permanent dipoles of molecules. Microwaves, which are 1 m to 1 cm (300 MHz to 30 GHz respectively) in wavelength[110], interact with the dipoles of the molecules. Chemistry applications use microwaves at 2.45 GHz or 900 MHz. The rate at which the heating of the sample occurs is due to three factors. These factors are the dielectric constant or real permittivity, ε', the dielectric loss, ε", and the dissipation factor, tan δ. The dielectric constant describes the ability of a molecule to be polarized by an electric field[110] and is a function of the frequency and the temperature. The dielectric loss factor describes how well the sample material can convert electromagnetic energy into heat and finally, the dissipation factor is a measure of the ability of a material to convert electromagnetic energy into other forms of energy at a given frequency and temperature. The dissipation factor or the dielectric loss tangent is the ratio of the dielectric loss to the dielectric constant. Not all materials with high dielectric permittivity exhibit a high loss factor. The two types of dielectric polarization that are involved in microwave frequencies are orientation polarization and space charge polarization. Orientation polarization is from the organization and disorganization that occurs as the microwaves are applied in pulses to the material[109] (Figure 59).

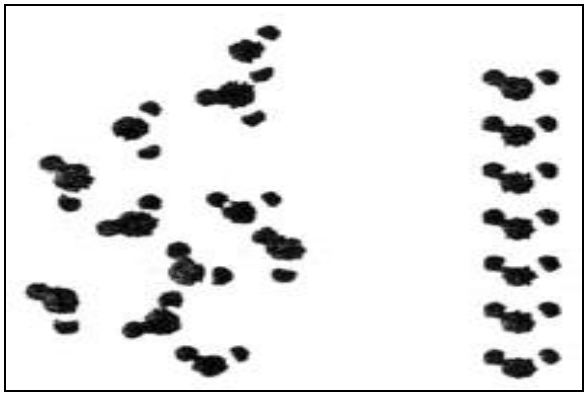

a b

Figure 59. Orientation Polarization: a) disorganized, no field applied; b) organized, applied field

Space charge polarization is when materials with free electrons have restricted movement. This causes entire regions to become charge polarized.[109] (Figure 60).

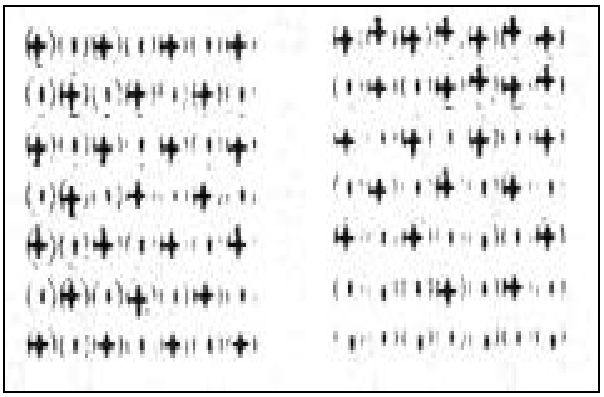

a) No electric field b) Applied Electric Field

Figure 60. Space Charge Polarization Under Applied Microwave Field

The alternating field in the polarization orientation varies cyclically with the field. At high frequencies, the inertia of the molecules lags behind the field. This lag leads to

absorption of energy and Joule heating. The rate at which the temperature will rise is calculated from eq. 45.[109]

$$\frac{dT}{dt} = \frac{cnst * e'' * f * E^2}{r * C_p} \tag{45}$$

dT/dt = rate of temperature change

e" = dielectric loss, Hz

f = frequency of the electromagnetic field, Hz

E = electric field intensity

r = density of the material, g/mL

C_p = specific heat capacity, cal/g* °C

In organic liquids as well as in solids the dissipation factor rises with temperature. The degree of heating depends only on the dielectric properties of the processed material so that it is possible to target specific analytes. A final parameter of interest is the penetration depth. This is the depth into a material where the power falls to ½ of its surface value.[110] It can be described by eq. 46.[110]

$$D_p \propto l_o \sqrt{\frac{e'}{e''}} \tag{46}$$

D_p = penetration depth, cm

l_o = wavelength of the radiation, cm

e' = dielectric constant, Hz

e" = dielectric loss, Hz

Different materials have different penetration depths and this affects the heating of the sample.

There is an increased speed of reaction rates and extraction efficiency when using microwave energy versus conventional heating methods. For a closed vessel system temperatures higher than the normal boiling points of the solvents can be reached due to

the increased pressures. Another theory is that the increased reaction and extractions rates are partially due to localized superheating.

Generally, the mass transport of the analyte is increased at the higher temperatures leading to faster diffusion of the analyte into the extraction solvent. These are the basic principles of MAE.

Applications

One of the first to use microwave extraction was Ganzler.[111] She worked with plants and food materials and found extraction efficiencies comparable to Soxhlet and shaking methods, however, the microwave method was much faster.[112] Microwave extractions have also been used to extract antibodies from red blood cells;[113] to rapidly separate stabilizers from plastics with greater than 90% recovery;[114] and to extract polycyclic aromatic hydrocarbons from soil samples.[115] MAE degradation of analytes is a potential problem according to some researchers. Lopez-Avila showed that the recoveries for some pesticides were reduced in the presence of soil, but not in the absence of soil.[116] Shape, dimensions and water content all affect microwave extraction efficiencies for different applications. The types of samples involved in this work are food samples. The dielectric is an important parameter of the molecule as seen in the previous discussion when working with microwaves. The dielectric properties vary with different types of food products.[117] In addition to interaction with the molecular rotation of the polar molecules, microwaves can also linearly accelerate the ions of salts in the food product. The use of microwave interactions with food products has largely been for testing or food processing, for example decreasing the moisture content. There has been little work done with extraction of analytes of interest from food products using microwave assisted extraction. For this reason and for the desired increase in the speed of sample preparation, microwave assisted extraction of food products is examined as a way to efficiently extract analytes from food products prior to a fast chromatographic analysis.

Extraction Parameters

The extraction parameters must be optimized for each sample type and matrix. This is because the matrix will cause interferences in the chromatographic analyses. When analyzing food, it is important to not "cook" the sample and generate more compounds in the matrix, but to heat the sample to order to extract the analyte of interest.

The parameters for the chewing gum sample to be optimized were the power, time, temperature, sample size and solvent. The power was set at 100% to get the maximum heating as fast as possible. The temperatures and pressures reached by the system are functions of the power applied and the dielectric properties of the solvent and the sample. Several different solvent systems were investigated. The Greenberg paper used toluene to extract the BHT and isopropanol to precipitate the gum base. The microwave vessels are not compatible with toluene, so toluene could not be used here. The solvent system that gave the best results with relatively clean chromatography and good extractions was a 9:1 mixture of hexane:isopropanol. The following chromatograms illustrate this point.

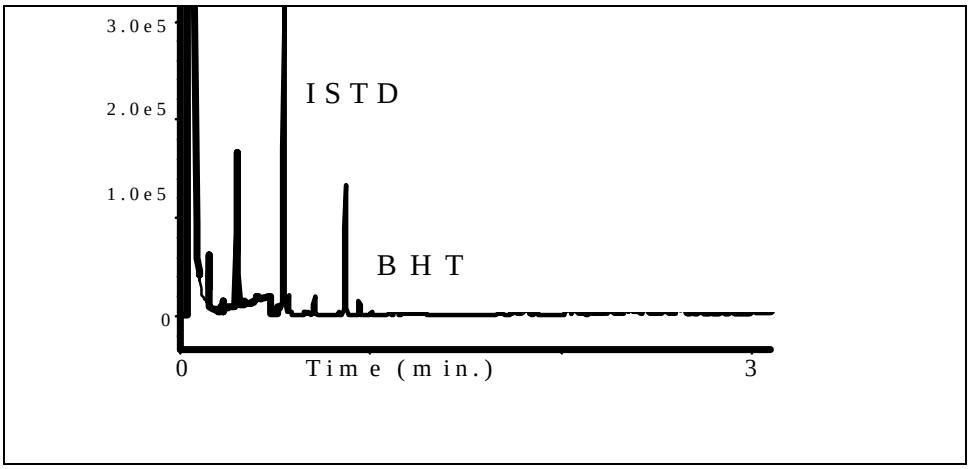

Figure 61. 9:1 Mixture of Hexane and Isopropanol

Conditions: 5 minute MAE extraction, Analysis - Rtx-5, 5 m x 0.32 mm i.d., 0.25 μm d_f, 8 psi He, 1 uL, split flow – 50 mL/min, oven temperature program – 60 °C program at 180 °C/min to 300 °C

Figure 61 shows the extraction of a chewing gum in a 9:1 hexane:isopropanol mixture. This extract gave the best results of the three solvents systems investigated. The baseline is relatively flat and there are no interferences that can not be separated from the internal standard and the BHT peaks. It also appears to have less high molecular weight compounds than the other two extracts. (Figure 62 and Figure 63)

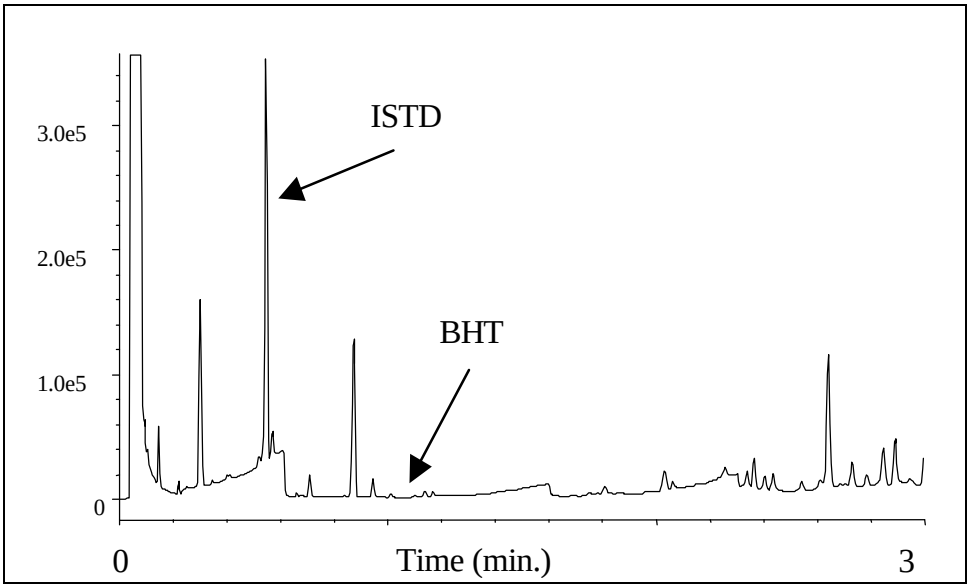

Figure 62. 1:1 Mixture of Hexane and Isopropanol

Conditions: 5 minute MAE extraction, Analysis - Rtx-5, 5 m x 0.32 mm i.d., 0.25 μm d_f, 8 psi He, 1 uL, split flow – 50 mL/min, oven temperature program – 60 °C program at 180 °C/min to 300 °C

Figure 62 is a chromatogram of the extract after a 1:1 hexane:isopropanol extraction. In this chromatogram the baseline is not nearly as flat and it be difficult to get good reproducibility on the internal standard peak. It also appears that more higher molecular weight compounds are being extracted.

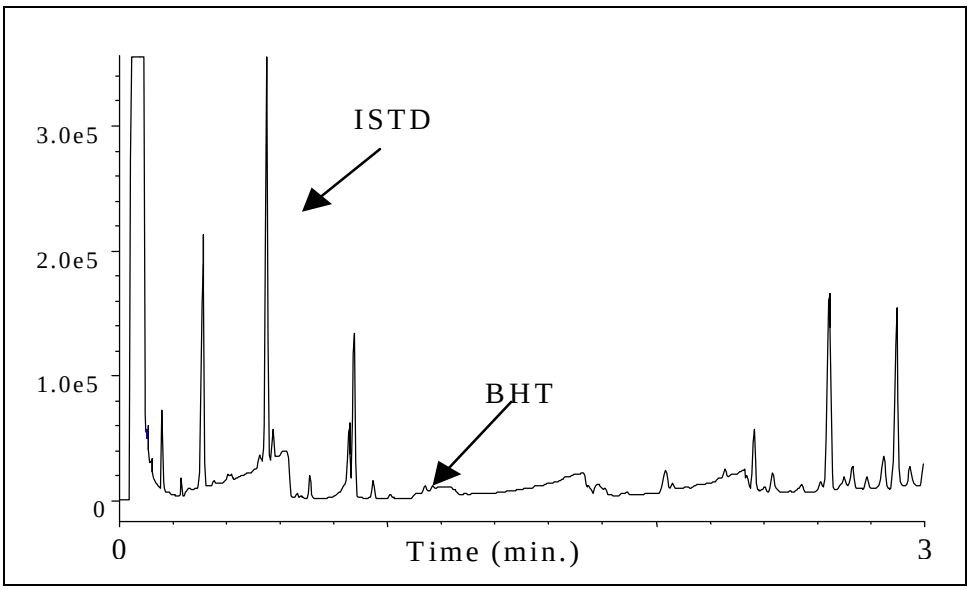

Figure 63. 1:9 Mixture of Hexane and Isopropanol

Conditions: 5 minute MAE extraction, Analysis - Rtx-5, 5 m x 0.32 mm i.d., 0.25 μm d_f, 8 psi He, 1 uL, split flow – 50 mL/min, oven temperature program – 60 °C program at 180 °C/min to 300 °C

Figure 63 shows the worst extract of all. The extract was obtained using a 1:9 mixture of hexane:isopropanol. The isopropanol is extracting too much of the matrix (extra peaks). Again, it would be hard to obtain reproducible peak areas for the internal standard and the BHT peaks in this chromatogram. There appears to be even higher molecular weight compounds extracted with this solvent system. The 9:1 hexane:isopropanol solvent system was chosen to do the extractions.

The next parameter to be optimized was the extraction time. For the chewing gum sample, a one, two, and five minute microwave time and a two minute shaking extraction time were compared. From an average of three trials at each extraction condition an extraction time of one minute was chosen (Figure 64).

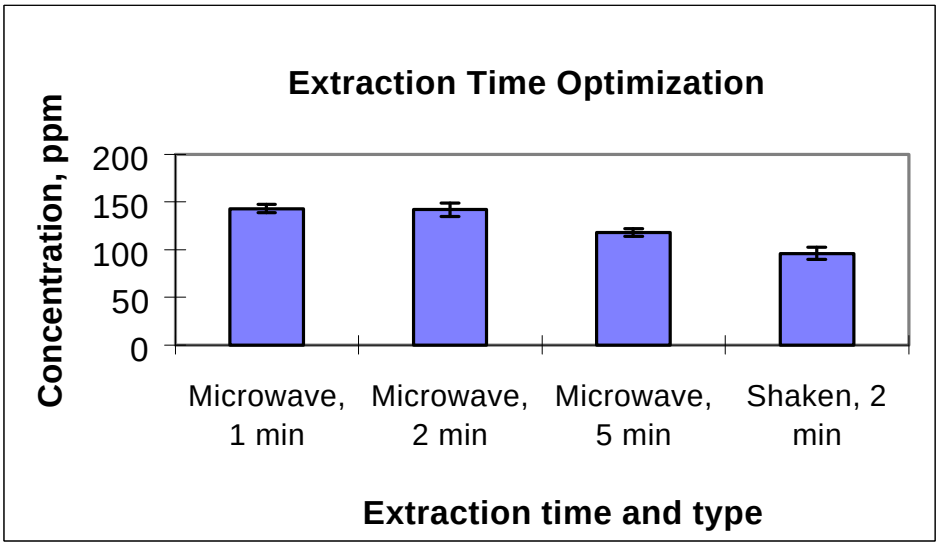

Figure 64. Extraction Time Optimization for Chewing Gum

Conditions: 0.1 g chewing gum extracted at 100% power in 5 mL 9:1 hexane:isopropanol solvent mixture, Analysis conditions in Table 33.

The two minute extraction, extracted a slightly higher concentration of BHT, than the one minute extraction. The standard deviation for the two minute analysis was also larger than for the one minute analysis. A two-tailed statistical analysis was done using Form 2 of the *t*-test at the 95% confidence level (Table 28). All extraction times are compared to the one minute microwave extraction. H_o is that there is no statistical difference in the extraction efficiencies and H_1 is that there is a statistical difference in the extraction efficiencies.

Table 28. Statistical Analysis of Various Extraction Times for Chewing Gum, (n = 3)

	t_{calc}	$t_{tab(95\%)}$[118]	Conclusion
2 min microwave extraction vs. 1 min	2.492	2.776	$t_{calc} < t_{tab}$ ∴accept H_o
5 minute microwave extraction vs. 1 min	10.8	2.776	$t_{calc} > t_{tab}$ ∴reject H_o
2 minute shaking vs. 1 min	24	2.776	$t_{calc} > t_{tab}$ ∴reject H_o

The two minute extraction was not statistically different than the one minute analysis so a one minute extraction time was chosen. The concentration of BHT in chewing gums is typically greater than 100 ppm; consequently, a small sample size was needed. A 0.1 g sample size was chosen to be extracted in 5 ml of solvent. Prior to extraction the chewing gum was cut into pieces so that 0.1 g would be three separate pieces. The internal standard used was naphthalene at a concentration of 1.2 mg/mL. This was added prior to the extraction to also account for losses in the sample handling. The final extraction parameters are listed in Table 29.

Table 29. Extraction Conditions for Chewing Gum

Parameter	Value
Solvent	9:1 hexane:isopropanol
Time	1 minute
Power	100%
Internal Standard	Naphthalene
Sample Size	0.1 g
Amount of Solvent	5 ml

The microwave extractor was a MES 1000 from CEM (Matthews, NC). It is capable of extracting twelve identical samples simultaneously. The power is controlled as well as the maximum temperature reached and the hold time at the maximum temperature. The microwave system operates at 950 Watts. The extraction vessels are closed systems so that no sample or solvent is lost during the extraction. One of the vessels is a control vessel where a fiber optic probe monitors the temperature and a pressure transducer monitors the pressure.[119] It was necessary to cool the vessels after the extraction prior to opening them. The average temperature and pressure reached by the gum samples was 37 °C and 13 psi respectively. The water content and other gum components affect these values. The gum samples and were filtered through a 0.45 μm syringe filter and then the extract was ready for analysis.

Many of the same steps were followed for the breakfast cereal extraction. Once again the power was chosen at 100%. The same solvent system, 9:1 hexane:isopropanol was chosen as for the chewing gums after investigation of several other solvents and solvent systems. The other solvents included hexane and methanol, ethanol and hexane, methylene chloride, hexane and hexane and ethyl acetate. The 9:1 hexane: isopropanol system was chosen for the cereal samples for the same reasons that it was chosen for the chewing gum samples.

The time chosen for the extraction was five minutes after investigating three extraction times at one minute, five minutes and ten minutes. (Figure 65).

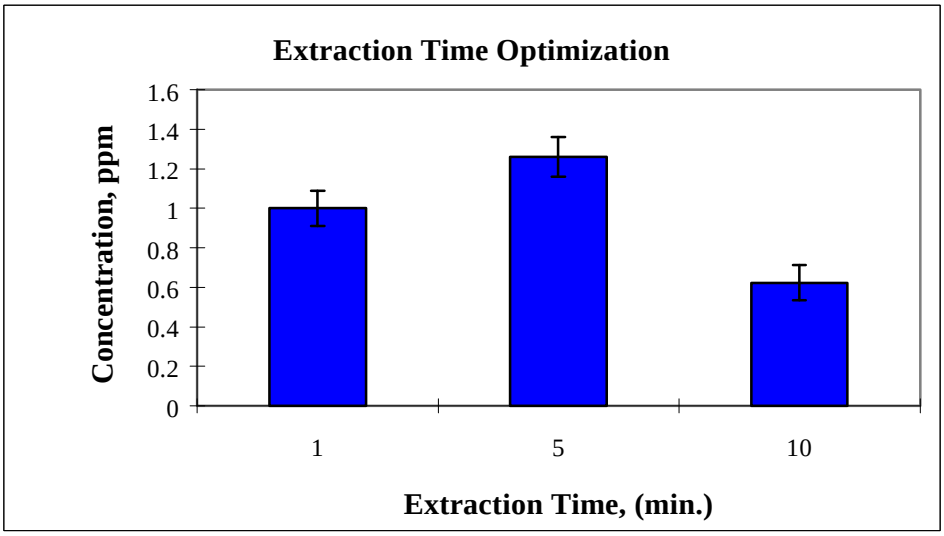

Figure 65. Extraction Time Optimization for Cereal

Conditions: 1 g breakfast cereal extracted at 100% power in 5 mL 9:1 hexane:isopropanol solvent mixture, Analysis conditions in Table 33.

The extraction values were again, statistically compared using a two-tailed Form 2 of the t-test at the 95% confidence level. (Table 30). The values in the table were compared against the five minute extraction and are shown to be statistically different. H_o is that there is no statistical difference in the extraction efficiencies and H_1 is that there is a statistical difference in the extraction efficiencies.

Table 30. Statistical Analysis of Various Extraction Times for Breakfast Cereal, (n = 3)

	t_{calc}	$t_{tab(95\%)118}$	Conclusion
1 min microwave extraction	4.71	2.776	$t_{calc} > t_{tab}$ ∴reject H_o
10 minute microwave extraction	11.25	2.776	$t_{calc} > t_{tab}$ ∴reject H_o

The internal standard remained the same for the cereal samples. The sample size was increased to one gram in 5 ml of solvent due to the approximate 10 to 100 fold decrease in concentrations of BHT in cereal compared to chewing gum. The concentration of BHT in cereal is less than 50 ppm. Prior to weighing the cereal samples, the cereal was crushed in a food blender to a fine particle size and the large pieces sifted out of the crushed cereal. An attempt was made to extract the cereal without crushing it first (Table 31). This attempt was unsuccessful using the extraction conditions listed in Table 32. Despite the microwaves ability to penetrate the sample, it was not possible to extract the BHT from the cereal prior to crushing it. A longer extraction time or a pre-soaking time may eliminate the need for crushing the sample. The concentration in the crushed sample was determined to be 0.3 ppm, but in the uncrushed sample the BHT was not detected, "nd". This indicates that even with the higher diffusivities possible with solvent when using microwave extraction there is still a limit as to what can be rapidly extracted.

Table 31. Crushed vs. Uncrushed Extraction Concentrations of Cereal Samples

	Crushed Cereal Sample	Uncrushed Cereal Sample
Concentration of BHT	0.3 ppm	nd

The final extraction conditions for the cereals are shown in Table 32.

Table 32. Extraction Conditions for Breakfast Cereal

Parameter	Value
Solvent	9:1 hexane:isopropanol
Time	5 minutes
Power	100%
Internal Standard	Naphthalene
Sample Size	1 g
Amount of Solvent	5 ml

The solvent amount was kept as low as possible so that no additional concentrating steps would be needed. The cereal extract was filtered through 70 mm Whatman glass microfiber filter paper and concentrated in a few samples under a stream of nitrogen. The extract was then ready for analysis.

Standard Preparation

To obtain quantitative data from the extracts, a series of standards was prepared. For the chewing gum samples, 6 standards were prepared ranging in concentration from 200 ppm to 2.5 ng/mL. See the calibration curve in Figure 66.

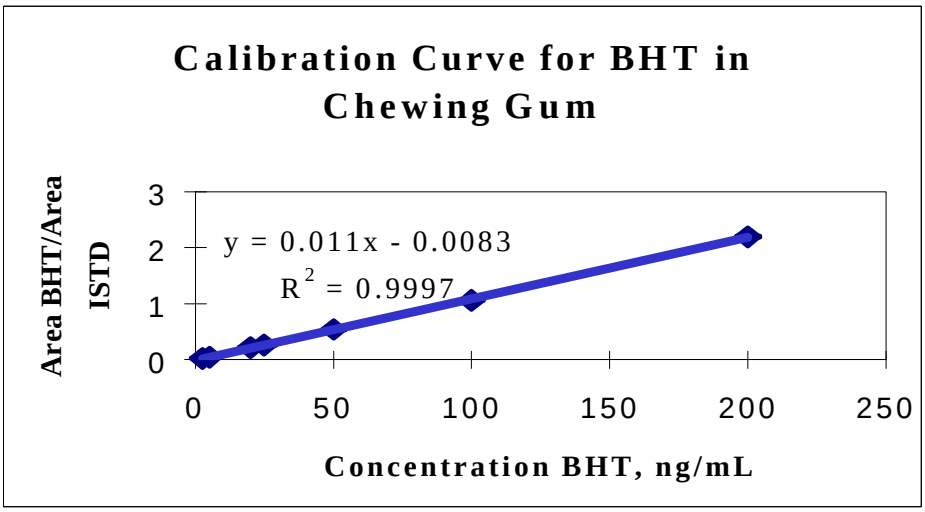

Figure 66. Calibration Curve for BHT in Chewing Gum

Conditions: 6 standards ranging from 200 to 2.5 ng/mL, n = 3 at each concentration. Analysis conditions listed in Table 33.

The equation of the line is y = 0.011x – 0.0083, with an R^2 value of 0.999, which indicates good linearity over the concentration range used. Each data point is an average of three injections. A new calibration curve was prepared for the cereal samples using 5 standards ranging in concentration from 0.05 ppm to 50 ppm. See the calibration curve in Figure 67.

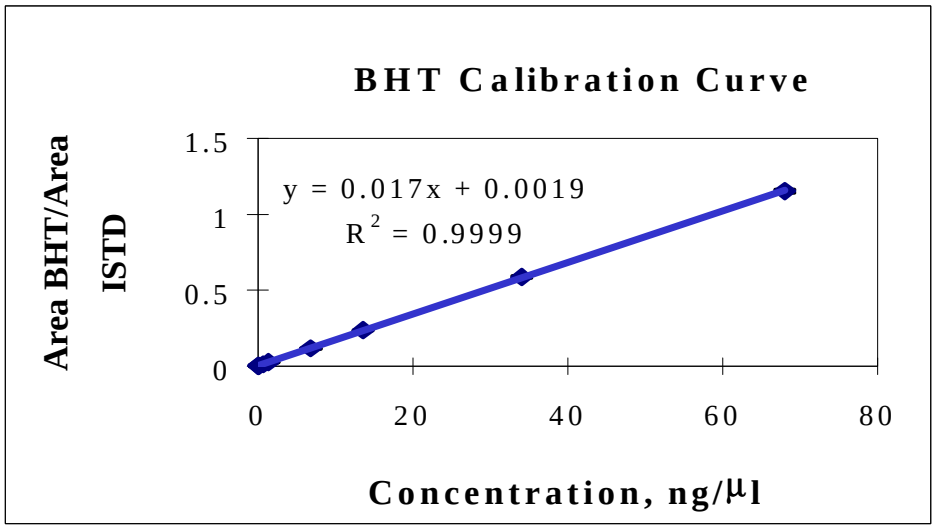

Figure 67. Calibration Curve Used for Quantitation of BHT in Breakfast Cereal

Conditions: 5 standards ranging from 50 to 0.05 ng/mL, n = 3 at each concentration. Analysis conditions listed in Table 33.

Each data point in the calibration curve is an average of three injections. The equation of the line is, y = 0.017x – 0.0019, with an R^2 value of 0.999, again indicating good linearity over the concentration range. The limit of detection (LOD) and the limit of quantitation (LOQ) were calculated for the BHT using the eq. 47 and eq. 48.

$$\text{LOD} = \frac{k s_{background}}{slope} \tag{47}$$

$$\text{LOQ} = \frac{10 s_{background}}{slope} \tag{48}$$

k = constant, dimensionless

$s_{background}$ = standard deviation of the chromatographic baseline

slope = from the signal vs. concentration graph, pA/concentration

The standard deviation of the baseline is determined by integrating the chromatographic baseline 20 times and calculating the standard deviation of these 20 baseline measurements. The constant k is either 2 or 3, based on whether or not a Gaussian

distribution is assumed. A value of 3 was used in this work, which assumes a non-Gaussian distribution. The slope term is obtained from a graph of the signal of the analyte plotted vs. the analyte concentration. The graph shown in Figure 68 was used to determine the slope.

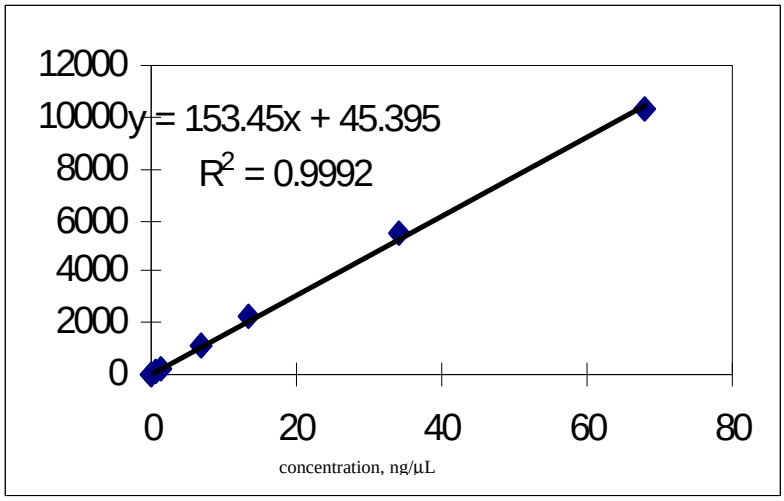

Figure 68. Calibration Curve Used to Calculate LOD and LOQ

The LOD was calculated to be 0.02 ng/µL and the LOQ was calculated to be 0.06 ng/µL. Finally, a spiking study was done at a concentration of 50 ppm using a cereal containing no BHT. There was no label claim of BHT on this particular cereal, and the absence of BHT was confirmed by extracting and analyzing the cereal prior to spiking; BHT was not detected. After spiking, the sample was allowed to sit for several hours and then the BHT was extracted and analyzed in the same way as the samples. The recovery was 98.7 $\pm$ 3.7%.

Analysis

The analysis of the extracts was done on a HP (Wilmington, DE) model 5890 GC. The GC was equipped with an EZFlash™ from Thermedics Detection, (Chelmsford, MA). The EZFlash™ system is described in Chapter 4 of this thesis. The column used

was a Rtx-5, (5% phenyl, polydimethylsiloxane), 5 m x 0.32 mm, 0.25 μm d_f. Table 33 describes the remainder of the GC conditions.

Table 33. Analysis Conditions for BHT in Food Matrices

Parameter	**Condition**
Injection Volume	1 μL
Split Ratio	20:1 to 50:1
Injector/Injector Interface Temperature	250 °C
Carrier Gas	Helium, at 4-5 mL/min
Oven Temperature Program	Variable, 60 °C to 300 °C for total time of 3.5 min
Detector	Flame Ionization Detector
Detector Sampling Rate	20 Hz
Detector/Detector Interface Temperature	325 °C

The extracts were analyzed using the conditions listed in Table 33. The mean values, standard deviations, and %RSDs were calculated for each sample. Several representative chromatograms are shown below for the chewing gums, breakfast cereals and a granola bar.

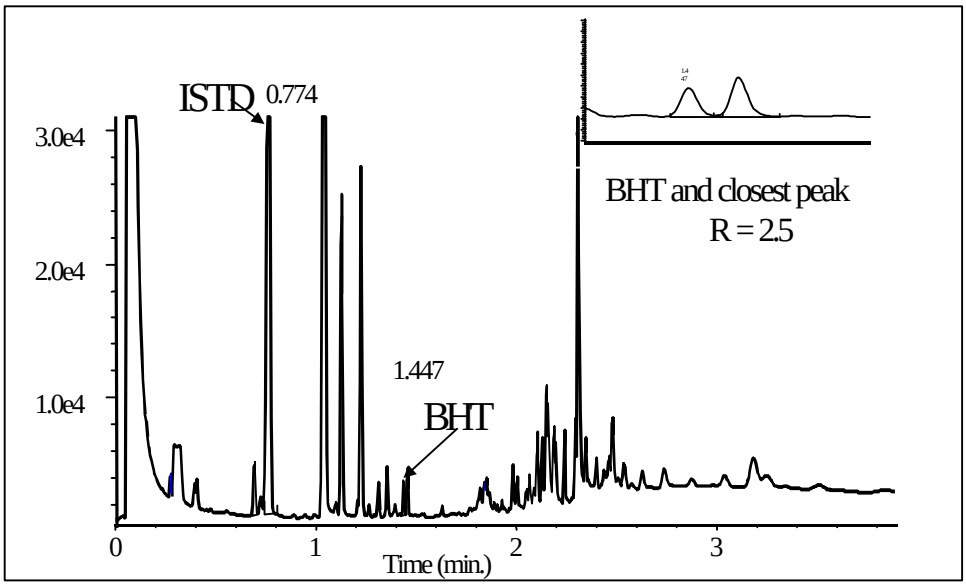

Figure 69. Chromatogram of Cinnamon Chewing Gum

Conditions: Rtx-5, 5 m x 0.32 mm i.d., 0.25 µm d_f, 7 psi, helium, split flow – 50 mL/min, 1 µL injections, oven temperature program – 60 °C, 40 °C/min to 100 °C, 150 °C/min to 300 °C

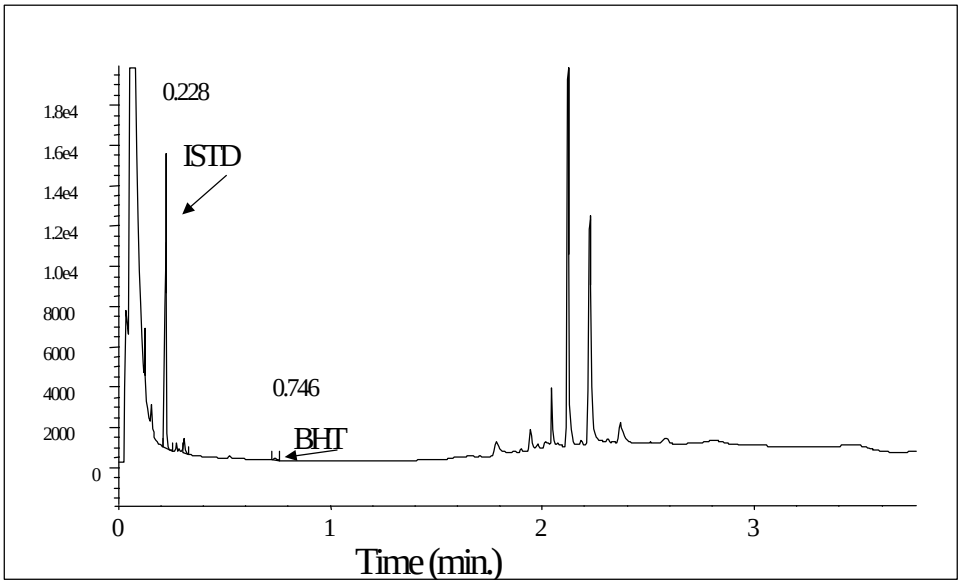

Figure 70. Chromatogram of Breakfast Cereal

Conditions: Rtx-5, 5 m x 0.32 mm i.d., 0.25 µm d_f, 6.5 psi, helium, split 23:1, 1 µL injections, oven temperature program – 100 °C, 40 °C/min to 100 °C, 150 °C/min to 300 °C

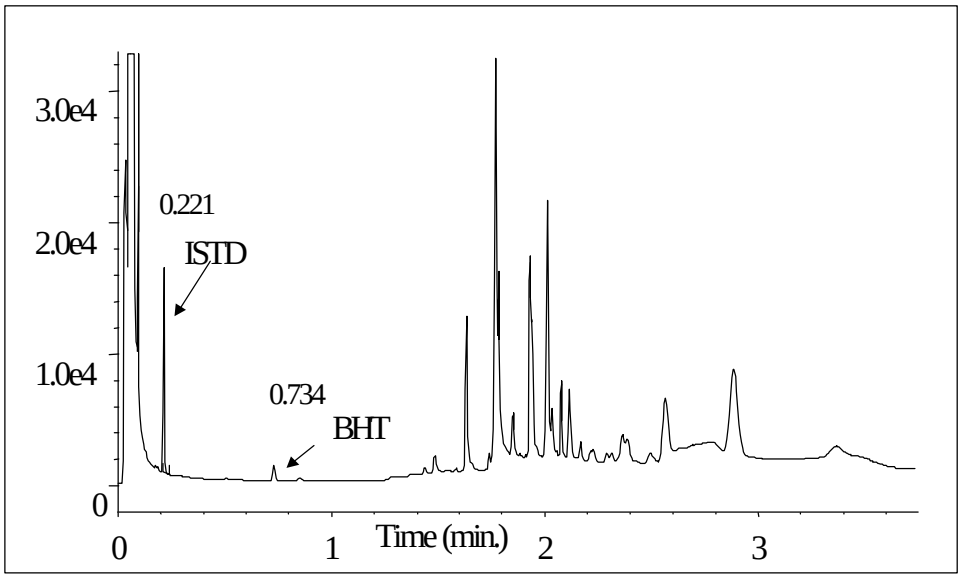

Figure 71. Chromatogram of a Granola Bar

Conditions: Extracted for 4 min. at 100% power, Rtx-5, 5 m x 0.32 mm i.d., 0.25 µm d_f, 6.5 psi, helium, split 23:1, 1 µL injections, oven temperature program – 100 °C, 40 °C/min to 100 °C, 150 °C/min to 300 °C

The peak identities were confirmed by injecting the standards for retention time confirmation as well as using a HP model 6890/5973 benchtop GC/MS system. The GC/MS was operated in the electron impact mode, scanning from 50 to 400 amu. A sample experimental mass spectrum for BHT is shown in Figure 72 and a library spectrum is shown in Figure 73.

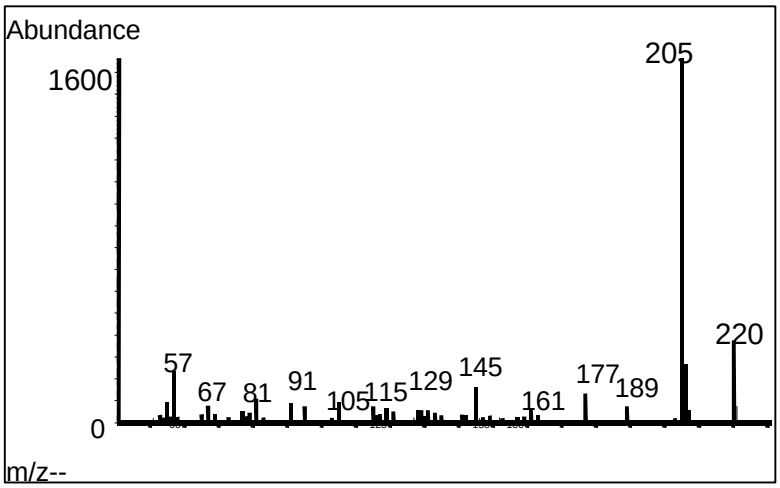

Figure 72. Experimental Mass Spectrum of BHT

Conditions: 70 eV ionization, benchtop, quadrupole mass spectrometer

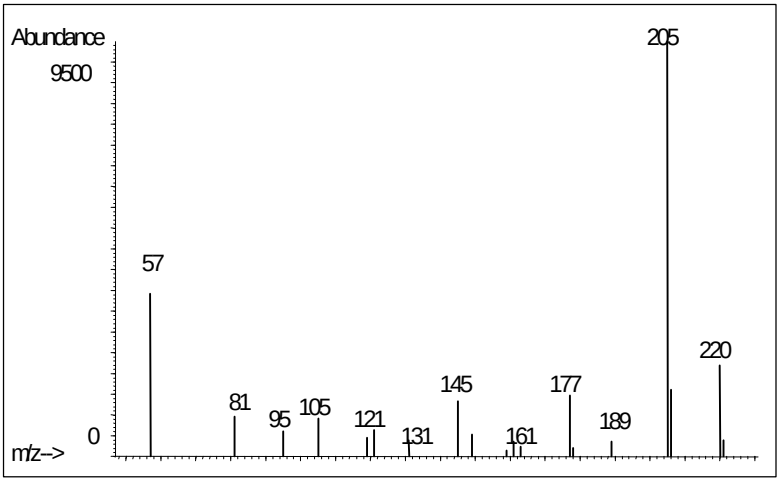

Figure 73 Library[124] Mass Spectrum of BHT

Conditions: 70 eV ionization, benchtop, quadrupole mass spectrometer

Results

The results of the analyses are shown in the following tables. Table 34 is for the chewing gum, Table 35 lists the results for the bubble gum and Table 26 tabulates the results for the cereal extracts.

Table 34. Results for Chewing Gum, (n = 3)

	Mean (ppm)	Std. Dev. (ppm)	%RSD
Bubble Gum	130	4	3.1
Cinnamon	64	5	7.1
Mint	145	5	4.0
Fruit	98	3	2.8

Table 35. Results for Bubble Gum, (n = 3)

	Mean (ppm)	Std. Dev. (ppm)	%RSD
Original	143	7	5.0
Fruit	161	2	1.3
Watermelon	173	14	8.0
Berry	172	11	6.3

Table 36. Results for Breakfast Cereal, (n = 3)

	Mean (ppm)	Std. Dev. (ppm)	%RSD
Cereal #1	1.00	0.09	8.8
Cereal #2	0.29	0.05	16
Cereal #3	8.87	0.09	1.0
Cereal #4 no claim of BHT	nd	0	0
Cereal #5	4.01	0.5	13
Cereal #6	21.6	2	9.1

The result for the granola bar was 23 ppm $\pm$ 1 ppm, %RSD of 4.3%. All results are based on 3 extractions, n = 3. The results for the BHT in the chewing gum and the breakfast

cereals are compared to the results obtained in the studies mentioned in the introduction to this chapter[107],[108]. See the table below.

Table 37. Comparison of Results

	Chewing Gum	Breakfast Cereal
J Food Sci Study[107]	53 – 118 ppm	
LC-GC Study[108]	70 – 220 ppm	0.2 – 32.3 ppm
Virginia Tech Study	64 – 172 ppm	0.06 – 22 ppm

Discussion

Microwave extraction has been shown to be a fast sample preparation method to precede a fast GC analysis. The graph in Figure 74 compares the times of GC analysis and sample preparation of the previously mentioned studies and this study.

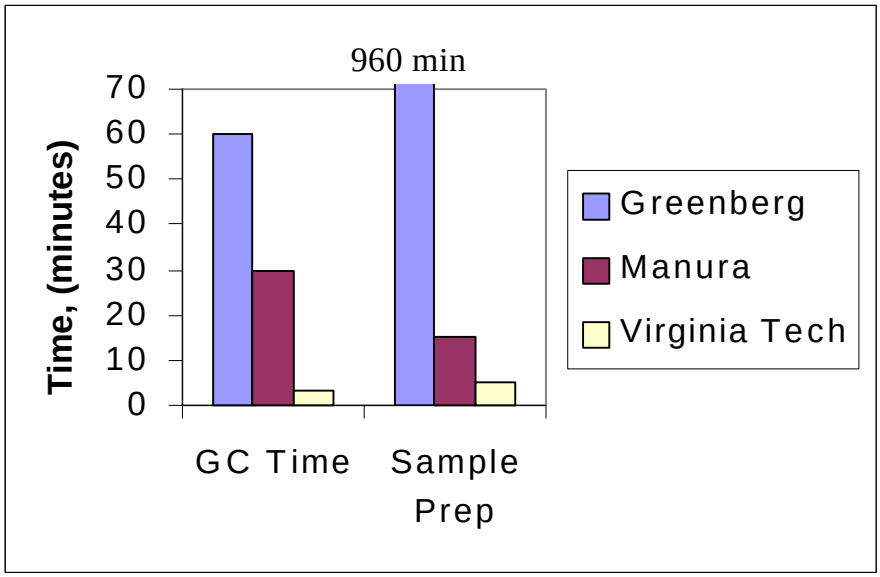

Figure 74. Time Comparison

This graph demonstrates the increase in speed that the fast GC analysis and the microwave extractions give in comparison to a traditional GC analysis and a liquid

extraction as well as thermal desorption. The validity of this study has also been shown by comparing the results of this study to the results of the other studies previously mentioned, as well as by a spiking study. The method was linear over a wide concentration range.

The %RSDs were somewhat higher than is desirable, although they were not beyond acceptable standards for the food industry. Less than 5% would be good and under 2% is great, however half of the results had %RSDs greater than 5%. This could be due to determinate errors, but the use of the internal standard should minimize that type of error. This led to a possibility of uneven heating by the microwaves. One experiment indicated that this might be true. Three samples were extracted for 45 minutes. After the extraction two of the samples looked "normal" and the third sample was black, like it was burnt. This would lead to the conclusion that uneven heating occurred in the microwave. This effect has not been reported in other studies. This effect may be more pronounced when using food samples and a cooking effect can occur.

Another question that remained was the significant decreasing recoveries at longer extraction times. (Figure 64 and Figure 65). The expected effect is to see an increase in recovery and then a leveling off of the recoveries. The fact that the recovery decreased may indicate degradation or adsorption occurring. The extractions were performed on the cereal again using a wider range of extraction times. The results obtained are shown in Figure 75.

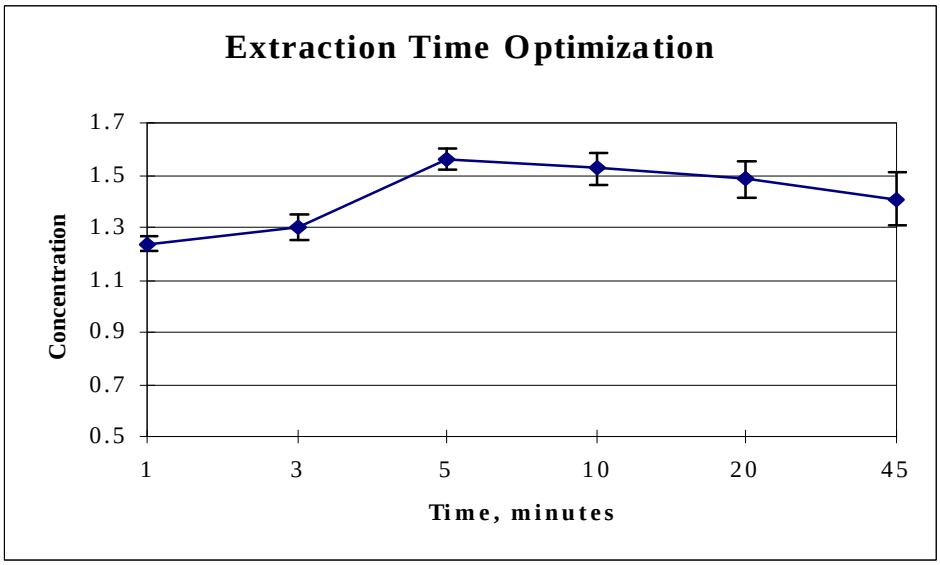

Figure 75. Extraction of BHT From Cereal Products, Degradation Study

Conditions: extraction - 1 g cereal extracted at 100% power in 5 mL 9:1 hexane:isopropanol; analysis - Rtx-5, 5 m x 0.32 mm i.d., 0.25 μm d_f, 7 psi, helium, split flow – 50 mL/min, 1 μL injections, oven temperature program – 60 °C, 40 °C/min to 100 °C, 150 °C/min to 300 °C

The extraction efficiencies seem to reach a maximum at 5 minutes. Beyond this the extraction efficiency seems to decrease. There is no statistical difference between the sequential extraction efficiencies beyond 5 minutes. The extractions at 5 minutes and at 45 minutes are almost statistically different. Whether the original extractions efficiencies decreased due to lack of skill or some other experimental factor is uncertain. However, one would expect that the extraction efficiencies should deviate above and below a mean and not continually decrease. In Figure 75, after 5 minutes the extraction efficiency decreases and does not go above this mean. This led to an investigation into the possible degradation of BHT in the food samples at the higher temperatures and longer extraction times. The temperatures reached at the various extraction times are shown in Figure 76.

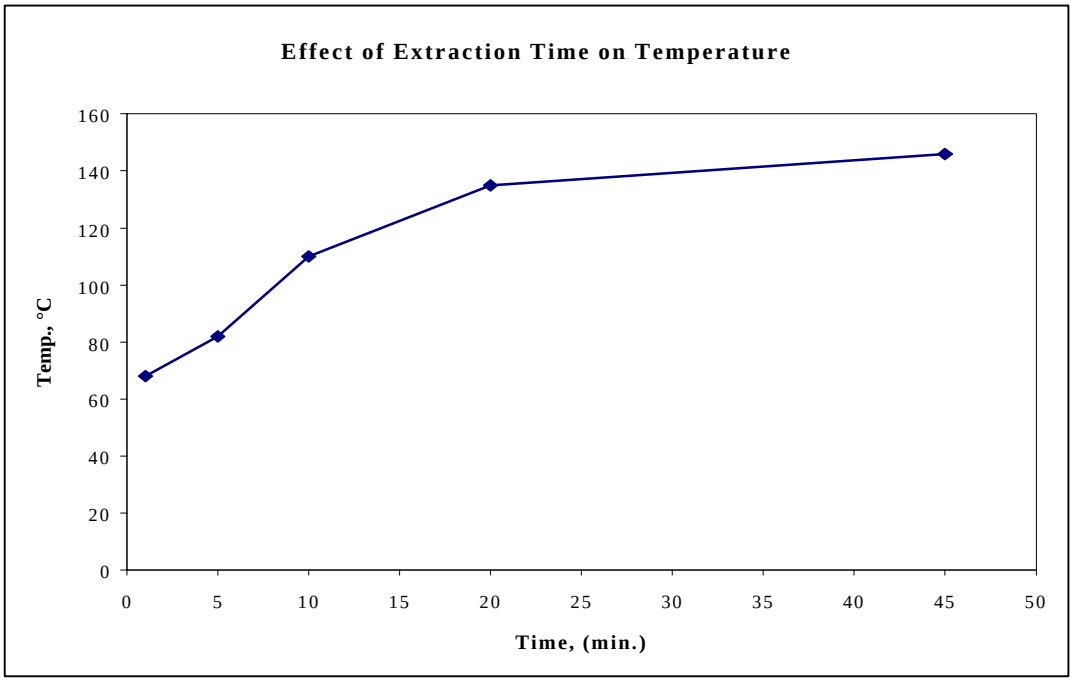

Figure 76. Effect of Extraction Time on Temperature

Conditions: Extraction and Analysis are the same as Figure 75.

The extraction temperatures increase with the longer extraction times. To investigate the possibility of BHT degradation, first the unmicrowaved standards were analyzed and the background checked for any small peaks that might be present. One was found and identified, using GC/MS, as 2-methylnaphthalene (Figure 77).

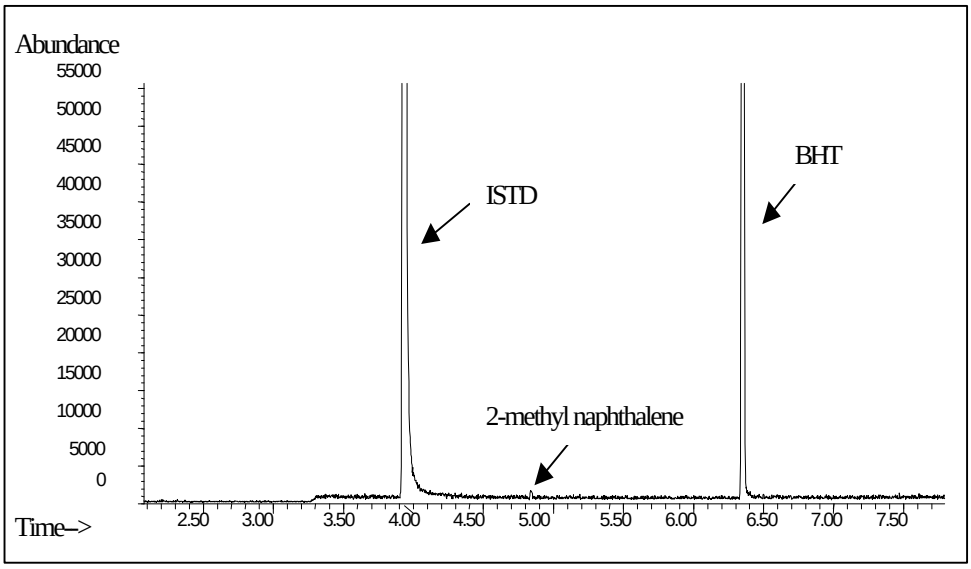

Figure 77. BHT and ISTD Prior to Microwave Extraction

Conditions: HP 6890/5973 GC/MS, HP-5 MS, 30 m x 0.25 mm i.d., 0.25 µm d_f, split 20:1, 1 µL injections, oven – 100 °C programmed at 25 °C/min to 300 °C, scanned 50 to 250 amu

Next, the internal standard and the BHT were microwaved in the solvent system for 5 minutes. The background of this total ion chromatogram (TIC) was carefully checked for small impurity peaks that might be arising. None were found (Figure 78).

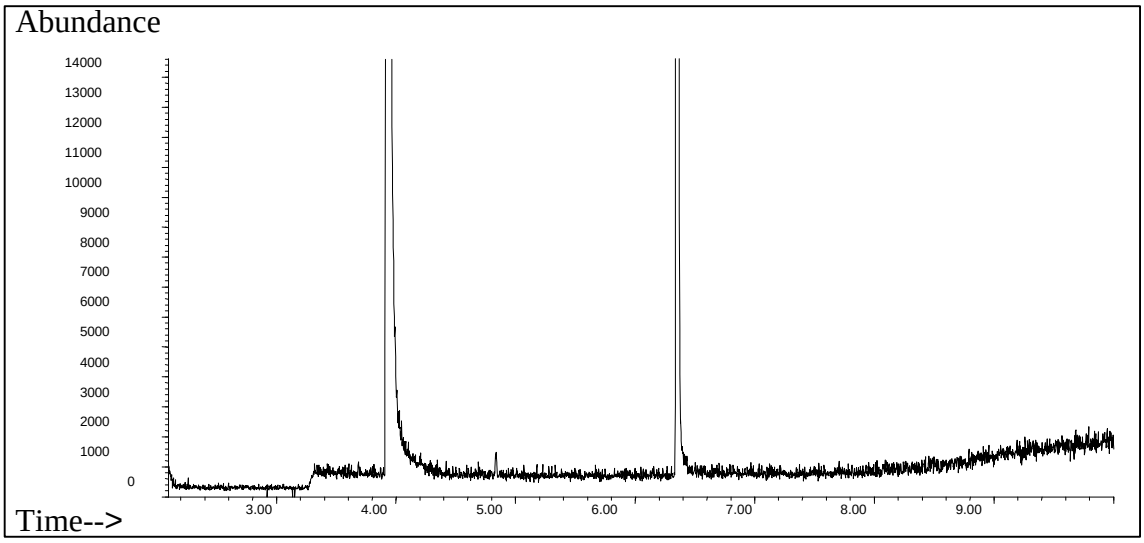

Figure 78. BHT and ISTD after Microwave Extraction

Conditions: Extraction – 5 mL standard extracted for 5 minutes at 100% power, Analysis - HP 6890/5973 GC/MS, HP-5 MS, 30 m x 0.25 mm i.d., 0.25 µm d_f, split 20:1, 1 µL injections, oven – 100 °C programmed at 25 °C/min to 300 °C, scanned 50 to 250 amu

The ISTD and the BHT were microwaved for 10 and 20 minutes to ensure that no extra peaks appeared at longer extraction times. The TICs appeared the same as the one shown in Figure 78. Once it was determined that the microwaving of the standards was not producing any "extra" peaks, the cereal was microwaved at various times and the TICs searched for the appearance of new peaks. The same impurity from the naphthalene is still present after microwave extraction of the cereal samples for 5, 10 and 20 minutes (Figure 79, Figure 80 and Figure 81).

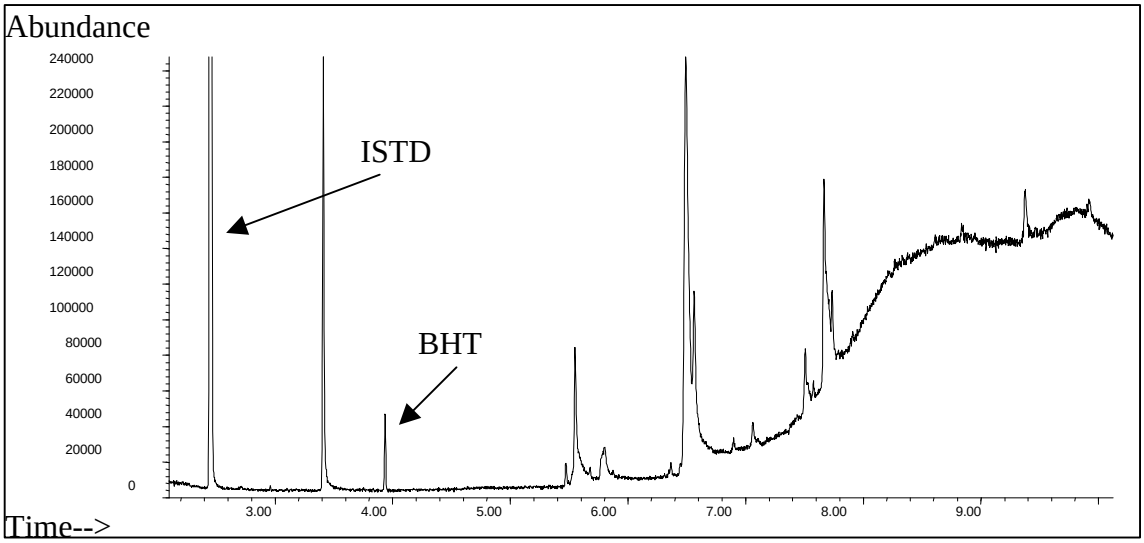

Figure 79 TIC of Cereal Extract After a 5 Minute Extraction

Conditions: Extraction – 5 mL standard extracted for 5 minutes at 100% power, Analysis - HP 6890/5973 GC/MS, HP-5 MS, 30 m x 0.25 mm i.d., 0.25 µm d_f, split 20:1, 1 µL injections, oven – 100 °C programmed at 25 °C/min to 300 °C, scanned 50 to 250 amu

The BHT and ISTD peaks are appearing as well as numerous other peaks. The impurity peak is still showing up, however since the temperature program was changed it appears at a retention time of 2.8 minutes instead of 4.8 minutes.

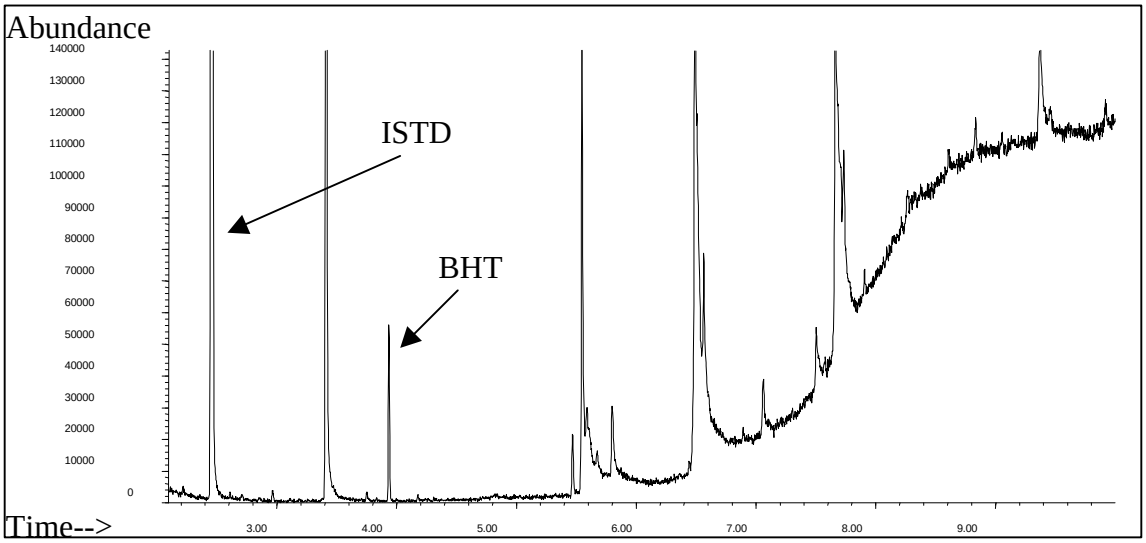

Figure 80. TIC of Cereal Extract After a 10 Minute Extraction

Conditions: Extraction – 1 g cereal extracted for 10 minutes in 5 mL 9:1 hexane:isopropanol at 100% power, Analysis - HP 6890/5973 GC/MS, HP-5 MS, 30 m x 0.25 mm i.d., 0.25 µm d_f, split 20:1, 1 µL injections, oven – 100 °C programmed at 25 °C/min to 300 °C, scanned 50 to 250 amu

There are more peaks in the TIC after 10 minutes than there were after the 5 minute extraction.

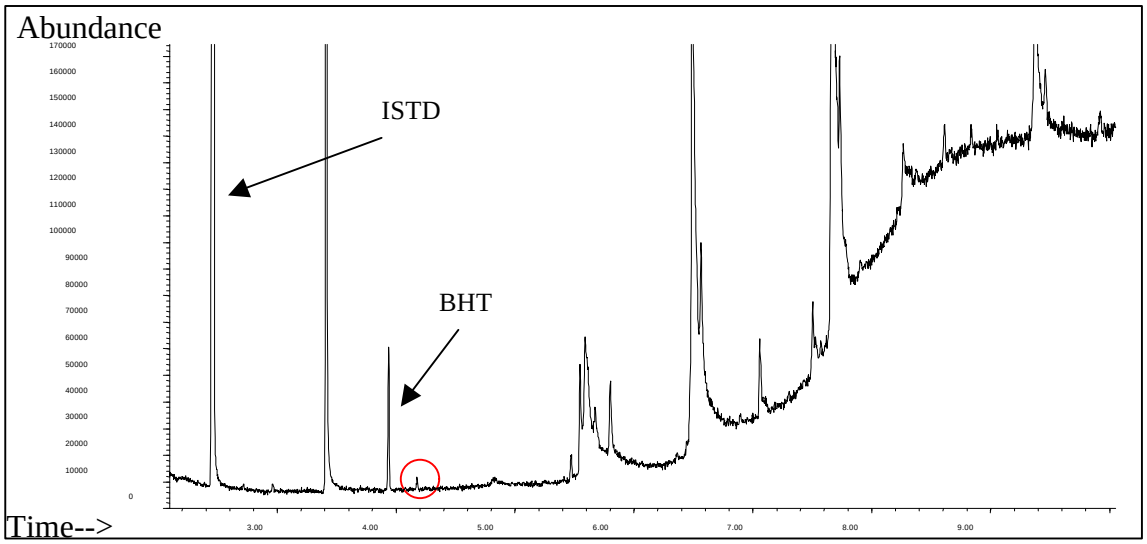

Figure 81. TIC of Cereal Extract After 20 Minute Microwave Extraction

Conditions: Extraction – 1 g cereal extracted in 5 mL 9:1 hexane:isopropanol for 20 minutes at 100% power, Analysis - HP 6890/5973 GC/MS, HP-5 MS, 30 m x 0.25 mm i.d., 0.25 µm d_f, split 20:1, 1 µL injections, oven – 100 °C programmed at 25 °C/min to 300 °C, scanned 50 to 250 amu

This TIC after 20 minutes has even more peaks. The peak that is circled at 4.2 minutes is a growing impurity peak from 10 to 20 minute extraction times. This is shown schematically in the following figure.

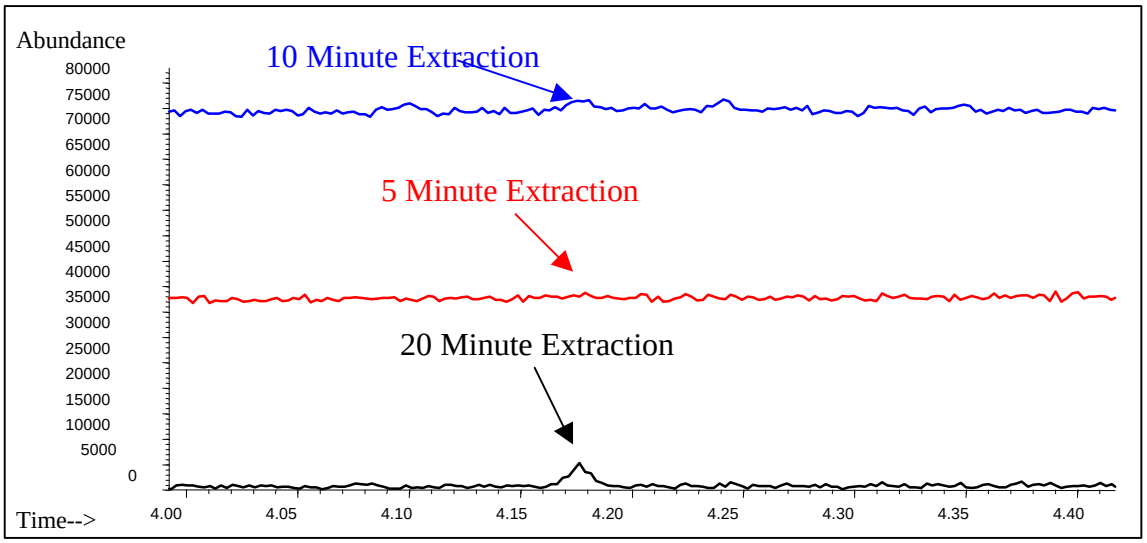

Figure 82. Overlay of TICs at Various Extraction Times

Conditions: 5, 10 or 20 minute extractions of 1 g cereal in 5 mL 9:1 hexane:isopropanol at 100% power, Analysis - HP 6890/5973 GC/MS, HP-5 MS, 30 m x 0.25 mm i.d., 0.25 µm d_f, split 20:1, 1 µL injections, oven – 100 °C programmed at 25 °C/min to 300 °C, scanned 50 to 250 amu

This impurity peak is very small, but Figure 82 shows that it is increasing with longer extraction times. It was thought that this might be a degradation product or a by-product of BHT in the cereal sample that is formed at higher temperatures. The role of BHT is to stop the oxidation of compounds such as lipids present in the same matrix. If a lipid is oxidized, the BHT reacts with the oxidized lipid and prevents further oxidation of the lipid.

This reaction occurs in several steps. First a lipid is oxidized by heat, oxygen, radiation or trace metals.[120] This forms a free radical in the form of RO•. The function of the antioxidant is to suppress the further oxidation of this lipid by donating a hydrogen to the oxidized lipid (Eq 49).

$$RO\bullet + AH \longrightarrow ROH + A\bullet \qquad (49)$$

AH is the antioxidant and A• is the antioxidant with a hydrogen removed. Various chemicals function as antioxidants and certain chemicals work better than others do in various conditions. The substitution of alkyl groups onto phenol at the 2, 4 or 6 positions, as in BHT, inductively increases the electron density on the hydroxyl group

and this increases the reactivity with the lipid radical. The radical formed by the reaction of the substituted phenol with an oxidized lipid is stabilized by the delocalization of an unpaired electron around the ring (Figure 83[121]).

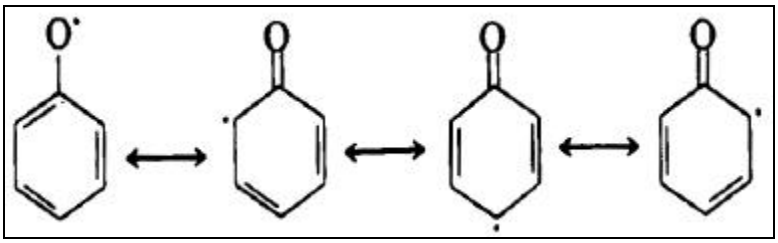

Figure 83. Stabilization by Delocalization[121]

The bulky groups, like the t-butyl group, in the 2 and 6 positions further increase the stability of the phenoxy radical. By an increase of steric hindrance, the alkyl substituents also reduce the rate of propagation reactions that involve the antioxidant radical. However, the bulky substituents also reduce the rate of reaction of the phenol with the oxidized lipid. The general reaction that an antioxidant can undergo with a lipid is shown in Figure 84.[122]

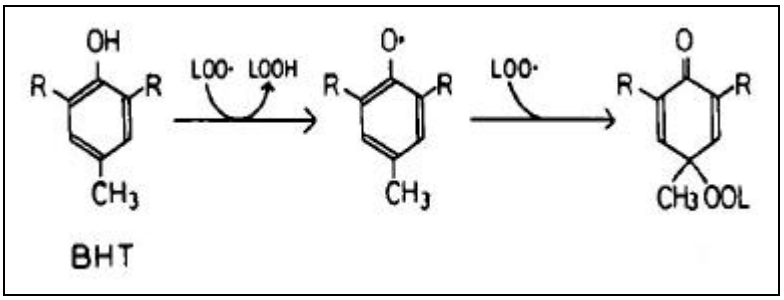

Figure 84. Degradation of Phenolic Antioxidants[122]

For BHT, the R group is t-butyl. It was of interest to this study to determine what the by-products of the antioxidant reactions were. A study[123] of soybean oil found 5 major degradation products of BHT. These products include 3,5-di-tert-butyl-4-hydroxy benzaldehyde, 3,5-di-tert-butyl-4-hydroxybenzylalcohol, 2,6-di-tert-butylbenzoquinone, 3,5,3',5'-tetra-tert-butyl-4-4'-dihydroxy-1,2-diphenylethylene and 3,5,3',5'-tetra-tert-

butylstilbenequinone. The molecular weight of each compound and the major ions are shown in Table 37.

Table 38. Degradation Products of BHT[124]

Compound	Molecular Weight	Major Ions
3,5-di-tert-butyl-4-hydroxy-benzaldehyde	234	219, 191
3,5-di-tert-butyl-4-hydroxy benzyl alcohol	236	221, 161, 147, 31
2,6-di-tert-butylbenzoquinone	220	205, 177, 149, 163, 149
3,5,3',5'-tetra-tert-butyl-4-4'-dihydroxy-1,2-diphenylethylene	438	not found
3,5,3',5'-tetra-tert-butyl stilbenequinone	434	419, 219, 57

The ions listed in Table 37 were searched for in the microwave extract filtrate. This was done using the extracted ion capabilities of the mass spectrometer software. The circled peak in Figure 81 has the major ions of BHT aldehyde. The mass spectrum for the unknown peak is shown in Figure 85.

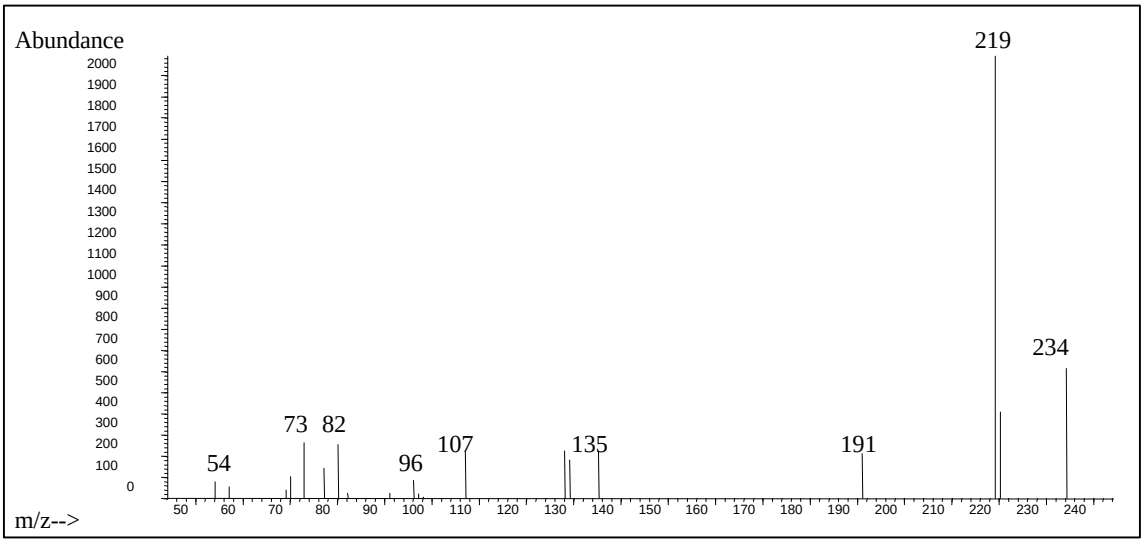

Figure 85. Experimental Mass Spectra of the Unknown Peak

Conditions: 70 eV ionization, benchtop, quadrupole mass spectrometer

From the spectra the compound was determined to be either BHT-aldehyde or 2,6-di-tert-butyl-4-ethylphenol. From the retention time of the standards, the compound was determined to be the latter. This is not one of the more common degradation compounds of BHT listed earlier, however it is appearing in these extracts. The last extraction time tested was 45 minutes. The TIC is shown below.

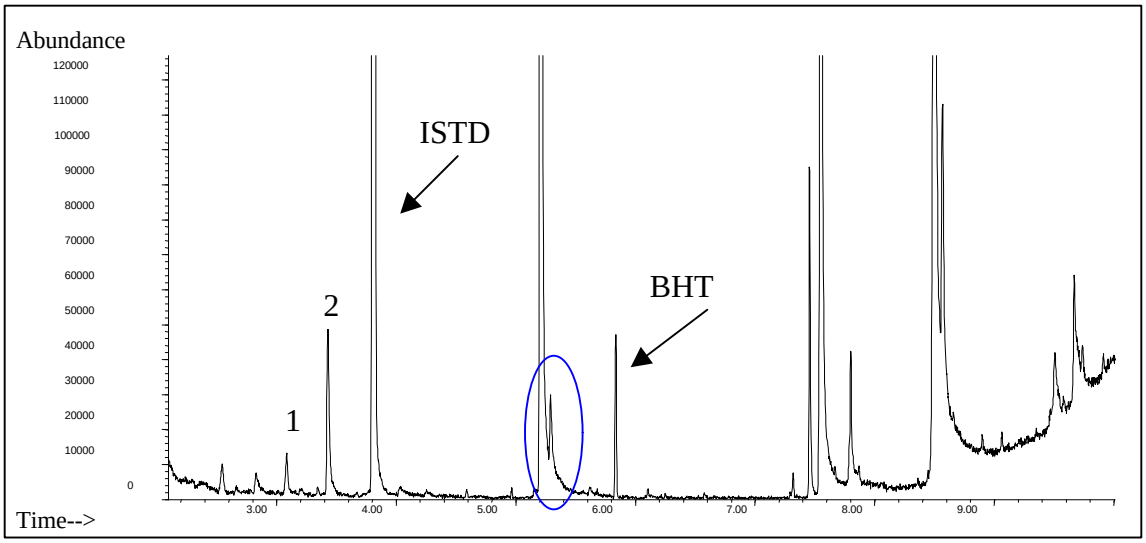

Figure 86. TIC of Microwave Extract After a 45 Minute Extraction

Conditions: Conditions: Extraction – 1 g cereal extracted in 5 mL 9:1 hexane:isopropanol for 45 minutes at 100% power, Analysis - HP 6890/5973 GC/MS, HP-5 MS, 30 m x 0.25 mm i.d., 0.25 µm d_f, split 20:1, 1 µL injections, oven – 100 °C programmed at 25 °C/min to 300 °C, scanned 50 to 250 amu

The peak that is circled in Figure 86 begins to appear sometime between 20 and 45 minutes extraction time, but it does not appear every time a 45 minute extraction is done. It appears to be a degradation peak of vanillin, which it co-elutes with. Peak 1 is nonanal at a 72% agreement with the Wiley mass spectral library spectra and Peak 2 is 4-H-Pyran-4-one, 2,3-dihydro-3,5-dihydroxy-5,6-dihydropyran-4-one at an 83% agreement with the Wiley mass spectral library spectrum. These peaks do appear every time that a 45 minute extraction is done. The difference in retention time of the ISTD and BHT in this figure are due to the fact that the TIC shown in Figure 86 was obtained from a splitless injection, which necessitated a change in the oven temperature program. The appearance of the aldehyde, peak 1, indicates that oxidation of the lipids in the cereal is occurring. This oxidation will cause the degradation of the BHT.

Microwave extractions of food products must be undertaken with care. Typical extractions of food products involve liquid extractions at room temperatures. These temperatures minimize decomposition of food products. It appears that there is a small decrease in the recovery of BHT over time using MAE. The initial experimentation with time indicated a statistically significant difference in the extraction of BHT from 5

minutes to 10 minutes. The results from the second extraction experiment indicated a decrease in extraction efficiencies from 5 to 45 minutes. The TICs showed an increase in the amount of peaks present as the extraction time increased. Some of the peaks in the 45 minute extraction TIC are indicative of compounds formed when a substance undergoes a Maillard reaction and when a lipid is oxidized.

This chapter has shown microwave extraction as a fast sample preparation method for fast GC. Microwave extraction can be used for the extraction of BHT from cereals and chewing gums, but care must be taken that there are no adverse temperature effects introduced. The use of fast GC for quantitative work for a complex matrix has been demonstrated.

Chapter 6 – Conclusions

Conclusions

The focus of this work was on fast GC and its capabilities. It should provide valuable help for those interested in initiating this technique. In Chapter Three experimental data was collected in comparing the Golay and Blumberg plots helps to validate the mathematically predicted Blumberg equation for GC under high pressure conditions. It was statistically shown that the Blumberg equation describes the experimental data better than the Golay equation. The Blumberg equation is a fundamental modification of the Golay equation, so that the equation describes the experimental data without using a pressure correction factor. The predicted effect of a long thick film column acting as a thin film column was seen. The predicted effect of the length on the rate equation plot was also experimentally confirmed. The predicted temperatures were experimentally found to be within experimental error. It is concluded that the Blumberg equation is statistically slightly better than the Golay equation and provides a means of describing the rate equations without introducing correction factors.

The investigation of fast temperature programming rates GC demonstrated that this is a good means of performing fast GC. It was shown here that the precision of the peak area and peak height of fast temperature programming rates is comparable to classical temperature programming rates. A loss of resolution is observed as the programming rate increases, but the unexpected detriment observed is that of peak broadening as the chromatogram becomes an isothermal analysis, rather than a temperature programmed analysis. Fast temperature programming rates should be used for fast GC if some loss in resolution is acceptable.

The first part of this work looked at the effect of high pressure drops caused by decreased internal diameters and the second part of this work looked at temperature programming rates. There is an important difference between using a small internal diameter column for fast GC and using fast temperature programming for fast GC. They both achieve faster analyses, however, the use of fast temperature programming allows

for the use of larger i.d. columns and longer columns to achieve fast analyses, with fewer problems with sample capacity. Fast temperature programming should be used for fast GC rather than a smaller internal diameter. Fast temperature programming has been largely underutilized; however, new instrumentation will make it possible to more fully exploit fast temperature programming rates. Fast temperature programming rates allow for the use of short columns with normal i.d.s and film thicknesses which makes sample capacity less of a problem for this mode of fast GC compared to other means of fast GC.

In the third part of this work, the use of fast GC to do fast analyses of more complex matrices was demonstrated. Along with the fast GC analyses was the use of microwave assisted extraction as a fast sample preparation method. This was to show that sample preparation times could be reduced to the same time scale or close to the same time scale as the analysis. Microwave extraction was used to extract BHT from breakfast cereals and chewing gum. It was found that long extraction times decreased the recovery of the analyte due to its possible thermal degradation.

A smaller internal diameter or faster temperature programming rate can be used to do a faster analysis. Faster sample preparation times can be used to reduce the total analysis time. Generally to do fast GC, the column length is reduced and then the carrier gas flow rate is increased, the film thickness is decreased and the column diameter is decreased in order to regain some of the efficiency lost in using shorter columns. Hydrogen or vacuum at the column outlet can also be used to preserve resolution lost by changing column parameters. The vacuum results suggest that the use of the mass spectrometer as a detector can speed up an analysis. The mass spectrometer is quite popular and becoming even more so as it becomes easier to use and lower in cost. The use of the vacuum at the column outlet will reduce the analysis time, but this is not always possible. In addition, the data sampling rate of a typical quadrupole benchtop mass spectrometer is not always fast enough for very fast GC analyses. In the scanning mode for a typical analysis on a benchtop quadrupole mass spectrometer scanning from 40 to 400 amu and using a sampling rate of 2, the mass spectrometer can sample 3.9 times per second.

Fast GC offers significant benefits, many of which are being underutilized at this point in time. The hope is that this work will inspire chromatographers to use fast GC and to take advantage of its benefits.

Future Work

Future work in the area of fast GC should involve several aspects. One of these is instrumentation. In the research presented here, the need for further improvements in the instrumentation became apparent. Figure 87 is a graph of the linear gas velocity as a function of the head pressure. The linear gas velocity is determined from the length of the column divided by the time for an unretained substance to travel through the column. See the following equation.

$$\bar{m} = \frac{L}{t_o} \tag{50}$$

$\bar{m}$ = average linear carrier gas velocity

L = length of the column

t_o = hold-up time

t_o was measured by injecting an unretained substance both manually and by using an autosampler. The startling effect was that the results for the linear velocity for the autosampler seemed to reach some limiting value and the results from the manual injections increased linearly as is expected.

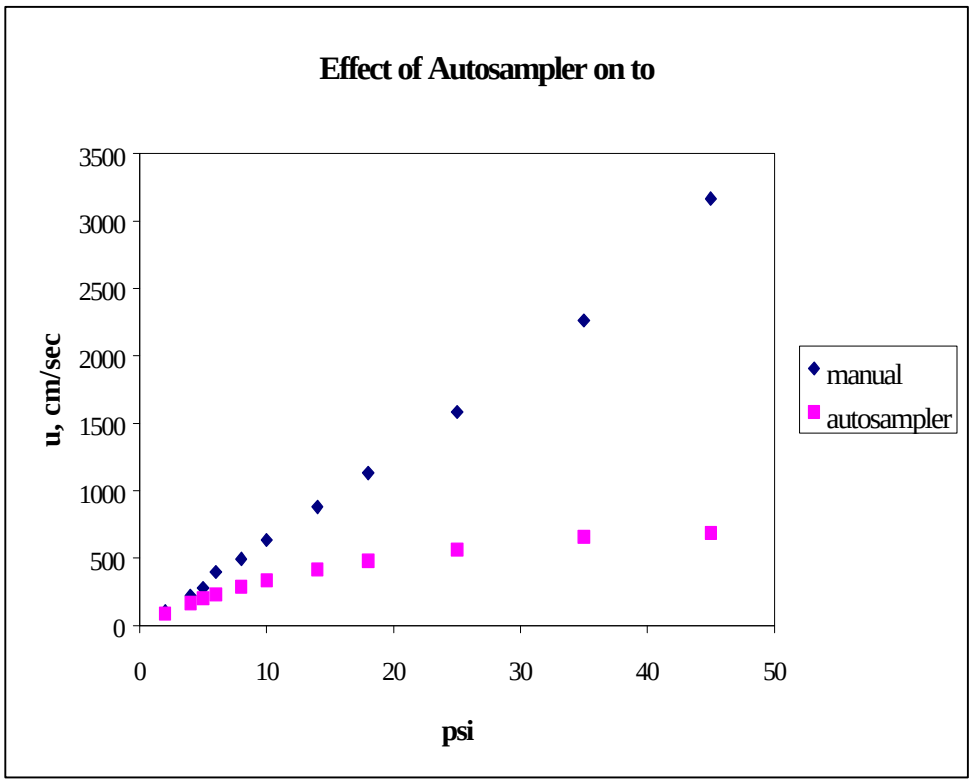

Figure 87. Effect of Autosampler on t_o

This figure indicates that work on the instrumentation is necessary in order to be able to maximize the capabilities of fast GC. A former researcher[125] at Hewlett Packard told me that the results just presented are due to an offset start time. There is a small delay from the time the injection is made until the integrator clock begins. This is not important when the analysis times are minutes, but it becomes more important as the analysis times are reduced.

Further work also needs to be done on proving that fast GC is reliable and rugged for routine analyses and for quantitation. This work demonstrated quantitation for one analysis, but more work needs to be done with other sample types. The future for fast GC columns lies in the development of highly specialized phases that are specific for a specific analysis, (large α). This is good for those who use routine analysis, but not for a research lab where much of the method development is done.

References

[1] M. J. E. Golay in: *Gas Chromatography*, V. J. Coates, H. J. Noebles, I. S. Fagerson (eds), Academic Press, New York, **1958**, p. 1.

[2] M. J. E. Golay in: *Gas Chromatography*, D. H. Desty, (ed), Butterworths, London, **1958**, p. 36, 62.

[3] J. de Zeeuw, Varian Chrompack, **1987**.

[4] D. H. Desty, A. Goldup in: *Gas Chromatography*, R. P. W. Scott, (ed), Butterworths, Washington, 1960, p. 162.

[5] M. J. E. Golay, Patent # 2,920,478, January 12, **1960**.

[6] R. P. W. Scott, C. A. Cumming in: *Gas Chromatography*, R. P. W. Scott, (ed), Butterworths, Washington, 1960, p. 117.

[7] R. P. W. Scott, C. A. Cummings in: *Gas Chromatography*, R. P. W. Scott, (ed), Butterworths, Washington, 1960, p. 127.

[8] L. S. Ettre, *Golay Award Address*, 14th Int. Sym. on Cap. Chrom. May 25-29, Baltimore MD, **1992**.

[9] A. Van Es, J. Rijks, C. Cramers, *J. Chromatogr*. **1989**, 477, 39.

[10] R. J. Jonker, H. Poppe, J. F. K. Huber, *Anal. Chem*. **1982**, 54, 2447.

[11] T. A. Rooney, L. H. Altmayer, R. R. Freeman, E. H. Zerenner, *Am. Lab*. **1979**, 81.

[12] H. M. McNair, G. L. Reed, *Flash Chromatography: Use of Fast Oven Temperature Programming*, 21st International Symposium on Capillary Chromatography & Electrophoresis, Park City, Utah, June **1999**.

[13] S. Dobanovic-Slavica, B. Slavica, B. Brantne, Application Note, Hewlett Packard, March **1999**.

[14] G. Gaspar, *J. Chromatogr*. **1991**, 556, 221.

[15] J. C. Miller, J. N. Miller, *Statistics for Analytical Chemists*, John Wiley & Sons, New York, 1988, p. 46.

[16] M. V. Russo, *Chromatographia*, **1995**, 41, 419.

[17] M. van Lieshout, M. van Deursen, R. Derks, H. Janssen, C. A. Cramers, .*J High Resol. Chromatogr*. **1999**, 22, 116.

[18] Hewlett Packard Web Page, http://chem.external.hp.com/cag/products/microecd.html, **1999**.

[19] A. van Es, J. Janssen, R. Bally, C. Cramers and J. Rijks, *J. HRC&CC*, **1987**, 10, 273.

[20] L. S. Ettre, J. V. Hinshaw, *Basic Relationships of Gas Chromatography*, Advanstar, Cleveland, OH, 1993, p.134.

[21] P. Sandra, *LC.GC*, **1987**, 5, 236.

[22] L. S. Ettre, J. V. Hinshaw, *Basic Relationships of Gas Chromatography*, Advanstar, Cleveland, OH, 1993, p. 131.

[23] L. S. Ettre, J. V. Hinshaw, *Basic Relationships of Gas Chromatography*, Advanstar, Cleveland, OH, 1993, p. 111.

[24] R. P. W. Scott, G. S. F. Hazeldean, *Gas Chromatography*, R. P. W. Scott, ed., Butterworths, London, 1960, p 144.

[25] K. J. Hyver, P. Sandra, *High Resolution Gas Chromatography*, Hewlett-Packard Co. **1989**, p. 1-18.

[26] P. A. Leclercq, *J. High Resol. Chromatogr*. **1992**, 15, 531.

[27] P. A. Leclercq,, Ca. A. Cramers, *J. High Resol. Chromatogr. Chromatogr. Comm*. **1985**, 8, 764.

[28] J. V. Hinshaw, L. S. Ettre, *Introduction to Open-Tubular Column Gas Chromatography*, Advanstar Communications, Cleveland, OH, 1994, p. 119.

[29] J. Heng, M.S. Thesis, Virginia Polytechnic Institute and State University, Blacksburg, VA, **199**

[30] Understanding Your Chemstation, Hewlett Packard, **1995**, p. 150.

[31] C. Leonard, A. Grall, R. Sacks, *Anal. Chem*. **1999**, 71, 2123.

[32] Flash GC Brochure, Thermedics Detection Inc., Chelmsford MA, USA, **1996**.

[33] M. van Lieshout, R. Derks, H. Janssen, C. A. Cramers, *J. High Resol. Chromatogr*. **1998**, 21, 583.

[34] T. A. Williams, M. Riddle, S. L. Morgan, W. E. Brewer, *J. Chrom Sci*. **1999**, 37, 210.

[35] G. L. Reed, K. Clark-Baker, H. M. McNair, *J. Chrom. Sci*., **1999**, 22, 300.

[36] J. Dalluge, R. Ou-Aissa, J. J. Vreuls, U. A. Th. Brinkman, *J. High Resol. Chromatogr*. **1999**, 22, 459.

[37] K. J Hyver, R. J. Phillips, *J. Chromatogr*. **1987**, 399, 33.

[38] M. E. Hail, R. A. Yost, *Anal. Chem*. **1989**, 61, 2402.

[39] J. C. Giddings, *Anal. Chem*. **1962,** 34, 314.

[40] P. G. Van Ysacker, H. M. Janssen, H. M. J. Snijders, P. A. Leclercq, C. A. Cramers, H. J. M. van Crutchen, *J. Microcol. Sep*. **1993**, 5, 413.

[41] L. S. Ettre, J. V. Hinshaw, *Basic Relationships of Gas Chromatography*, Advanstar, Cleveland, OH, 1993, p. 123.

[42] J. V. Hinshaw, L. S. Ettre, *Introduction to Open-Tubular Column Gas Chromatography*, Advanstar Communications, Cleveland, OH, 1994, p. 100.

[43] C. P. M. Schutjes, Ph.D. Thesis, Eindhoven University of Technology, Eindhoven **1983**, p 37.

[44] D. H. Desty, A. Goldup, W. T. Swanton in: *Gas Chromatography*, N. Brenner, J. E. Callen and M. D. Weiss (eds), Academic Press, New York, 1962, p 105.

[45] G. Gaspar, P. Arpino, G. Guiochon. *J. Chrom. Sci*. **1977**, 15, 256.

[46] C. P. M. Schutjes, E. A. Vermeer, J. A. Rijks, C. A. Cramers, *Gas Chromatography*, **1981**, p. 687.

[47] C. P. M. Schutjes, E. A. Vermeer, J. A. Rijks, C. A. Cramers, *J. Chrom*, **1982**, 253, 1.

[48] F. I. Onuska, *J. Chromatogr*. **1984**, 289, 207.

[49] P. G. Van Ysacker, H. M. Snijders, H. M. Janssen, C. A. Cramers, *High Resol. Chromatogr*. **1998**, 21, 497.

[50] R. J. Yonker, H. Poppe, J. F. K. Huber, *Anal.Chem*. **1982**, 54, 2447.

[51] Y. Shen, M. L. Lee, *J. Micro. Sep*. **1997**, 9, 21.

[52] M. van Deursen, M. van Lieshout, R. Derks, H. Janssen, C. A. Cramers, *J. High Resol. Chromatogr*. **1999**, 22, 119.

[53] M. Akard, R. Sacks, *Anal.Chem*. **1994**, 66, 336.

[54] R. Sacks, M. Akard, *Environ. Sci. Technol*. **1994**, 28, 428A.

[55] R. Majors, LC-GC, **1991**, 9, 16.

[56] R. W. Current, a. J. Borgerding, *Anal. Chem*. **1999**, 71, 3513.

[57] T. Gorecki, J. Pawliszyn, *Anal. Chem*. **1995**, 67, 3265.

[58] T. Gorecki, J. Pawliszyn, *J. High Resol Chrom.* **1995**, 18, 161.

[59] C. Leonard, H. Liu, S. Brewer, R. Sacks, *Anal. Chem*. **1998**, 70, 3498.

[60] R. D. Dandeneau, E. H. Zerenner, *HRC/CC*, **1979**, 2, 351.

[61] M. J. E. Golay in: *Gas Chromatography*, D.H. Desty, (ed)., Butterworths Scientific Publications, London, 1958, pp. 36-55.

[62] H. M. McNair, J. M. Miller, *Basic Gas Chromatography*, John Wiley & Sons Inc., New York, 1998, p. 49.

[63] L. S. Ettre and J. V. Hinshaw, *Basic Relationships of Gas Chromatography*, Advanstar, Cleveland, OH, 1993, pp. 118-119.

[64] H. M. McNair, J. M. Miller, *Basic Gas Chromatography*, John Wiley & Sons, New York, 1998, p. 47.

[65] L. S. Ettre, J. V. Hinshaw, *Basic Relationships of Gas Chromatography*, Advanstar, Cleveland, OH, 1993, p 116.

[66] C. P. M. Schutjes, E. A. Vermeer, J. A. Rijks, C. A. Cramers, *J. Chromatogr*. **1982**, 253, 1.

[67] P. A. Lelcercq, *J. High Resol. Chromatogr*. **1992**, 15, 531.

[68] L. S. Ettre, J. V. Hinshaw, *Basic Relationships of Gas Chromatography*, Advanstar, Cleveland, OH, 1993, p. 44.

[69] J. V. Hinshaw, L. S. Ettre, *Introduction to Open-Tubular Column Gas Chromatography*, Advanstar Communications, Cleveland, OH, 1994, p.20

[70] L. M. Blumberg, *Chromatographia*, **1995**, 41, 15.

[71] L. M. Blumberg, *J. High Resol. Chromatogr*. **1997**, 20, 597.

[72] L. M. Blumberg, *J. High Resol. Chromatogr*. **1997**, 20, 679.

[73] L. M. Blumberg, *J. High Resol. Chromatogr*. **1999**, 22, 403.

[74] L. M. Blumberg, *J. High Resol. Chromatogr*. **1999**, 22, 501.

[75] J. H. Purnell, *Ann. New York Acad. of Sci.* **1959**, 72, 592.

[76] P. A. Leclercq, C. A. Cramers, *J. High Resol. Chromatogr*. **1985**, 8, 764.

[77] C. A. Cramers, P. A. Leclercq, *CRC Critical Reviews in Analytical Chemistry*, 20/2, CRC Press Inc. **1988**, pp. 117-147.

[78] Kaleida Graph, Abelbeck Software, Reading, PA,

[79] J. C. Miller, J. N. Miller, *Statistics for Analytical Chemists*, John Wiley & Sons, New York, 1988, p. 217.

[80] L. S. Ettre, J. V. Hinshaw, *Basic Relationships of Gas Chromatography*, Advanstar, Cleveland, OH, 1993, p. 46.

[81] C. P. M. Schutjes, Ph.D. Thesis, Eindhoven University of Technology, Eindhoven 1983, p. 39.

[82] L. S. Ettre, J. V. Hinshaw, *Basic Relationships of Gas Chromatography*, Advanstar, Cleveland, OH, 1993, p. 38.

[83] A. T. James, A. J. P. Martin, *Biochem. J.* **1952**, 50, 679.

[84] J. C. Giddings, *Third Int. Sym. by Analysis Instrumentation Division of the Instrument Society*, June 13-16, 1961, Academic Press, NY, **1962**.

[85] W. E. Harris, H. W. Habgood, *Programmed Temperature Gas Chromatography*, John Wiley & Sons, Inc., New York, 1966, p. 8.

[86] J. H. Griffiths, D. H. James, C. S. G. Phillips, *Analyst*, **1952**, 77, 897.

[87] M. Lee, K. D. Bartle, S. J. Yang, *Open Tubular Gas Chromatography*, John Wiley & Sons, New York, NY, 1984.

[88] M. E. Hail, R. A. Yost, *Anal. Chem*. **1989**, 61, 2410.

[89] V. Jain and J. B. Phillips, *J. Chromatogr. Sci*. **1995**, 33, 55.

[90] V. Jain, J. B. Philips, *J Chrom. Sci*. **1995**, 33, 601.

[91] E. U. Ehrmann, H. P. Dharmasena, K. Carney and E. B. Overton. *J. Chromatogr. Sci*. **1996**, 34, 533.

[92] C. Leonard, A. Grall, R. Sacks, *Anal.Chem*. **1999**, 71, 2123.

[93] J. C. Giddings, *J Chem Ed*. **1962**, 39, 569.

[94] R. Rowan, Jr., *Anal Chem*, **1961**, 33, 510.

[95] H. W. Habgood, W. E. Harris, *Anal. Chem*. **1960**, 32, 450.

[96] S. Dal Nogare, W. E. Langlois, *Anal. Chem*. **1960**, 32, 767.

[97] J. C. Giddings, *Facts and Methods*, **1962**, 3, 1.

[98] L. S. Ettre, J. V. Hinshaw, *Basic Relationships of Gas Chromatography*, Advanstar, Cleveland, OH, 1993, p. 75.

[99] L. S. Ettre, J. V. Hinshaw, *Basic Relationships of Gas Chromatography*, Advanstar, Cleveland, OH, 1993, p. 81.

[100] L. S. Ettre, J. V. Hinshaw, *Basic Relationships of Gas Chromatography*, Advanstar, Cleveland, OH, 1993, p. 63.

[101] K. Clark-Baker, M.S. Thesis, Virginia Polytechnic Institute and State University, Blacksburg, Virginia, 1997.

[102] Y. Wang, Ph.D. Thesis, Virginia Polytechnic Institute and State University, Blacksburg, Virginia, 1997.

[103] Hewlett Packed Chemical Analysis Catalog, **1998-1999**, p. 212.

[104] FDA web page, http://www.verity.fda.gov/search97, June **1999**.

[105] R. W. Moch, *Food Chem. Toxicol*. **1986**, 24, 1167.

[106] Fisherman and Cohen, *Ann. of Allergy*, 31, 126.

[107] M. Greenberg, J. Hoholick, R. Robinson, K. Kubis, J. Groce, L. Weber, *J. Food Sci*, **1984**, 49, 1622.

[108] J. J. Manura, *LC-GC*, **1993**, 11, 140.

[109] A. Zlotorzynski, *Crit. Rev. in Anal.Chem*. **1995**, 25, 43.

[110] D. M. P. Mingoes, D. R. Baghurst in: *Applications of Microwave Dielectric Heating Effects to Synthetic Problems in Microwave Chemistry*, H. M. Kingston, S. J. Haswell, (eds), Microwave-Enhanced Chemistry Fundamentals, Sample Preparation and Applications, ACS, Washington, D. C. 1997, p. 4.

[111] K. Ganzler, A. Salgo, K. Valko, *J. Chromatogr*. **1986**, 371, 299.

[112] K. Ganzler, J. Bati, and K. Valko, *Chromatograph, the State of the Art*, Akademiai Kiado, Budapest, **1985**.

[113] T. Meier, S. L. Wilkinson, G. Utz, *Transfusion 23 (Abstr S16)*, **1983**, 411.

[114] W. Frietag. O. John, *Die Angew, Makromol. Chem*., **1990**, 175, 181.

[115] L. B. Jassie, S. A. Margolis, N. E. Craft, M. J. Heys, *PittCon Abstr*. **1993**, 171.

[116] V. Lopez-Avila, R. Young, W. R. Beckert, *Anal. Chem*. **1994**, 66, 1097.

[117] A. G. Gaonkar, *Characterization of Food Emerging Methods*, Elsevier, NY, 1995, p. 214.

[118] D. C. Harris, *Quantitative Chemical Analysis, 3rd ed*. W. H. Freeman and Co. NY, 1991, p. 53.

[119] MES-1000 Operation Manual, CEM Corporation, Matthews, NC, **1993**.

[120] S. J. Jadhav, S. S. Nimbalkar, A. D. Kulkarni, D. L. Madhavi in: *Food Antioxidants, Technological, Toxicological and Health Perspectives*, D. L. Madhavi, S. S.Deshpande, D. K. Salunkhe, (eds), Marcel Dekker, Inc. New York, 1996, p. 6.

[121] M. H. Gordon in: *Food Antioxidants*, B. J. F. Hudson, (ed), Elsevier Applied Science, New York, 1990, p. 20.

[122] K. Kikugawa, A. Kunugi, T. Kurechi in: *Food Antioxidants*, B. J. F. Hudson, (ed), Elsevier Applied Science, New York, 1990, p. 67.

[123] K. Kikugawa, A. Kunugi, T. Kurechi in: *Food Antioxidants*, B. J. F. Hudson, (ed), Elsevier Applied Science, New York, 1990, p. 66.

[124] Wiley Mass Spectrometry Database, Hewlett Packard ChemStation, **1996**.

[125] L. Blumberg, personal communication, **1998**.

Vita

Gail L. Reed was born in Bloomsburg, PA, on September 28, 1971 to Frank and Lois Reed. Gail was raised in Pennsylvania as the eldest child in a family of five. After graduation from Manheim Central High School in June 1990 she attended Millersville University, Millersville, PA. She obtained her B.S. degree in chemistry from Millersville University in May 1994, when she also received the American Institute of Chemists Award. In August 1994 she began teaching at Terre Hill Mennonite High School where she taught ninth through twelfth graders chemistry, biology, physics, earth & space science and general science. After a year of teaching she decided to further her education and came to Virginia Polytechnic Institute and State University in August 1995. There she worked under the direction of Dr. Harold M. McNair. The summer of 1996 was spent working at S. C. Johnson Wax, Racine, WI under the direction of Mr. Don Hansen and the summer of 1997 was spent working at IRI.TMC, under the direction of Dr. Jonathan Crowther. She completed her Ph.D. in Analytical Chemistry in September 1999. During her time at Virginia Polytechnic Institute and State University she was involved in teaching the undergraduate chemistry laboratories including general chemistry, analytical chemistry for the life sciences and analytical chemistry. She was also involved in teaching ACS short courses including Gas Chromatography, Liquid Chromatography and Gas Chromatography/Mass Spectrometry. She has accepted a position at Janssen Pharmaceutica, Titusville, NJ beginning October 1999.